Engineering Journal

American Institute of Steel Construction

Third Quarter 2010 Volume 47, No. 3

www.aisc.org

Transfer Forces in Steel Structures

BO DOWSWELL

ABSTRACT

Transfer forces are loads that are transmitted across joints in a structure. For connections to be designed properly, the transfer forces must be communicated to the connection designer. This paper discusses the calculation of transfer forces and how the connection configuration affects the calculations. Two examples are provided to illustrate the calculation process.

Keywords: transfer forces, connections

Transfer forces are loads that are transmitted across joints in a structure. For connections to be designed properly, the transfer forces must be communicated to the connection designer. In simple structures, the force paths can be easily identified, but for more complicated structures such as the one shown in Figure 1, the force paths are not obvious. The process is further complicated by the fact that multiple load cases must be considered.

This paper discusses the calculation of transfer forces and how the connection configuration affects the calculations. Two examples are provided to illustrate the calculation process.

BRACING CONNECTIONS

A standard vertical bracing connection is shown in Figure 2. When this type of connection is used, the transfer forces should be calculated assuming the horizontal component of the brace load is transferred through the gusset-to-beam interface and the vertical component is transferred through the gusset-to-column interface. Technically, this assumption may not be true, because the connection designer may choose to transfer the forces in a different way, but the additional loads will be accounted for in the connection design process and the end result will be as assumed. There are many different methods to determine the force distribution in bracing connections, but to illustrate this point, only the KISS method and the Uniform Force Method will be used.

The lower bound theorem of limit analysis states that a load calculated based on an assumed force distribution that satisfies equilibrium conditions with forces nowhere exceeding the capacity will be less than or equal to the true limit load. The designer can choose any force path that is convenient, if the following three conditions are satisfied:

1. Equilibrium must be satisfied.
2. All components in the force path must be designed for the assumed force distribution.
3. All components in the joint must have adequate ductility to allow the stresses to redistribute so the assumed force distribution can be achieved.

Although condition 1 must always be satisfied, the contract drawings usually show the maximum load in the members. In most cases, the maximum loads for each member at a particular node will occur at different load cases, and a free body diagram of the node using these maximum loads will not be in equilibrium.

The external loads acting on a vertical bracing joint are shown in Figure 3.

The KISS method, described by Thornton (1984), has been used extensively in the past to distribute the brace forces through the connection. The assumed force distribution is

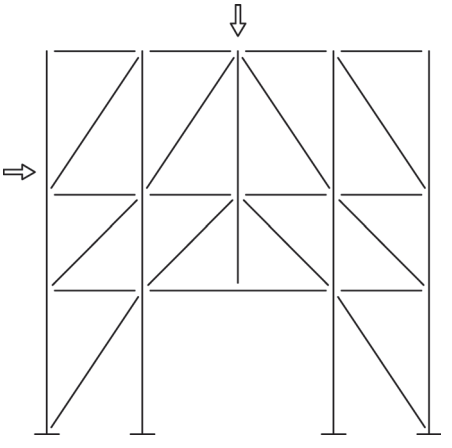

Fig. 1. Elevation of a braced frame.

Bo Dowswell, Principal, SDS Resources, LLC, Birmingham, AL.
E-mail: bo@sdsresources.com

shown in Figure 4. Because the horizontal load at the gusset-to-beam interface, H_b, is equal and opposite to the horizontal component of the brace load, P_h, the beam-to-column connection is not affected by the brace load. Therefore, the beam connection can be designed as if the brace were not present.

The force distribution for the general condition of the Uniform Force Method (AISC, 2005) is shown in Figure 5. In addition to the beam reaction and transfer force, the beam-to-column connection must be designed for additional forces generated by the assumed force distribution. To maintain equilibrium, the horizontal force at the gusset-to-column interface, H_c, must be transferred into the beam. Similarly, the vertical force at the gusset-to-beam interface, V_b, should be added (algebraically) to the beam reaction.

Although the beam-to-column connection can be affected by the gusset interface loads, the transfer forces are calculated independently, and the beam-to-column connections are designed considering the transfer force and any additional load from the assumed distribution of the brace loads. This can be seen in the free-body diagram of the column in Figure 5, where the horizontal force carried by the beam-to-column connection, H, must equal the algebraic sum of F_t and H_c.

Conversely, this assumption is not correct if the gusset plate is attached at only one interface as shown in Figure 6. For the connection in Figure 6(a), the horizontal component of the brace goes into the column through the gusset-to-column interface. Then it passes through the beam-to-column connection. If no other forces are acting on the joint, the transfer force is equal and opposite to the horizontal component of the brace. In Figure 6(b), a similar situation exists, and the vertical component of the brace must be transferred into the column. In this case, the beam end connection should be designed to carry the algebraic sum of the beam end reaction and the vertical component of the brace.

Standard horizontal bracing connections are shown in Figure 7. When these connections are used, the components of the brace force transfer directly into the beams. The components at each gusset-to-beam interface are parallel to the longitudinal axis of the beam.

BEAM CONNECTIONS FOR LARGE TRANSFER FORCES

It is common to use 5/16-in.-thick clip angles for standard double angle connections; however, the axial capacity of these connections is low. For axial loads exceeding the capacity of

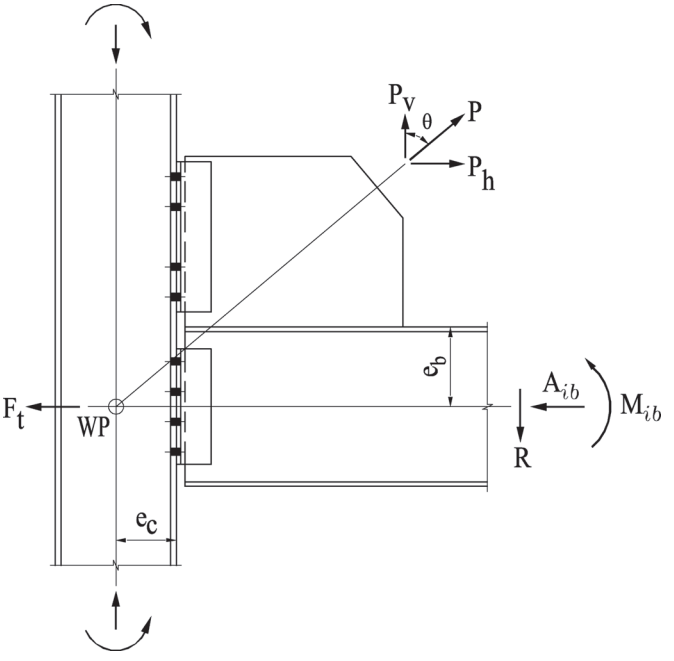

Fig. 3. External loads acting on a vertical bracing joint.

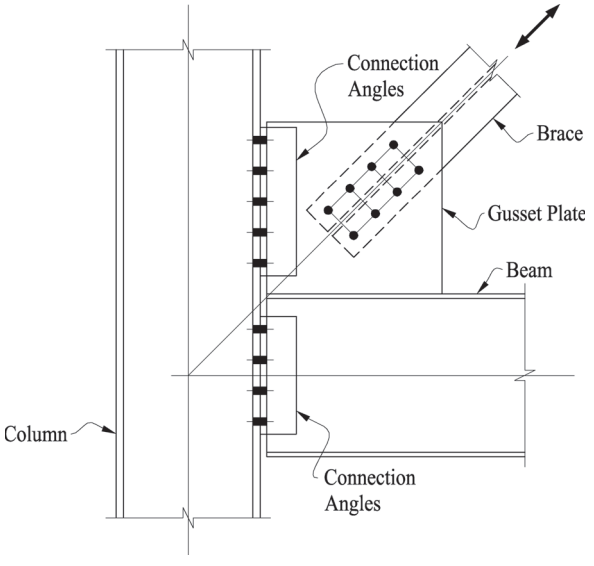

Fig. 2. Standard vertical brace connection.

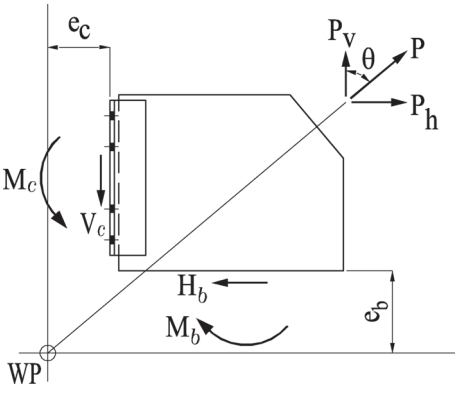

Fig. 4. Gusset plate interface forces for the KISS method.

standard connections, the most common connections are the double-angle connection and the shear end plate connection shown in Figures 8(a) and 8(b), respectively.

Transfer forces occasionally exceed the axial capacity of the common connection configurations. In these cases, alternative connections must be used. If the connection is required to carry axial load only, it can be designed as a strut connection with a gusset plate as shown in Figure 9. If the beam shear is significant, the connections in Figure 10 can be used. These connections have a significant rotational stiffness and will behave as moment connections in the real structure. The fin plate connection in Figure 10(a) has traditionally been used by fabricators to increase the axial load capacity of beam-to-column connections. Williams (1986) showed that the plates cause the connection to perform as a fully fixed moment connection. Figure 10(b) shows a flush end plate connection that can be used to carry very large compression loads and moderately large

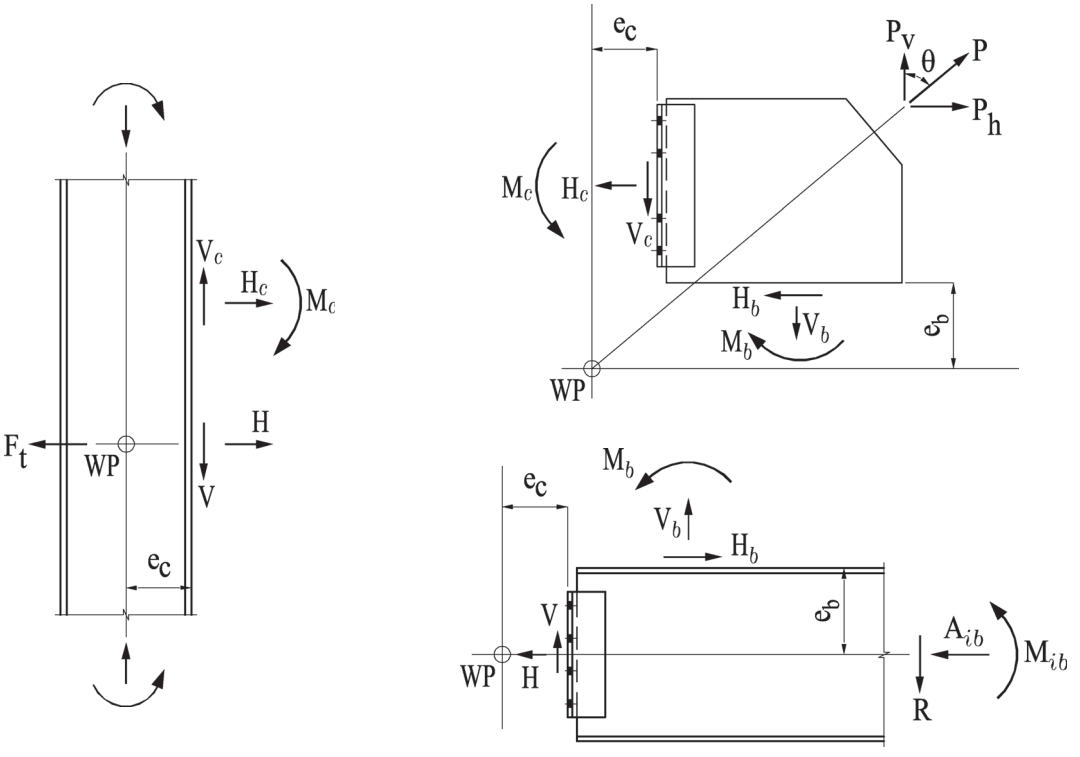

Fig. 5. Gusset plate interface forces for the Uniform Force Method.

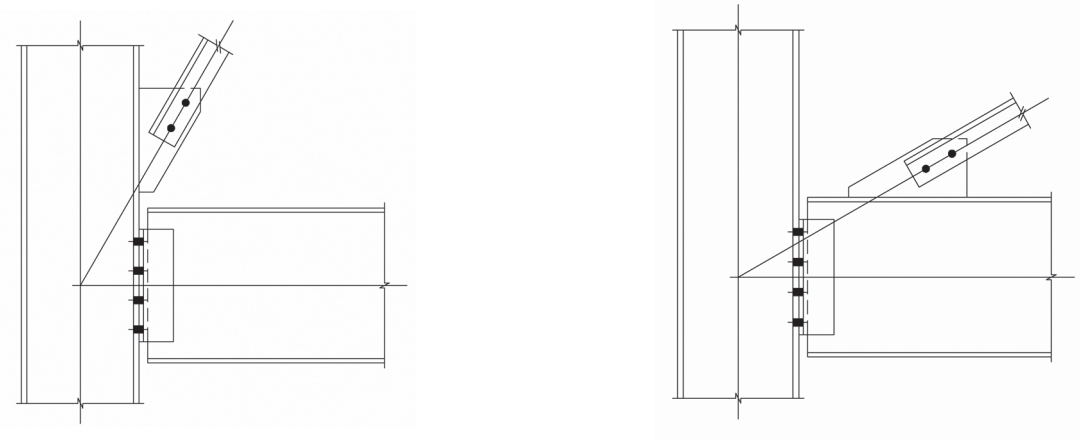

(a) *(b)*

Fig. 6. Nonstandard vertical brace connections. (a) Gusset plate welded directly to column. (b) Gusset plate welded directly to beam.

tension loads. Figure 10(c) shows an extended end plate that can be designed for large tension and compression loads. If designed correctly, this connection can develop the full strength of the member. Figure 10(d) shows a flange plate connection that can carry very large loads, such as truss chord pass-through loads.

VERTICAL TRANSFER FORCES

Generally, transfer forces are thought of as acting in the horizontal plane of a structure, but there are cases where vertical transfer forces should be indicated on the drawings. The connections shown in Figure 11 have vertical loads entering the gusset plate from a beam or truss chord. Figure 11(a) shows a truss panel point with a vertical transfer force across the chord due to the purlin load. In most cases, if the transfer force is not shown, the gusset-to-chord interface will be designed for the horizontal force only. Figure 11(b) shows an inverted V-brace with a vertical transfer force due to the gravity floor load. Figure 11(c) shows an inverted V-brace with a vertical transfer force due to column above. Figure 11(d) shows the mid-point of an X-brace, where vertical forces may be transferred from one gusset plate to the other.

DIAPHRAGM FORCES

Forces in the horizontal plane of a structure can be transferred to the vertical bracing system with a horizontal bracing system or a diaphragm. If a diaphragm is used, the forces can be transferred to the struts using deck welds, screws or composite studs. Forces can also be transferred from a concrete floor diaphragm into the column by bearing directly on the column. The forces will then be transferred from the column into the strut. The transfer mechanism for these forces dictates the amount of load in the beam-to-column connections.

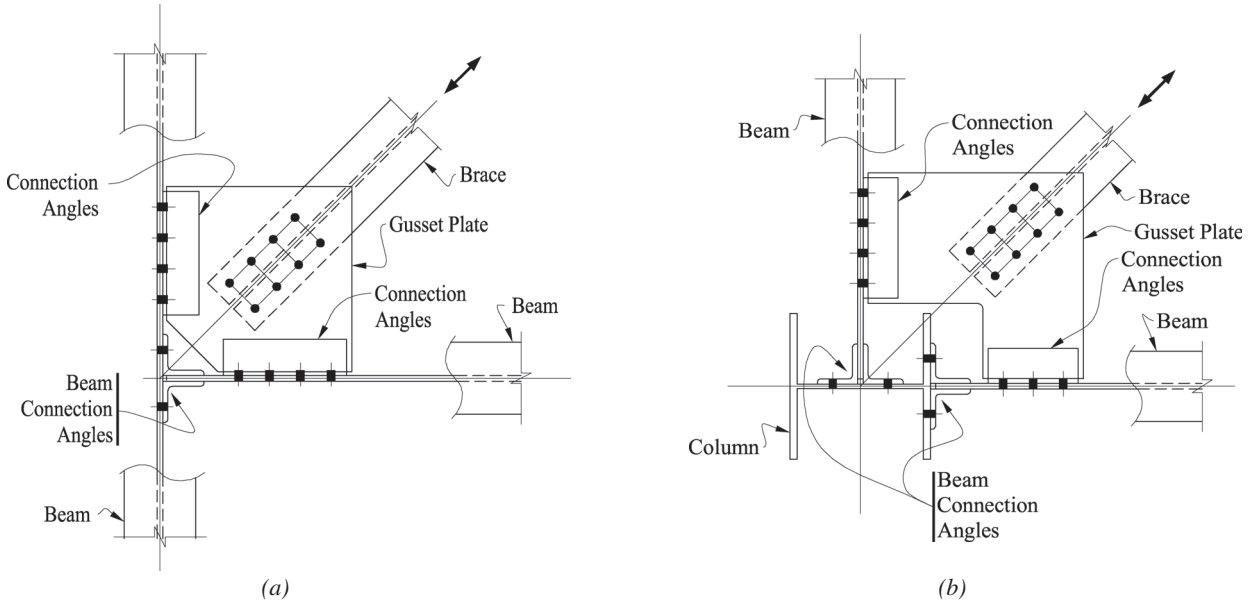

Fig. 7. Standard horizontal brace connections. (a) Beam-to-beam interface. (b) Beam-to-column interface.

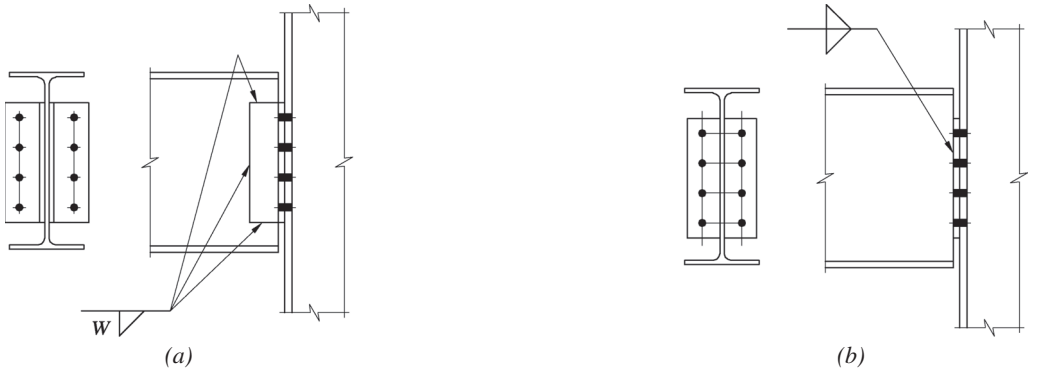

Fig. 8. Common beam connections for axial loads. (a) Double clip angle connection. (b) Shear end plate connection.

EXAMPLE 1

Example 1 shows the calculation of transfer forces in a simple structure as it would be done by hand. The structure has a horizontal bracing system at level 2 and a diaphragm at level 3, which are shown in Figures 12(b) and 12(a), respectively. Three different vertical bracing arrangements are considered. The elevations along lines A and B are identical and are shown in Figure 13 for each of the three bracing arrangements considered.

An 80-kip lateral load is applied at level 2 simultaneously with a 100-kip lateral load applied at level 3. The forces will be calculated by hand and will not include the effects of member stiffness. Standard connections will be assumed.

Figure 14 shows the forces entering the beams from the diaphragm and horizontal braces. The component from each horizontal brace is 10 kips. This load enters the beam through the standard gusset plate connection. The horizontal component of the top vertical brace is 50 kips.

Figure 15 shows the transfer forces and axial loads in the beams, which were calculated using simple statics. The transfer force across column line 2 at level 2 for each bracing arrangement are:

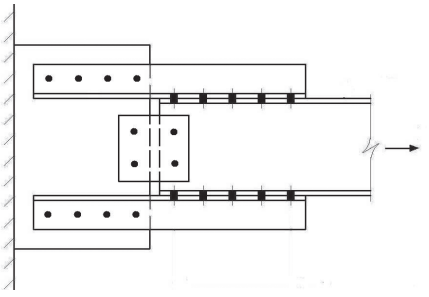

Fig. 9. Strut connection.

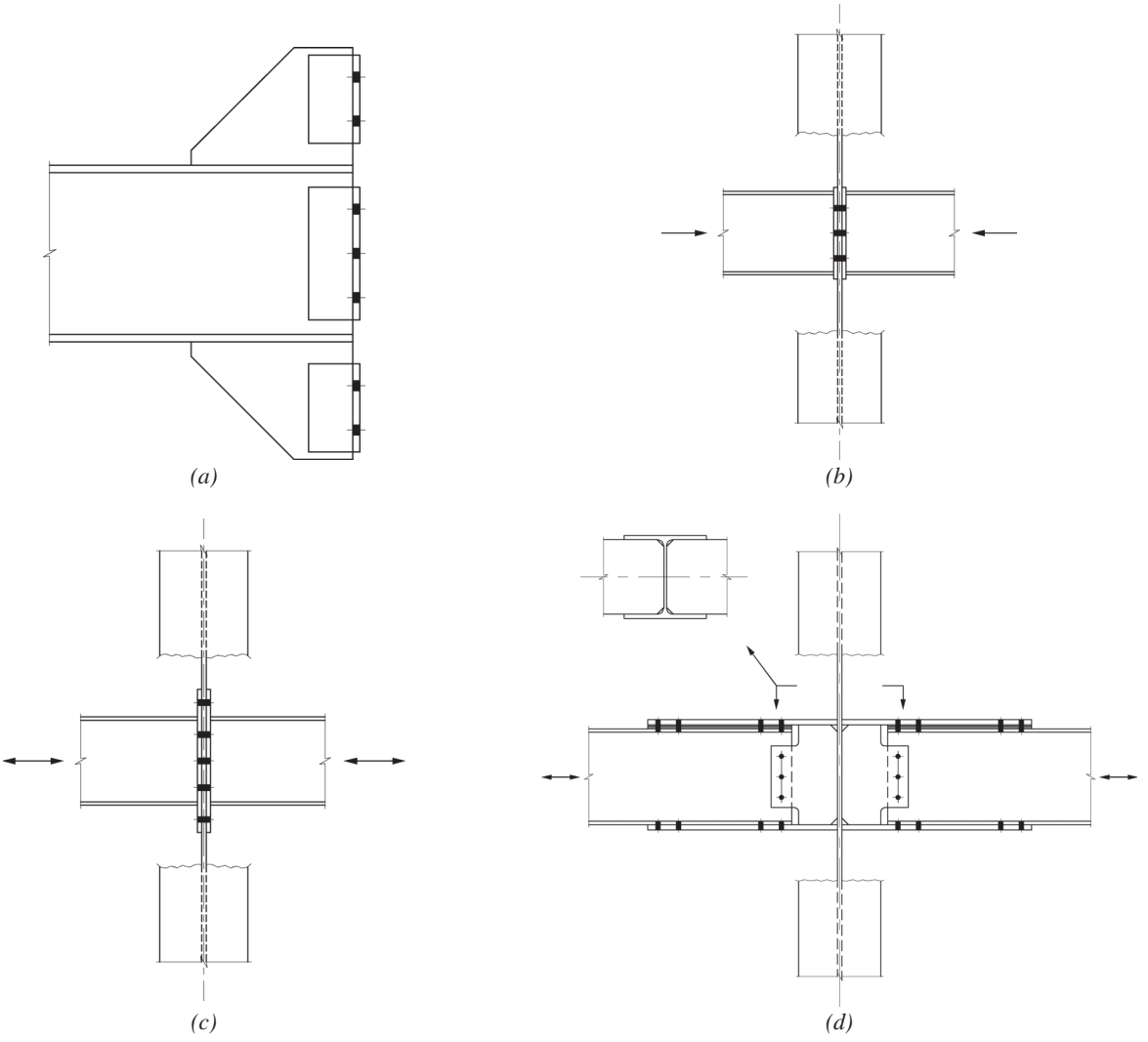

Fig. 10. Connections for very large axial loads. (a) Fin plate connection. (b) Flush end plate. (c) Extended end plate. (d) Flange plate connection.

Bracing arrangement 1
F_t = 10 kips + 10 kips = 20 kips (compression)

Bracing arrangement 2
F_t = 50 kips + 10 kips + 10 kips = 70 kips (compression)

Bracing arrangement 3
F_t = 10 kips + 10 kips + 50 kips = 70 kips (compression)

This example clearly shows that the axial load in the beam is not a good indicator of the transfer force. For bracing arrangement 3, the transfer force at level 2 and column line 2 is 70 kips, but the axial load in the beams is only 10 kips. If the axial load in the beam was used to design the beam-to-column connection, the connection would be underdesigned.

The opposite problem occurs at the same location for bracing arrangement 1. The axial load in the beam is 80 kips on one side of the column and 10 kips on the other side, but the transfer force is 20 kips. In this case, using the largest axial load instead of the transfer force would be conservative, but this could cause the connection to be much more expensive than is required.

The transfer force will be zero at column lines 1 and 3 for all three vertical bracing configurations, but the beam-to-column connections must be adequate to brace the columns against buckling. Except for structures with very high column loads, most standard connections have enough strength and stiffness to act as a brace point.

EXAMPLE 2

Example 2 shows the transfer force calculation for a joint in a large industrial structure as it would be done using the output from a finite element model. For simplicity, only one load case is considered. The node has two vertical braces and three horizontal braces, and standard connections are assumed. The structural elements and loads are shown in Figure 16.

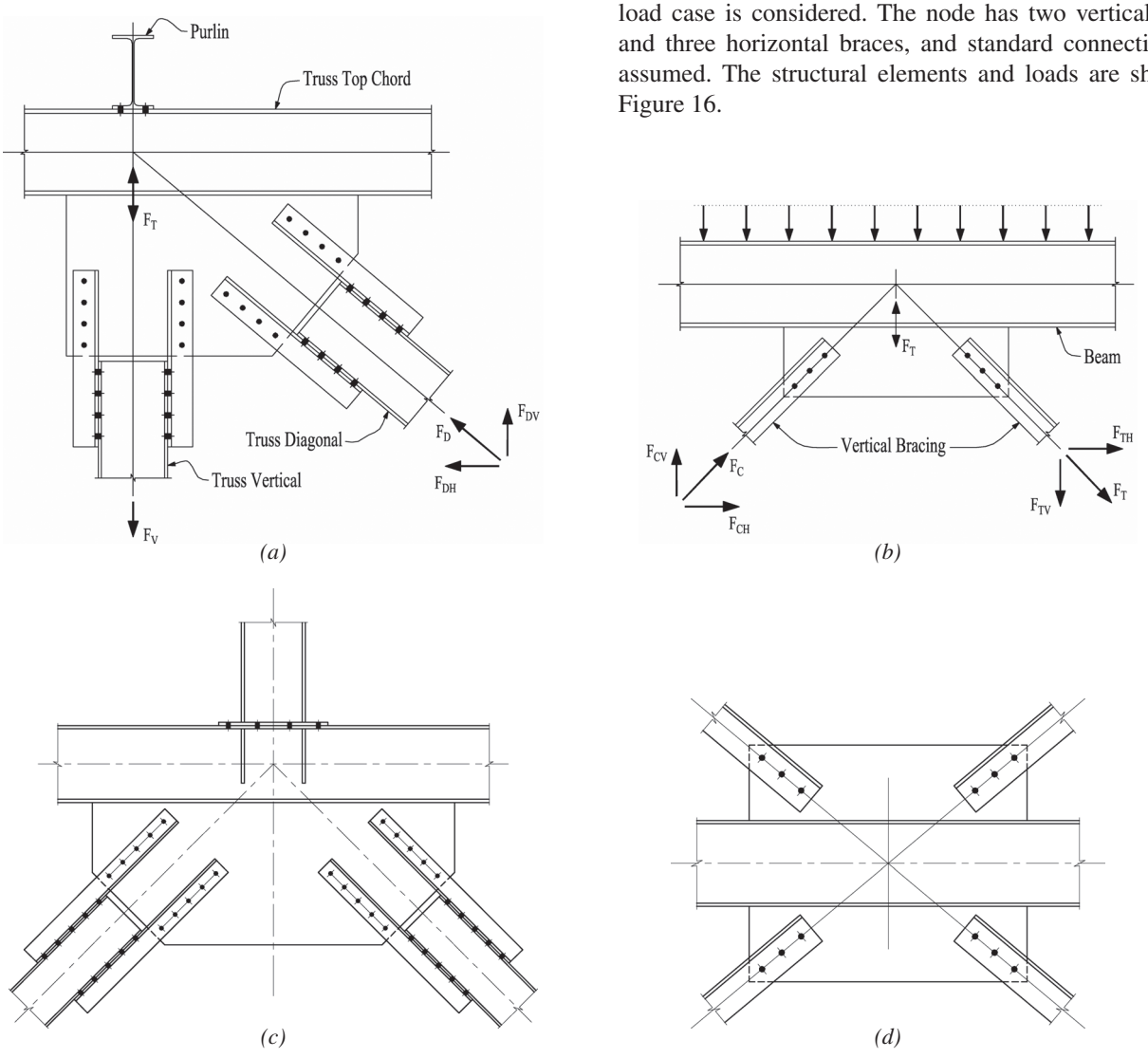

Fig. 11. Joints with vertical transfer forces. (a) Truss panel point with purlin. (b) Inverted V-brace with gravity floor load. (c) Inverted V-brace with column above. (d) Mid-point of an X-brace.

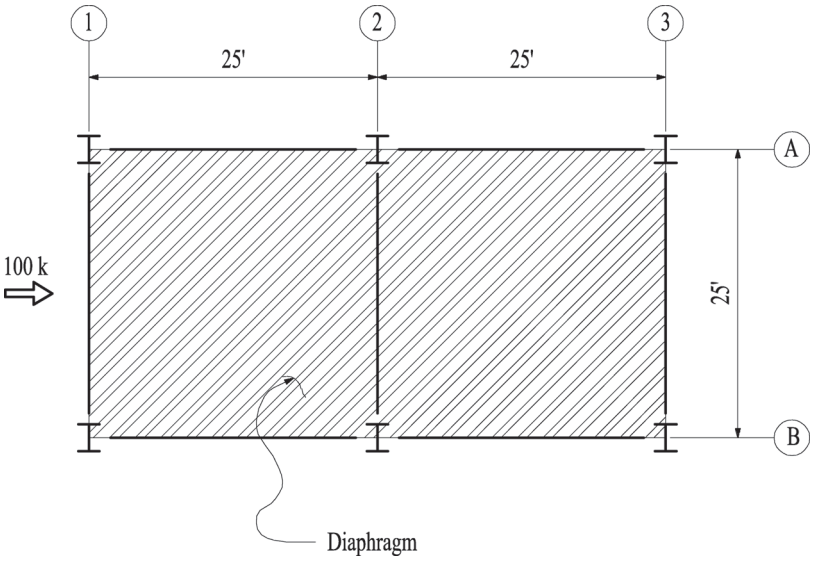

(a)

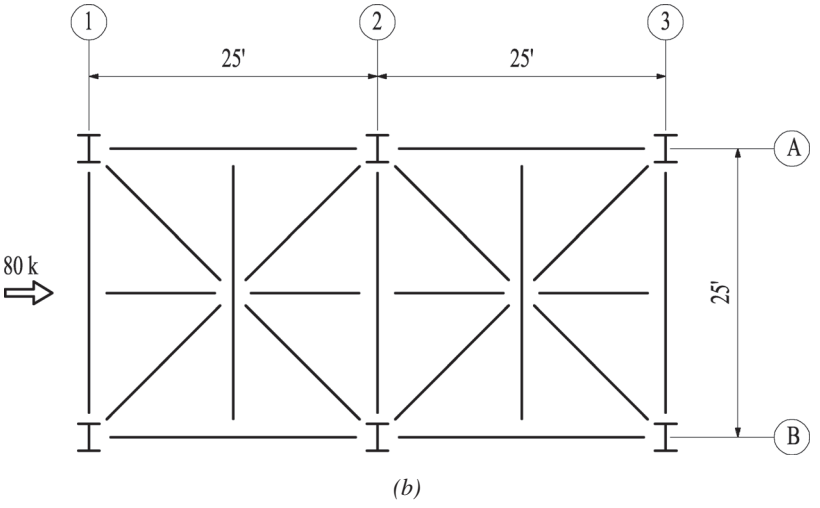

(b)

Fig. 12. Plan views of example structure. (a) Level 3. (b) Level 2.

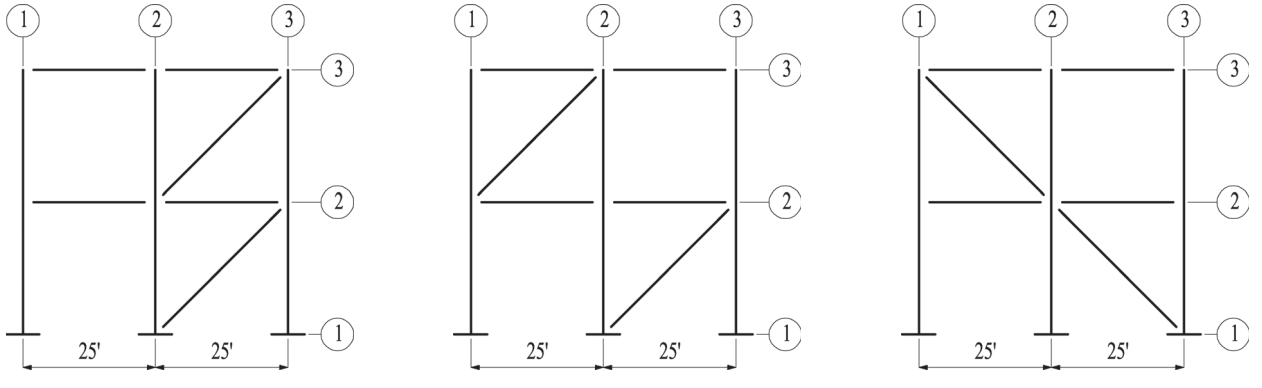

(a) *(b)* *(c)*

Fig. 13. Elevation along lines A and B. (a) Bracing arrangement 1. (b) Bracing arrangement 2. (c) Bracing arrangement 3.

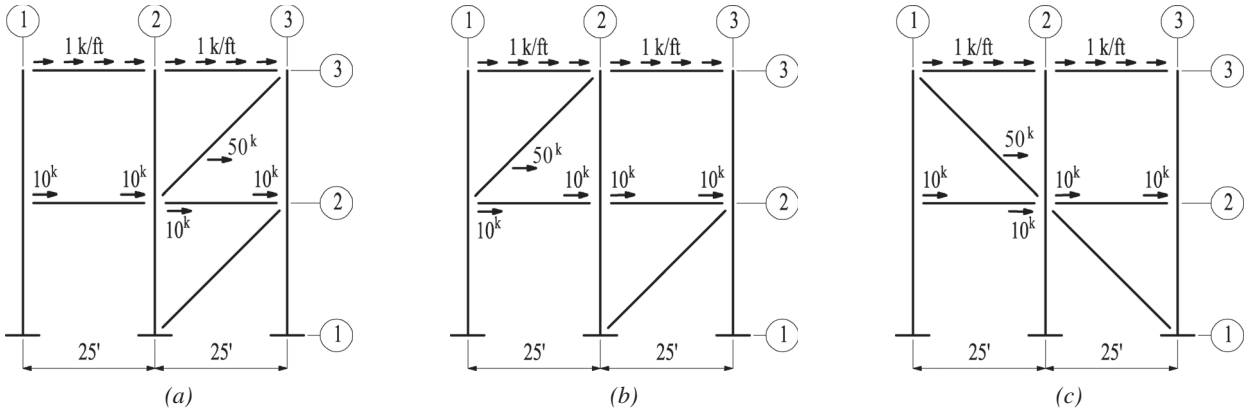

Fig. 14. Forces entering beams from diaphragm and horizontal bracing. (a) Bracing arrangement 1. (b) Bracing arrangement 2. (c) Bracing arrangement 3.

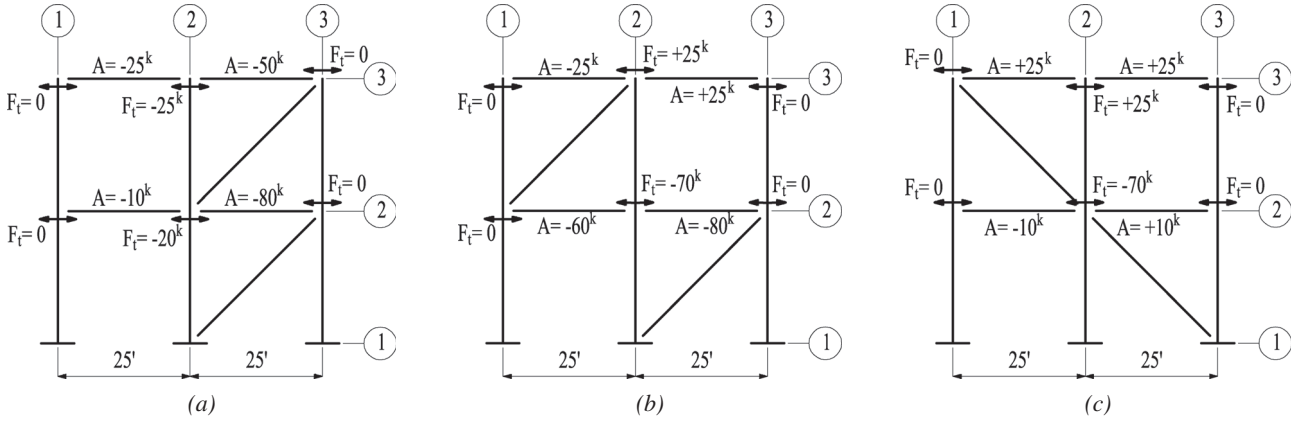

Fig. 15. Transfer forces and axial loads in beams. (a) Bracing arrangement 1. (b) Bracing arrangement 2. (c) Bracing arrangement 3.

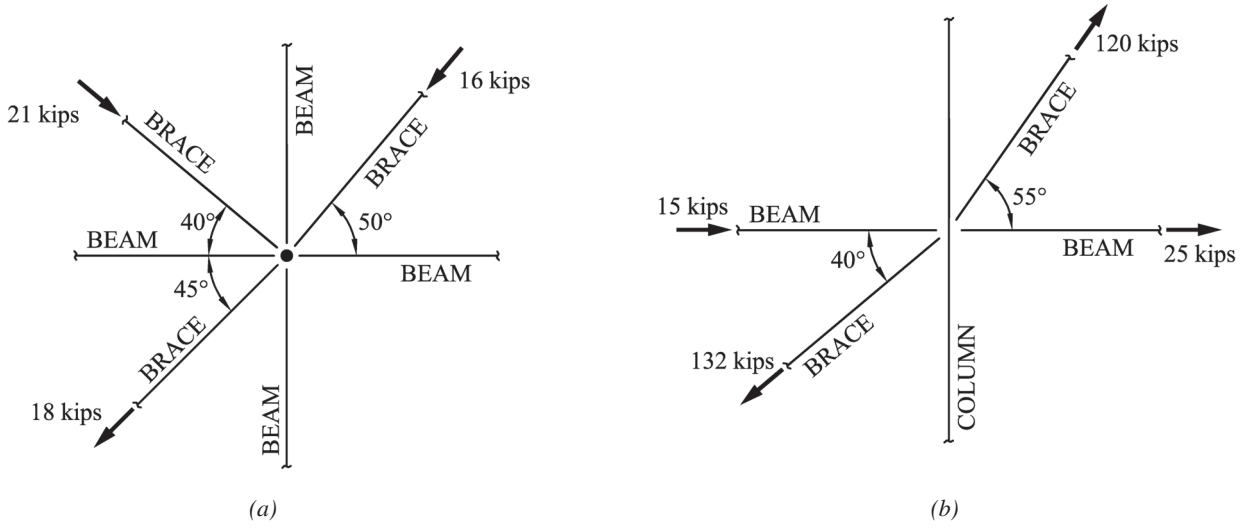

Fig. 16. Partial structure for Example 2. (a) Plan. (b) Elevation.

The net horizontal load on the right-hand side of the column is

$$F_R = 25 \text{ kips} + (120 \text{ kips})\cos(55°) - (16 \text{ kips})\cos(50°)$$
$$= 83.5 \text{ kips}$$

The net horizontal load on the left-hand side of the column is

$$F_L = -15 \text{ kips} + (132 \text{ kips})\cos(40°) + (18 \text{ kips})\cos(45°) - (21 \text{ kips})\cos(40°)$$
$$= 82.7 \text{ kips}$$

Note that F_R and F_L will be equal and opposite if the column is pinned at the node; however, if the column is modeled as a continuous member, some of the load will transfer into the column causing flexural stresses. For design purposes, the transfer force can be the largest of F_R and F_L; therefore, the transfer force is 83.5 kips.

CONCLUSIONS

For connections to be designed properly, transfer forces must be communicated to the connection designer. General guidance was provided on nonstandard beam-to-column connections that can accommodate large transfer forces, and the importance of providing vertical transfer forces in special situations was discussed. Two examples were provided—one showing the basic calculation procedure and one showing the procedure for calculating transfer forces from computer output. These examples were very simple, but for most real structures, the determination of transfer forces can be a time-consuming, but essential step in the design of safe and economical structures.

REFERENCES

AISC (2005), *Steel Construction Manual*, 13th Ed., American Institute of Steel Construction, Chicago, IL.

Thornton, W.A. (1984), "Bracing Connections for Heavy Construction," *Engineering Journal*, 3rd quarter, American Institute of Steel Construction, Chicago, IL.

Williams, G.C. (1986), "Steel Connection Designs Based on Inelastic Finite Element Analysis," Doctoral Dissertation, The University of Arizona.

Limit States for Horizontal Shear at a Braced Frame Beam Flange

BRENT E. HUNGERFORD

ABSTRACT

The most common design methodologies for bracing connections are based on the lower bound theorem. If the lower bound theorem is the basis cited for a steel connection design, the theorem's requirements must be satisfied. While the ductility requirement is essential to the theorem, it is the implications of the equilibrium and material strength limit requirements that will be investigated here for a portion of a common load path in a braced frame connection. Two limit states will be outlined that precisely define and expand on a limit state for web horizontal yielding. The limit states are also applicable to other types of connections with similar loading and geometry. These limit states are rational approaches to ensure that adequate resistance is provided to critical portions of a commonly assumed load path for braced frame connections. The limits likely will not control many typical braced frame configurations, but several conditions in which they may govern have been outlined for consideration. Additionally, it has been shown that it may be too conservative to require that all horizontal force from the gusset plate be transferred by shear into the beam web within the length of the gusset connection, although there are defined limits to the local beam capacity that can be obtained in these connections.

Keywords: beam flange, horizontal shear, limit states.

The most common design methodologies for bracing connections are based on the lower bound theorem, based on the author's experience and observations. For example, the Uniform Force Method is recommended by AISC for bracing connections (AISC, 2005), and it is an application of the lower bound theorem. Also, the KISS method, a common alternate method, is also an application of the lower bound theorem. If the lower bound theorem is the basis cited for a steel connection design, the theorem's requirements must be satisfied. While the ductility requirement is essential to the theorem, it is the implications of the equilibrium and material strength limit requirements that will be investigated here for a portion of a common load path in a braced frame connection. In this portion of the load path, two limit states will be outlined that precisely define and expand on a limit state for web horizontal yielding described by Thornton (Tamboli, 1999). The limit states are also applicable to other types of connections with similar loading and geometry.

CONNECTION CONFIGURATION AND LOAD PATH

Consider the braced frame connection shown in Figure 1. Here a gusset plate is directly welded to the top flange of a beam, and that weld will be expected to transfer some combination of shear, axial load and moment.

Of the resisted loads, shear is frequently a dominant component because a large portion of the horizontal component of the brace force is typically required to be transferred at the gusset-to-beam weld. The forces to be transferred in the braced frame connection are shown in Figure 2(a), and the horizontal forces are isolated and labeled in Figure 2(b). Refer to Part 13 of the *Steel Construction Manual* (AISC, 2005) for forces not labeled.

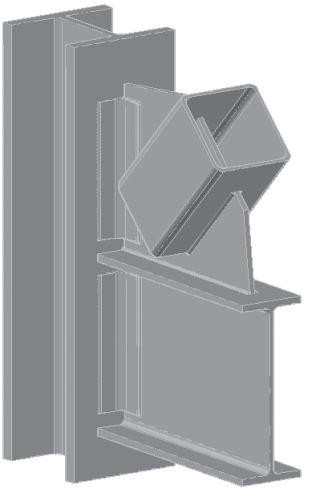

Fig. 1. Connection configuration for a braced frame.

Brent E. Hungerford, P.E., Associate, Walter P Moore and Associates, Tampa, FL. E-mail: bhungerford@walterpmoore.com

It is expected for member design that the axial load from the beam end connection and shear from the gusset connection will distribute uniformly in the beam cross section at a distance away from the connection. The lower bound theorem requires an engineer to ensure this load path has adequate resistance by investigating equilibrium and material strength limit states between the gusset-to-beam weld and the beam section at a distance away from the connection. To make certain that the assumed load path has adequate resistance, two rational limit states for load transfer at critical sections of the beam are developed using the basic AISC equations for shear [2005 *Specification* Equation J4-3, $\phi R_n = (1.0)(0.60)F_y A_s$] and axial resistance [2005 *Specification* Equation J4-1, $\phi R_n = 0.9F_y A_s$] in a connection. Both limits should be checked in order to verify that the gusset-to-beam connection has adequate length for load transfer into the beam.

Limit State 1: Web Shear Yielding and Axial Yielding of the Top Flange and k-Area (see Figure 3)

Much of the horizontal load transferred from the gusset to the beam must also pass through the top edge of the beam web. However, some load will remain in the top flange and k-area based on an assumed uniform stress distribution in the beam cross section away from the connection. The load that must transfer to the beam web in excess of the web shear capacity along the connection length must initially be transmitted as axial load in the top flange and k-area of the beam. Then, away from the connection along the beam length, the excess load is expected to migrate by shear from the top flange and k-area into the beam web in order to attain a uniform stress distribution. In this event, the top flange and k-area may be compared to a collector beam, dragging load into the beam web away from connection. If the axial capacity of the top flange and k-area is less than needed for the required axial load, the gusset-to-beam connection must be lengthened or the beam reinforced. This limit state is intended to preclude a failure that may be analogous to block shear rupture: there is a portion of the steel member that may fail with shear along one edge and axial load on its perpendicular edge. A comparable failure mode was indicated by Epstein and D'Aiuto (2002) in their Figure 2(c), reproduced here as Figure 4.

Limit State 1 for web shear yielding and axial yielding of the top flange and k-area is developed in the following manner (refer to Figure 5 for variable definitions):

1. Determine the maximum possible resistance that the top flange and k-area, A_{f+k}, can provide by axial yielding.
2. Determine the minimum connection length, L_c, needed to provide the balance of the required force resistance by beam web shear.

$$\phi R_{n,w+f+k} \geq H_{ub} \tag{1}$$

$$\phi V_{n,w} + \phi P_{n,f+k} \geq H_{ub}$$

$$(1.0)(0.6)F_y L_c t_w + 0.9F_y A_{f+k} \geq H_{ub} \tag{2}$$

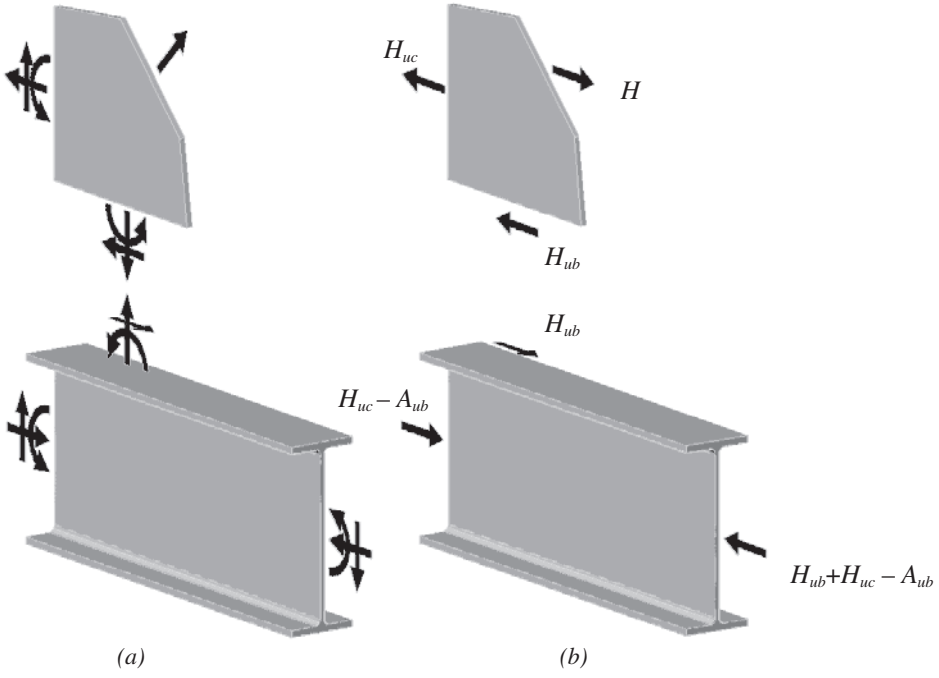

Fig. 2. Free-body diagrams for forces on (a) gusset plate and beam and (b) only horizontal forces on gusset plate and beam.

where

$$A_{f+k} = 0.5\left[A_g - t_w\left(d - 2k_{des}\right)\right]$$

Minimum connection length format:

$H_{ub} - 0.9F_yA_{f+k} \le 0$:

$$L_{c,\min,w} = 0 \quad (3)$$

$H_{ub} - 0.9F_yA_{f+k} > 0$:

$$L_{c,\min,w} \ge \frac{H_{ub} - 0.9F_yA_{f+k}}{0.6F_yt_w} \quad (4)$$

The use of Equation 3 would indicate that the connection length is not governed by horizontal shear of the beam web because the top flange and k-area has sufficient capacity to drag the required force into the web beyond the connection length.

Limit State 2: Shear Yielding of Flanges (see Figure 6)

If the horizontal load to be transferred to the beam exceeds the web shear capacity over the gusset-to-beam connection length, the balance of the load must be resisted by axial load in the top flange and k-area of the beam. To achieve the required load distribution in the top flange and k-area, some axial load may need to distribute beyond the toes of the fillets

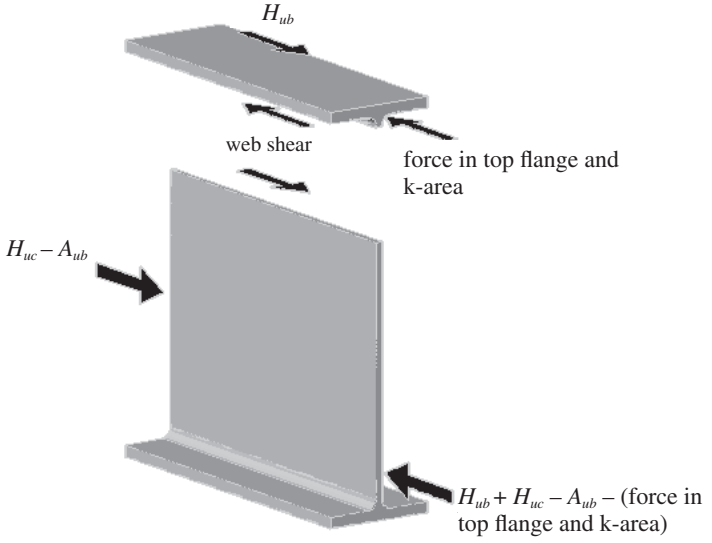

Fig. 3. Horizontal forces with section cut at beam web.

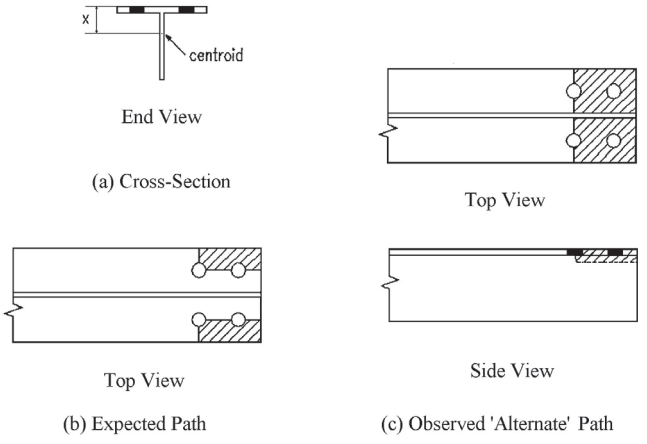

Fig. 4. Block shear paths in structural tees (Epstein and D'Aiuto, 2002).

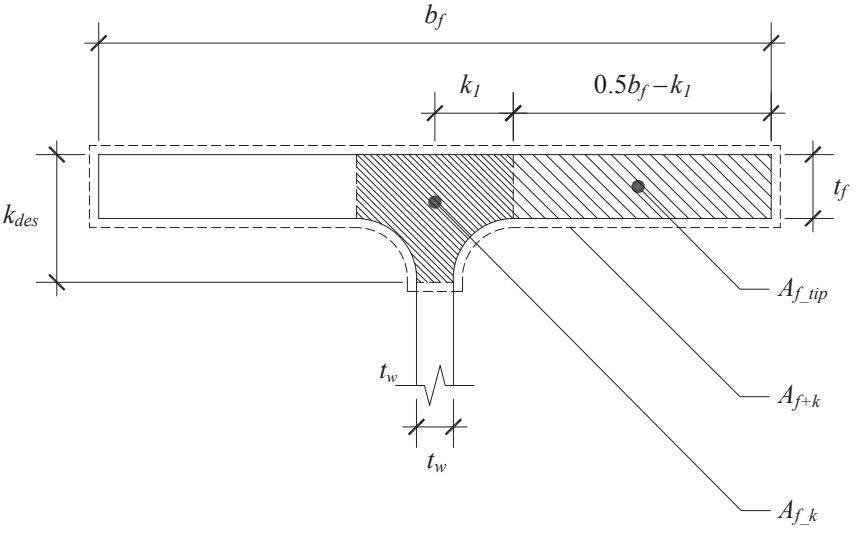

Fig. 5. Top flange cross-section variables for Limit States 1 and 2.

on the flange. The axial load must distribute to this area over the length of the gusset-to-beam connection, and so the shear capacity of the flange must be capable of transferring this load. If the flange shear capacity is less than required, the gusset-to-beam connection must either be lengthened or the beam reinforced.

Limit State 2 for the shear yielding of flanges is developed in the following manner (refer to Figure 5 for variable definitions):

1. Determine the minimum axial force required to be resisted in the beam flange tips, A_{f_tip}, at the end of the connection length. This is horizontal force in the beam, less the maximum possible resistance by beam web shear over the connection length and axial yielding in the top flange k-area, A_{f_k}.
2. Determine the minimum connection length needed to transmit the required axial load to the beam flange tips by beam flange shear.

$$\phi V_{n,f\_tips} \geq P_{u,f\_tips,\min} \tag{5}$$

$$2(1.0)(0.6)F_y L_c t_f \geq P_{u,f+k,\min} - P_{u,f\_k,\max}$$

$$2(1.0)(0.6)F_y L_c t_f \geq P_{u,f+k,\min} - 0.9F_y A_{f\_k} \tag{6}$$

where

$$P_{u,f+k,\min} = H_{ub} - (1.0)(0.6)F_y L_c t_w$$
$$A_{f\_k} = A_{f+k} - 2A_{f\_tip}$$
$$A_{f\_tip} = t_f\left(0.5b_f - k_1\right)$$

Minimum connection length format:

$H_{ub} - 0.9F_y A_{f\_k} \leq 0$:

$$L_{c,\min,f} = 0 \tag{7}$$

$H_{ub} - 0.9F_y A_{f\_k} > 0$:

$$L_{c,\min,f} \geq \frac{H_{ub} - 0.9F_y A_{f\_k}}{0.6F_y\left(2t_f + t_w\right)} \tag{8}$$

The use of Equation 7 would indicate that the connection length is not governed by horizontal shear of the beam flange because the top flange k-area alone has sufficient axial capacity to drag the required force into the web beyond the connection length.

ADDITIONAL COMMENTS

Net Section Capacity

In both of the limit states previously described, the effect of net section on the shear and tension areas should be incorporated into design calculations. That is, the gross area minus the area of the bolt holes, copes and blocking of flange tips should be reflected in the input dimensions. It is also suggested to use the resistance factor and material limit for shear and tension rupture—0.75 and ultimate stress, respectively (AISC, 2005)—when material is removed from the failure planes. When beam material is removed from the failure planes and the brace in Figure 1 is in compression, Limit State 1 appears to address a failure very similar to the block shear failure observed by Epstein and D'Aiuto (2002).

Are These Limit States Significant?

If the assumed load path requires horizontal shear transfer at a beam flange, the flange and web must have adequate material strength to resist the loads that satisfy equilibrium. The limit states described here are intended to address conceivable failure modes on this load path. Therefore, they are suggested to be considered and applied to braced frame and similarly configured connections. Typically sized connection configurations for braced frames will not often have these limit states govern unless material is removed from the top flange or web of the beam in the vicinity of the connection. Furthermore, it may be excessively conservative to require that the length of the gusset connection be such that all the horizontal force from the gusset plate is transferred to the beam web over that length because the substantial axial capacity of the top flange and k-area is neglected.

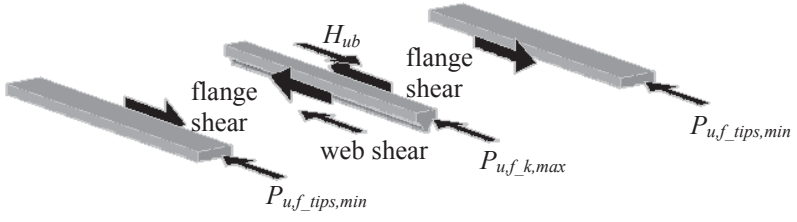

Fig. 6. Horizontal forces with section cuts at beam flange.

Although perhaps uncommon, there are conditions that may cause these limit states to govern. Several of these conditions are listed here:

1. High horizontal shear at the gusset-to-beam connection:
   - The braced frame beam is near yielding due to the brace force.
   - The brace connection is to column web rather than column flange.
   - There is no brace connection to the column.
   - The brace angle to the horizontal is small.
   - The KISS method is used.
2. Short gusset-to-beam connection:
   - The ratio of the gusset plate yield strength to the beam yield strength is greater than 36 to 50 ksi.
   - The gusset plate is very thick.
   - There is an architectural or spatial constraint.
3. Braced frame beams that are not rolled wide flange sections:
   - The braced frame beam is a hollow structural section (HSS).
   - The braced frame beam is a built-up section.
4. Material removed from the braced frame beam:
   - The top flange of the braced frame beam is coped.
   - The top flange tips are coped to fit beam between column flanges.
   - The top flange tips are blocked to allow a double-angle connection that is continuous across the gusset plate and beam web.
   - There are bolt holes within the gusset connection length in the beam top flange or web.

DESIGN EXAMPLE

AISC *Manual*, 13th Ed., Example II.C-2 (see Figure 7)

Given

W18×106 beam:

A_g = 31.1 in.^{2}
d = 18.7 in.
b_f = 11.2 in.
t_f = 0.94 in.
t_w = 0.59 in.
k_{des} = 1.34 in.
k_1 = 1.125 in.
F_y = 50 ksi
L_c = 42 in.
H_{ub} = 355 kips

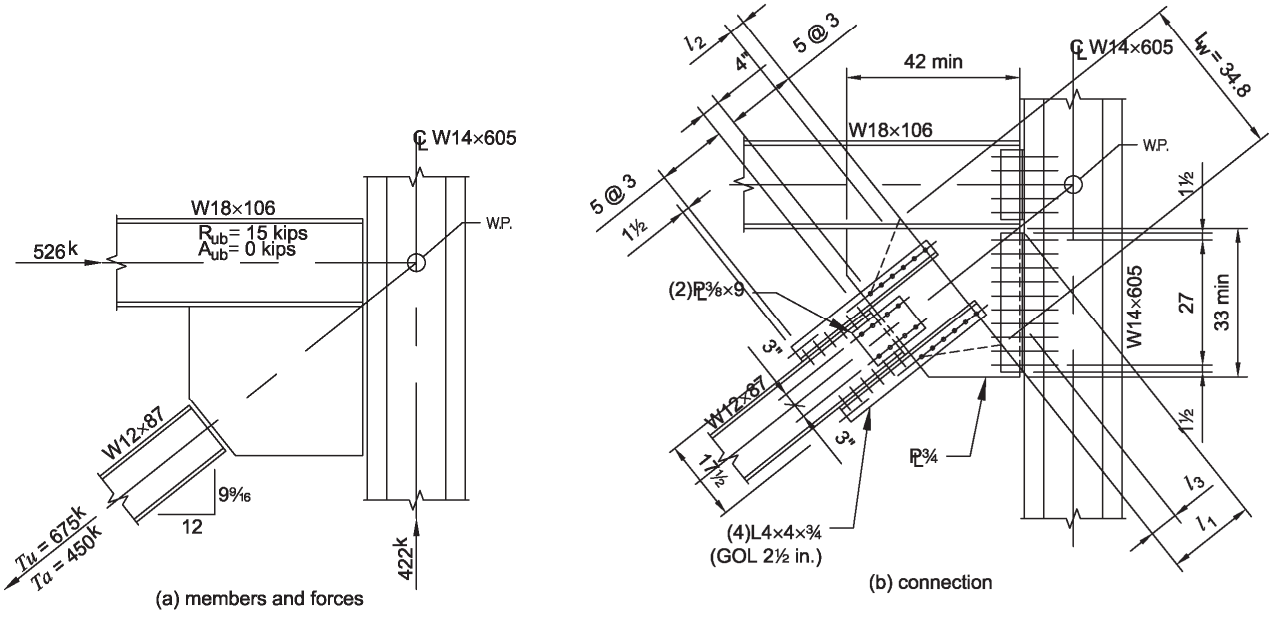

Fig. 7. AISC Manual, 13th Ed., Example II.C-2.

Area of the flange and k-area:

$$A_{f+k} = 0.5\left[A_g - t_w\left(d - 2k_{des}\right)\right]$$

$$A_{f+k} = 0.5\left\{31.1 \text{ in.}^2 - (0.59 \text{ in.})\left[18.7 \text{ in.} - 2(1.34 \text{ in.})\right]\right\}$$

$$A_{f+k} = 10.8 \text{ in.}^2$$

Area of the flange tip:

$$A_{f\_tip} = t_f\left(0.5b_f - k_1\right)$$

$$A_{f\_tip} = (0.94 \text{ in.})\left[0.5(11.2 \text{ in.}) - 1.125 \text{ in.}\right]$$

$$A_{f\_tip} = 4.21 \text{ in.}^2$$

Area of the k-area:

$$A_{f\_k} = A_{f+k} - 2A_{f\_tip}$$

$$A_{f\_k} = 10.8 \text{ in.}^2 - 2\left(4.21 \text{ in.}^2\right)$$

$$A_{f\_k} = 2.38 \text{ in.}^2$$

Limit State 1:

$$\phi R_{n,w+f+k} \geq H_{ub}$$

$$\phi V_{n,w} + \phi P_{n,f+k} \geq H_{ub}$$

$$(1.0)(0.6)F_y L_c t_w + 0.9F_y A_{f+k} \geq H_{ub}$$

$$(1.0)(0.6)(50 \text{ ksi})(42 \text{ in.})(0.59 \text{ in.}) + 0.9(50 \text{ ksi})\left(10.8 \text{ in.}^2\right) \geq 355 \text{ kips}$$

1230 kips ≥ 355 kips **o.k.**

Minimum axial load in the flange and k-area:

$$P_{u,f+k,\min} = H_{ub} - \left(1.0\right)\left(0.6\right)F_y L_c t_w$$

$$P_{u,f+k,\min} = 355 \text{ kips} - (1.0)(0.6)(50 \text{ ksi})(42 \text{ in.})(0.59 \text{ in.})$$

$$P_{u,f+k,\min} = -388 \text{ kips} \rightarrow P_{u,f+k,\min} = 0 \text{ kips}$$

Minimum axial load required to be in the flange tips:

$$P_{u,f+k,\min} = 0 \text{ kips} \rightarrow P_{u,f\_tips,\min} = 0 \text{ kips}$$

Limit State 2:

$$\phi V_{n,f\_tips} \geq P_{u,f\_tips,\min}$$

$$2(1.0)(0.6)F_y L_c t_f \geq P_{u,f\_tips,\min}$$

$$2\left(1.0\right)\left(0.6\right)\left(50 \text{ ksi}\right)\left(42 \text{ in.}\right)\left(0.94 \text{ in.}\right) \geq 0 \text{ kips}$$

2369 kips ≥ 0 kips **o.k.**

Both Limit State 1 (capacity 1,230 kips) and Limit State 2 (capacity 2,369 kips) are satisfied because the resistance of each significantly exceeds the required horizontal force of 355 kips. The same conclusion may be reached by verifying that the design connection length, L_c, exceeds both minimum connection lengths $L_{c,\min,w}$ and $L_{c,\min,f}$. Those calculations are performed next.

Minimum connection length based on maximum axial capacity of flange and k-area (Limit State 1):

$$L_c \geq L_{c,\min,w}$$

$$L_c \geq \frac{H_{ub} - 0.9F_y A_{f+k}}{0.6F_y t_w}$$

$$42 \text{ in.} \geq \frac{355 \text{ kips} - 0.9(50 \text{ ksi})\left(10.8 \text{ in.}^2\right)}{0.6(50 \text{ ksi})(0.59 \text{ in.})}$$

42 in. ≥ –7.40 in. → $L_{c,\min,w} = 0$ in. **o.k.**

Minimum connection length based on maximum shear capacity of web and maximum axial capacity of the k-area (Limit State 2):

$$L_c \geq L_{c,\min,f}$$

$$L_c \geq \frac{H_{ub} - 0.9F_y A_{f\_k}}{0.6F_y\left(2t_f + t_w\right)}$$

$$42 \text{ in.} \geq \frac{355 \text{ kips} - 0.9(50 \text{ ksi})\left(2.38 \text{ in.}^2\right)}{0.6(50 \text{ ksi})\left[2(0.94 \text{ in.}) + 0.59 \text{ in.}\right]}$$

42 in. ≥ 3.35 in. **o.k.**

The design connection length of 42 in. is much more than both $L_{c,\min,w}$ (0 in.) and $L_{c,\min,f}$ (3.35 in.), and so the connection as detailed is sufficiently long. The calculated minimum connection length $L_{c,\min,w}$ is negative, indicating that the axial capacity of the flange and k-area alone exceeds the applied horizontal force. As a result, the flange and k-area may drag shear into the web over the necessary beam length as determined by the web shear capacity.

Additionally, if the length of the gusset to beam connection were limited by requiring that all horizontal force from the brace must transfer to the beam web over the connection length, the resulting connection length would be:

$$L_c = \frac{H_{ub}}{(1.0)(0.6)F_y t_w}$$

$$L_c = \frac{355 \text{ kips}}{(1.0)(0.6)(50 \text{ ksi})(0.59 \text{ in.})}$$

$$L_c = 20.1 \text{ in}$$

This connection length, when only considering beam web shear, is six times the length required when the axial capacity of the top flange and k-area is considered.

CONCLUSION

The two limit states suggested here are rational approaches to ensure that adequate resistance is provided to critical portions of a commonly assumed load path for braced frame connections. The applicability of the two limit states is derived from the requirements of the lower bound theorem on which common connection design methodology is based. The limits likely will not control many typical braced frame configurations, but several conditions in which they may govern have been outlined for consideration. Additionally, it has been shown that it may be too conservative to require that all horizontal force from the gusset plate be transferred by shear into the beam web within the length of the gusset connection, but also there are defined limits to the local beam capacity that can be obtained in these connections.

NOTATION

A_g = gross cross-section area of a wide flange beam

A_{f+k} = area of the flange and k-area of a wide flange beam

A_{f_k} = k-area of a wide flange beam

A_{f_tip} = cross-section area of the flange tip beyond the toe of the fillet on the flange

A_{ub} = required transfer force from the adjacent bay

d = depth of a wide flange beam

t_w = web thickness of a wide flange beam

t_f = flange thickness of a wide flange beam

b_f = flange width of a wide flange beam

k_{des} = design fillet dimension along the web of the wide flange beam

k_1 = fillet dimension along the flange of the wide flange beam

L_c = length of the gusset-to-beam connection

$L_{c,\min,w}$ = minimum length of the gusset-to-beam connection required for web shear transfer without reinforcement

$L_{c,\min,f}$ = minimum length of the gusset-to-beam connection required for flange shear transfer without reinforcement

F_y = beam yield stress

H = horizontal component of the required brace axial force

H_{ub} = horizontal force transferred from the gusset plate to the beam

H_{uc} = horizontal force transferred from the gusset plate to the column

$P_{u,\, f\_tips,\, \min}$ = minimum axial force on the cross-section area of the flange tip beyond the toe of the fillet on the flange of a wide flange beam

$P_{u,f\_k,\, \max}$ = maximum axial force on the k-area of a wide flange beam

$P_{u,f+k,\, \min}$ = minimum axial force on the area of the flange and k-area of a wide flange beam

$\phi P_{n,f+k}$ = design axial strength of the flange and k-area of a wide flange beam

$\phi R_{n,w+f+k}$ = design strength for Limit State 1: design shear strength of the web along the length of the gusset-to-beam connection and axial strength of the flange and k-area

$\phi V_{n,f\_tips}$ = design strength for Limit State 2: design shear strength of the flange tips along the length of the gusset-to-beam connection

$\phi V_{n,w}$ = design shear strength of the web along the length of the gusset-to-beam connection

REFERENCES

AISC (2005), *Steel Construction Manual*, 13th Ed., American Institute of Steel Construction, Chicago, IL.

Epstein, H.I. and D'Aiuto, C.L. (2002), "Using Moment and Axial Interaction Equations to Account for Moment and Shear Lag Effects in Tension Members," *Engineering Journal*, AISC, 2nd Quarter, pp. 91–99.

Tamboli, A.R. (1999), *Handbook of Structural Steel Connection Design and Details*, McGraw-Hill Companies, New York.

An Experimental Analysis of Strength and Ductility of High-Strength Fasteners

AMY M. MOORE, GIAN A. RASSATI, and JAMES A. SWANSON

ABSTRACT

A total of 1,533 structural bolts, consisting of four different bolt grades and six different diameters, up to 5 in. long, were tested in direct tension and shear with the threads excluded and not excluded from the shear plane. Thread lengths, tensile and shear strength, and elongation at failure were measured. The experimental values were then compared to the requirements of the current AISC, RCSC, and ASTM specifications. This paper presents and discusses the results of the experimental tests and of the subsequent comparisons. It is concluded that all fasteners tested meet the minimum strength required by ASTM and RCSC. Furthermore, it is noted that while the strength in tension and in shear with the threads excluded from the shear plane are conservatively assessed by AISC specifications, the strength with the threads not excluded from the shear plane is often not conservatively predicted. As a consequence, an alternative expression for the shear strength with the threads not excluded from the shear plane is proposed. It is also concluded that the actual thread length can be different than the nominal values, potentially affecting the available cross section in shear. Finally, the measurement of the elongation at failure shows that all grades of fastener tested have a satisfactorily ductile behavior.

Keywords: structural bolts, threads excluded, threads included, shear strength, fastener ductility.

INTRODUCTION

High-strength structural bolts started becoming more economical in steel connections, completely replacing the use of rivets, during the 1950s. Installation of rivets required more and more trained manpower and more equipment, compared to that of high-strength bolts, which also offered more strength. The Research Council on Structural Connections (RCSC) was formed in 1947, with the main focus of a rapid development of high-strength fasteners in the United States. American Society of Testing and Materials (ASTM) designation A325 was approved in 1949 and revised in 1951 as a tentative specification for the material for high-strength bolts (Fisher and Beedle, 1967).

Based on Load and Resistance Factor Design, today's engineers are required to account for at most 75% of the bolt's tension and shear strength (AISC, 2005). Based on preliminary analyses on existing data in literature, supported by previous studies (Fischer et al., 1978), the authors believe that the resistance factor of 0.75 is not the direct result of a reliability analysis, but it is rather based on a perceived lack of ductility and on insecurities about consistent strength of fasteners and uncertainties about the force distribution among bolts in connections. This is particularly true for higher-grade bolts. The main goal of this research is to provide a more accurate statistical basis for the calibration of resistance factors for high-strength bolts in order to ensure a safe and potentially more economical design of bolted connections. This was achieved by testing a meaningful, statistical population of A325, F1852, A490, and F2280 bolts in direct tension and in shear, and then calculating resistance factors based on reliability indices and statistical reduction. Some of these results are summarized herein, and a full discussion on resistance factor calculations can be found in (Moore, 2007; Moore et al., 2008). Tensile and shear strengths were compared to the American Institute of Steel Construction *Specification for Structural Steel Buildings* equations (hereafter AISC *Specification;* AISC, 2005), and thread length and elongation at failure were also investigated. In the following, these results are presented and discussed, and some conclusions are drawn.

Amy M. Moore, Bridge/Structural Engineer, LJB Inc., Dayton, OH. E-mail: amoore@ljbinc.com

Gian A. Rassati, Assistant Professor, Department of Civil and Environmental Engineering, University of Cincinnati, Cincinnati, OH. E-mail: gian.rassati@uc.edu

James A. Swanson, Associate Professor, Department of Civil and Environmental Engineering, University of Cincinnati, Cincinnati, OH. E-mail: james.swanson@uc.edu

TENSILE AND SHEAR STRENGTH OF HIGH-STRENGTH FASTENERS

To determine the tensile strength of structural bolts, an effective area, calculated from the mean of the mean root and

pitch diameters, is used, because the threads are the weakest section of the fastener. The effective area is given by

$$A_{eff} = \frac{\pi}{4}\left(d - \frac{0.9743}{n}\right)^2 \quad (1)$$

where d is the nominal bolt diameter, and n is the thread pitch, i.e., the number of threads per inch in the fastener (ASTM F606-07, 2007).

Using the effective area, the nominal tensile strength of a structural bolt is given according to Kulak et al. (2001) as

$$R_n = F_u A_{eff} = F_u\left[\frac{\pi}{4}\left(d - \frac{0.9743}{n}\right)^2\right] \quad (2)$$

where F_u is the ultimate strength of the bolt material.

For easier design purposes, the effective area can be estimated as 75% of the nominal cross-sectional area of the shank, which is conservative for most sizes of structural bolts. AISC specifications follow a slightly different approach, by using nominal tensile stress values F_{nt} calculated as 75% of the tensile strength of the bolt material. Modifying the tensile strength of the bolt material allows the nominal area of the bolt shank to be used in the design calculations. Therefore, based on Section J.3.6 of the AISC *Specification* (AISC, 2005), the nominal tensile strength of a high-strength bolt is given by

$$R_n = F_{nt}A_b = \left(0.75F_u\right)A_b = \left(0.75\right)F_u\left(\frac{\pi d^2}{4}\right) \quad (3)$$

where A_b is the nominal bolt area.

In both Equations (2) and (3), F_u is the nominal tensile strength of the bolt material, which equals 120 ksi for A325 and F1852 bolts and 150 ksi for A490 and F2280 bolts. ASTM specifications provide a minimum strength value of 105 ksi instead of 120 ksi for A325 fasteners having a diameter larger than 1 in. None of the A325 bolts tested, including 1⅛-in. and 1¼-in.-diameter bolts, resulted in a strength below 120 ksi, thus the lower value is not considered herein.

As for shear, it has been shown in literature that the strength of a single fastener with the threads excluded from the shear plane is approximately equal to 62% of the tensile strength of the bolt regardless of the bolt grade (Kulak et al., 2001). It should be noted that this value was determined based on bolts tested in double shear in a tension jig. A modification factor of 0.80 is applied in the current specifications to accommodate configurations of fasteners in shear joints up to 50 in. long. This follows the observation that the distribution of shear force amongst bolts is nonuniform when more than two rows of bolts are in the line of force in a lap splice (RCSC, 2004; Moore, 2007). Thus, the nominal strength of a fastener with the threads excluded from the shear plane in a group of fasteners is given by (Section J3, AISC, 2005):

$$R_n = 0.80\left(0.62A_bF_u\right) = 0.50A_bF_u \quad (4)$$

It was also observed in literature that a fastener with the threads not excluded from the shear plane had a strength approximately equal to 83% of the strength of a fastener with the threads excluded (RCSC, 2004). The nominal shear strength of a fastener with the threads not excluded from the shear plane in a group of fasteners, taking 83% as roughly 80%, is given by (Section J3, AISC, 2005):

$$R_n = 0.80\left(0.50A_bF_u\right) = 0.40A_bF_u \quad (5)$$

The nominal shear strength of one isolated high-strength bolt, not part of a group of fasteners, can be thus obtained by dividing the AISC and Research Council on Structural Connections (RCSC) equations by 0.80. Therefore, for one bolt with the threads not excluded from the shear plane:

$$R_n = \frac{F_{nv,N}A_b}{0.80} = \frac{0.4F_uA_b}{0.80} = 0.5F_uA_b = 0.5F_u\left(\frac{\pi d^2}{4}\right) \quad (6)$$

and for one bolt with the threads excluded from the shear plane:

$$R_n = \frac{F_{nv,X}A_b}{0.80} = \frac{0.5F_uA_b}{0.80} = 0.625F_uA_b \approx 0.62F_uA_b = 0.62F_u\left(\frac{\pi d^2}{4}\right) \quad (7)$$

where $F_{nv,N}$ and $F_{nv,X}$ are the nominal strengths in shear provided in Table J3.2 of the AISC *Specification* (AISC, 2005) for the cases of threads not excluded (*N*) and excluded (*X*) from the shear plane, respectively. Equations (6) and (7) reflect the spirit of the shear strength models presented in AISC and RCSC in the context of the strength of a single fastener. It is worth noting that the provisions for tensile and shear strength of fasteners found within the RCSC *Specification* are consistent with those in the AISC *Specification* that are presented herein.

DESCRIPTION OF BOLTS OBTAINED AND TESTED

For this project, 100 lots of A325/F1852 and A490/F2280 high-strength bolts were tested with diameters ranging from ⅝ to 1¼ in. Table 1 shows the number of lots obtained and tested based on the grade of structural bolts. The bolts were acquired from seven different manufacturers or distributors. Approximately half of the bolts were sought from United States manufacturers through donations. The remaining bolts

Table 1. Test Matrix			
Diameter (in.)	Length (in.)	Lots of A325/F1852	Lots of A490/F2280
⅝	2¾ to 5	5	6
¾	2¾ to 5	10	12
⅞	3 to 5	10	13
1	3 to 5	10	12
1⅛	3¾ to 5	5	6
1¼	3¾ to 5	5	6
	Total	45	55

were purchased through local distributors. The decision to purchase half of the bolts was made to limit the possibility of preferential selection by the manufacturers and obtain a statistically sound sample. No differences were noted between donated and purchased fasteners. A larger number of A490/F2280 bolts were tested than A325/F1852 due to the smaller amount of data available from past research on these material grades. For each lot, five bolts were tested in direct tension, five in shear with the threads excluded from the shear plane, and five in shear with the threads not excluded from the shear plane. More details on the selection procedures that were followed to establish number of lots considered and the number of fasteners tested from each lot can be found in Moore (2007).

TEST PROCEDURE

The bolt testing procedure consisted of loading A325, F1852, A490 and F2280 bolts in direct tension and shear with both the threads excluded and not excluded from the shear plane. The standards for testing metallic materials in tension are given by ASTM E8-04 and ASTM A370-05. The standard test methods for the tensile and shear strengths of fasteners are given by ASTM F606-05.

Data were collected so that strength and bolt elongation information could be obtained. In tension, the force versus elongation plot provides a better set of information on the bolts' characteristics than a stress-strain curve, because the behavior of a fastener is governed primarily by its threaded part when subjected to an axial load (Kulak et al., 2001).

The tension and shear testing was carried out using a 400-kip universal testing machine in displacement control. More information on the fixtures and the transducers used can be found in Moore (2007).

The speed of testing has to be slow enough so that forces and strains are accurately indicated. Expecting the bolts to elongate more than 5%, per ASTM E8-04, the speed of testing has to be between 0.05 in. and 0.5 in. per inch of the length of reduced section per minute when determining the tensile strength (ASTM E8-04; ASTM A370-05). After conducting several tests using various strain rates, it was observed that the strength of a bolt is not greatly dependant on the strain rate. Therefore, a constant strain rate of 0.15 in./in./min was selected for all tension tests (Moore, 2007).

When testing a bolt in shear, according to F606-07, the speed of testing has to be between 0.25 in./min and 0.5 in./min. Several experiments were conducted using these two extreme load rates with the threads excluded and not excluded from the shear plane to determine the load rate to be used for testing in shear. The load rate was found not to be a factor on the strength of a high-strength fastener, so a load rate of 0.5 in./min was selected for all bolts tested in shear (Moore, 2007).

Tension testing was performed on full-sized fasteners as opposed to coupons machined from fasteners (ASTM A370-05; ASTM F606-07). Coupons were machined from a few fasteners and were tested to validate Equations 1 and 2. The results of this very limited number of experiments are almost identical to those on full-sized fasteners and can be found in Moore (2007).

The bolts tested in tension were tested in a holder with the load axially applied between the bolt head and a threaded fixture. To guarantee a conservative tensile response of the bolt, four complete threads were left unengaged within the grip of the bolt, as per ASTM F606-07, allowing for a complete fracture surface to freely develop in the threads (Moore, 2007). This was accomplished by fully threading the bolt into the holder and then applying four complete rotations to back it out. Tension tests were performed using a wedge washer (ASTM F606-07; ASTM A370-05). The purpose of using a wedge washer is to obtain the tensile strength while demonstrating the quality of the bolt head and the ductility of the fastener. The bolt head was oriented on the wedge washer to ensure that a flat edge of the hexagonal head was aligned with the high point of the wedge washer during testing.

Before a bolt was tested in tension, the diameter of the bolt shank was measured at five locations and recorded. The overall length of the bolt and that of its threaded portion were also measured. The bolt was then loaded until fracture occurred. Finally, the maximum load was recorded from the universal testing machine, and the final length of the threaded portion of the bolt was measured and recorded so that the elongation percentage of the fastener at failure could be computed.

Shear testing was performed to determine the failure load due to a load applied perpendicularly to the axis of the bolt according to ASTM F606-07, using a purposely fabricated shear fixture. This test fixture, pictured in Figure 1, was designed to be used with either a tensile or a compressive applied load. The measured shear strength of bolts tested in a shear fixture applying a tensile load is approximately 8 to 13% lower when compared to bolts tested in a compression shear fixture (Kulak et al., 2001). This is due to a "phenomenon that tends to bend the lap plates of the tension jig outward" (Kulak et al., 2001), known as lap plate prying. Even though this phenomenon has been observed and documented, the tension jig is preferred because it produces a conservative (lower) shear strength value and has more consistent test results when compared to the compression jig (Kulak et al., 2001). Thus, the shear tests were performed with the shear fixture arranged in tension. To provide sufficient durability to the fixture for the large projected number of fasteners to be tested, the fixture was designed so that replaceable inserts could be used as the bearing elements to apply shear forces on the bolts. Two sets of inserts were used: an outer set that would last for approximately 50 shear tests, and an inner set, in sizes corresponding to each bolt diameter that would last for approximately 8 to 10 tests. The outer inserts were made of D2 tool steel, to provide durability, while the inner inserts were made of 1045 steel (a medium carbon steel suitable for machining with mechanical characteristics similar to A36 steel), to provide boundary conditions similar to what would be encountered in an actual bolted connection. More details can be found in Moore (2007).

As was done for tension testing, before a bolt was tested in shear, the diameter of the bolt shank was measured at five locations and recorded. Spacers were used to position the bolt so that it could be tested with the threads excluded or not excluded from the shear plane as required. The bolt was installed in the shear fixture with a finger-tightened nut to hold the bolt in place while it was loaded. The bolt was then loaded until a shear fracture occurred and the maximum load was recorded.

THREAD LENGTH

Variability in the thread length of fasteners was also evaluated. The thread length of one bolt per lot was measured and compared to the values provided in the AISC *Steel Construction Manual* (2005), which are consistent with the values provided in ASME B18.2.6 (2006), to which in turn ASTM A325, F1852, A490 and F2280 make reference. Figure 2 shows the frequency distribution of the percentage error.

The average percent difference in the thread lengths is less than 5% for ⅝-in., ¾-in., and ⅞-in. bolts. However, as the bolt diameter increases, the percent difference in the thread length also increases to as much as 7.41% on average for 1¼-in. bolts (Moore, 2007). The overall average difference in the thread length was found to be 4.82%. The minimum and maximum error in the thread length, based on the 100 lots measured, were −1.34% (indicating that the thread length is shorter than the values provided in AISC's *Manual*) and 10.4%, respectively. This variability in the bolt thread length may be critical in situations in which a bolt is specified in *X* condition (i.e., with threads excluded from the shear plane) but the shear plane is close to the nominal thread run-out.

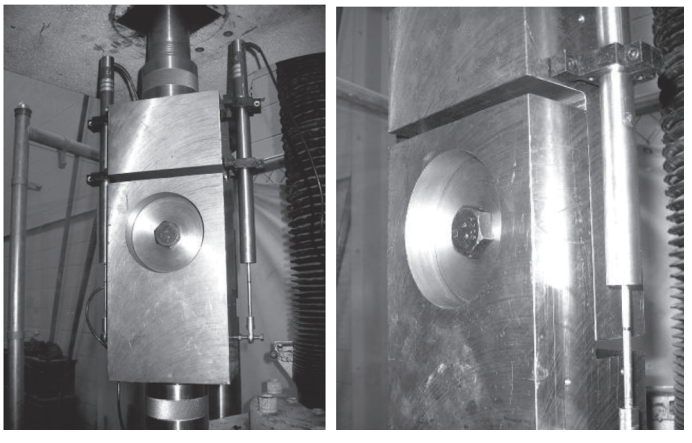

Fig. 1. Fixture used for shear testing.

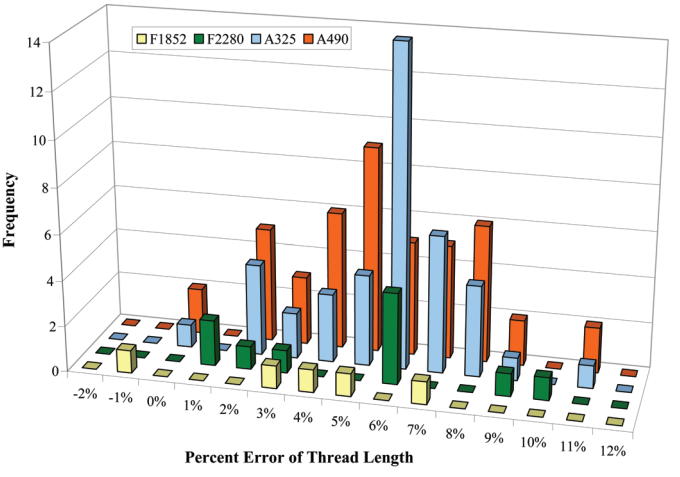

Fig. 2. Frequency distribution of percent error for bolt thread length.

Table 2. Tensile Strength of Bolts Tested Based on Grade											
Grade	Bolts Tested in Tension	Average (ksi)	Grade Standard Deviation (ksi)	Minimum (ksi)	Maximum (ksi)	Number (and Percentage) of Bolts Greater Than 150 ksi Tensile Strength		Number (and Percentage) of Bolts Greater Than 170 ksi Tensile Strength		Number (and Percentage) of Bolts Greater Than 173 ksi Tensile Strength	
A325	209	143.23	6.930	121.55	156.28	24	11.48%	Not Applicable			
F1852	28	148.71	6.043	135.46	156.09	13	46.43%	Not Applicable			
A325 F1852	237	143.88	7.046	121.55	156.28	37	15.61%	Not Applicable			
A490	228	163.71	4.234	152.06	173.06	Not Applicable		18	7.89%	1	0.44%
F2280	50	167.92	3.150	161.78	179.79	Not Applicable		12	24.00%	2	4.00%
A490 F2280	278	164.46	4.367	152.06	179.79	Not Applicable		30	10.79%	3	1.08%

EXPERIMENTAL TENSILE STRENGTH COMPARED TO MATERIAL DATA SHEETS

The results of the direct tension tests were compared to the values reported on the material data sheets that were obtained from the manufacturer or distributor. It should be noted that material sheets for only 79 out of the 100 lots were available for comparison (Moore, 2007). The ratio of the experimental tensile strength to the value obtained from the material data sheet was evaluated. Figure 3 shows the frequency distribution of the ratio of experimental tensile strength to the tensile strength reported on the material data sheets for the four grades of bolts investigated. Note that for the 100 lots tested in tension a wedge washer was used, whereas the tensile strength for the material data sheets was obtained using a proof (flat) washer. The experimental tensile strength was on average 99.8% of the strength reported on the manufacturers' material data sheets.

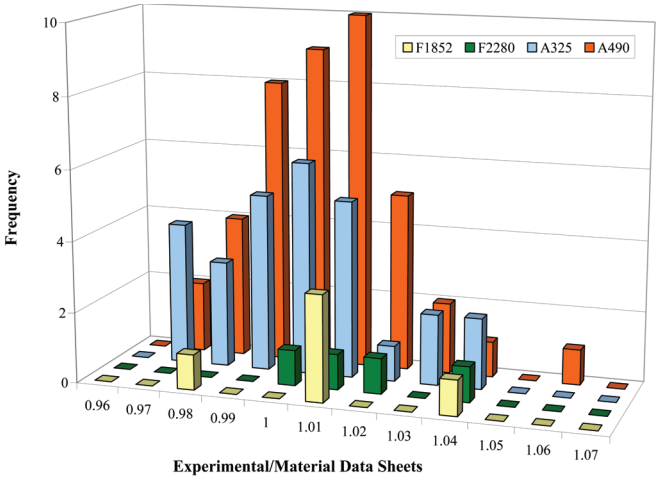

Fig. 3. Frequency distribution of experimental to data sheets strength.

TENSILE STRENGTH COMPARED TO ASTM AND RCSC

ASTM A325 (ASTM A325-04) and F1852 (ASTM F1852-05) specify a minimum tensile strength of 120 ksi for bolts less than or equal to 1 in. in diameter and of 105 ksi for bolts greater than 1 in. in diameter. Also, ASTM A490 (ASTM A490-04) and F2280 (ASTM F2280-06) bolts are specified to have a minimum tensile strength of 150 ksi as well as a maximum tensile strength of 173 ksi per ASTM or 170 ksi per RCSC (2004). As part of this study, the tensile strength of the 515 bolts tested in direct tension was compared to both ASTM and RCSC limits. The tensile strength was calculated using the failure tensile force, divided by the effective area, as given by Equation 1. Figure 4 shows the frequency distribution of the tensile strength for each bolt grade, while Table 2 summarizes the tensile strength of the 515 bolts tested based on the bolt grade.

A325 and F1852 bolts were never below the ASTM minimum tensile strength of 120 ksi, including diameters larger than 1 in., which should have had a minimum strength of 105 ksi. When considering A325 and F1852 bolts together, the average tensile strength of the 237 bolts tested is 143.9 ksi. There are 37 out of the 237 A325 and F1852 bolts tested in direct tension that have a tensile strength greater than 150 ksi. It was observed that the bolts that had a tensile strength greater than 150 ksi were 1 in. in diameter or less (Moore, 2007). AISC and RCSC do not recognize explicitly the 105-ksi strength level and use a minimum strength

of 120 ksi regardless of the bolt diameter. The experimental values validate this approach, considering that the tensile strength of the 237 A325 and F1852 bolts tested is always greater than 120 ksi, regardless of the bolt diameter.

The average tensile strength of the 278 A490 and F2280 bolts tested is 164.5 ksi. None of the A490 and F2280 bolts tested in direct tension has a strength smaller than the minimum tensile strength of 150 ksi specified by ASTM. Thirty out of the 278 A490 and F2280 bolts tested in direct tension had a tensile strength greater than the specified RCSC maximum (170 ksi). However, only 3 of the 278 A490 and F2280 bolts have a tensile strength greater than the maximum of 173 ksi as specified by ASTM. Taking into consideration the average tensile strength of the bolts tested per lot, there were 6 out of 55 A490 and F2280 lots that had an average tensile strength greater than 170 ksi. On the other hand, none of the A490 or F2280 lots had an average tensile strength greater than 173 ksi (Moore, 2007).

EXPERIMENTAL TO NOMINAL TENSILE STRENGTH—BASED ON AISC AND RCSC

Figure 5 shows the frequency distributions of the ratio of experimental strength to nominal AISC strength for the direct tension tests. The nominal tensile strength was calculated from Equation 3.

On average, the tensile strength for the A325 and F1852 bolts tested was 22.2% (5.75% standard deviation*) greater than the nominal tensile strength calculated based on AISC/RCSC equations. Also, on average, the measured tensile strength of the A490 and F2280 bolts was 11.9% (3.59%) larger than the nominal tensile strength based on AISC/RCSC equations (Moore, 2007). The ratio of experimental tensile strength to the nominal strength was never less than 1.023. Thus, it can be concluded that the AISC/RCSC equation conservatively predicts the strength of structural bolts in tension based on the 515 bolts tested.

EXPERIMENTAL TO NOMINAL TENSILE STRENGTH—BASED ON EFFECTIVE AREA

The frequency distributions of the ratio of experimental strength to nominal strength calculated based on the effective area are shown in Figure 6. The nominal tensile strength was calculated using the effective area from Equation 2.

On average, the measured tensile strength of the A325 and F1852 bolts tested was 19.9% (5.87%) greater than the

* Henceforth, standard deviations will be reported in parentheses immediately following the average values.

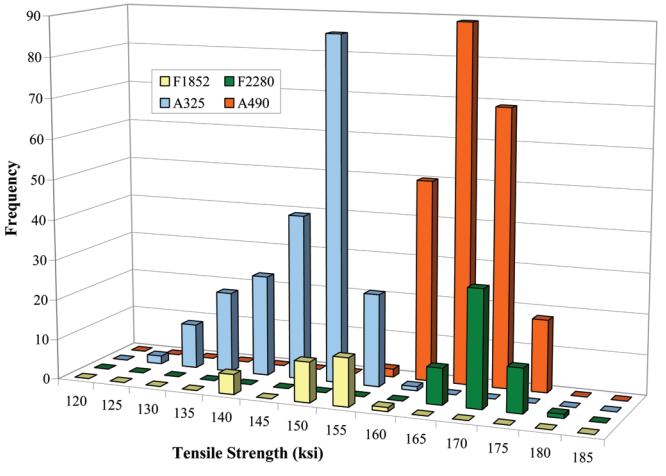

Fig. 4. Frequency distribution of tensile strength.

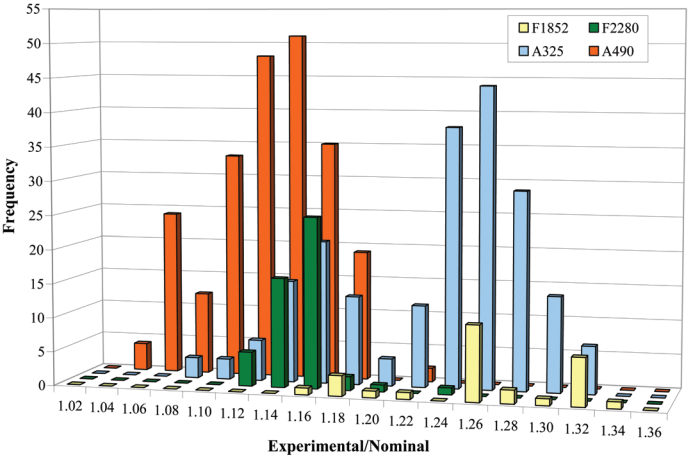

Fig. 5. Frequency distribution of experimental/nominal (AISC) for tensile strength.

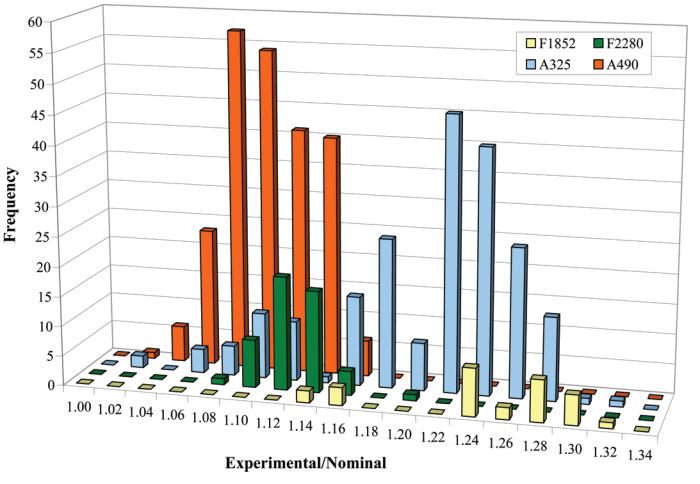

Fig. 6. Frequency distribution of experimental/nominal (effective area) for tensile strength.

nominal tensile strength calculated based on the effective area of the threaded section. The A490 and F2280 bolts had, on average, a measured tensile strength 9.64% (2.91%) larger than the nominal tensile strength based on the effective area (Moore, 2007).

The ratio of experimental tensile strength to nominal strength based on the effective area is 1.013 at a minimum, indicating that none of the high-strength bolts tested in tension had a tensile strength lower than the nominal strength based on the effective area (Moore, 2007). Comparing the ratio of experimental strength to nominal strength, it was determined that, on average, the nominal strength calculated using the effective area better predicts the failure load (i.e., the ratio of experimental to nominal strength is closer to unity, with similar or marginally smaller standard deviations).

EXPERIMENTAL TO NOMINAL SHEAR STRENGTH WITH THE THREADS EXCLUDED

The frequency distributions of the ratio of experimental strength to nominal strength in shear with the threads excluded from the shear plane are shown in Figure 7. Equation 7 was used to calculate the nominal shear strength with the threads excluded from the shear plane.

On average, the measured shear strength of bolts with the threads excluded from the shear plane was 18.1% (6.03%) greater than that specified by AISC/RCSC for the 233 tested A325 and F1852 high-strength bolts. Similarly, on average, a 5.63% (3.70%) greater strength was measured compared to AISC/RCSC's specified shear strength with the threads excluded from the shear plane for the 279 A490 and F2280 bolts tested (Moore, 2007). Of the 512 bolts tested in shear with the threads excluded from the shear plane, about 3.91% of the bolts have a shear strength smaller than the nominal AISC value. These bolts are of Grade A490. Therefore, based on the 512 bolts tested in shear with the threads excluded from the shear plane, it can be observed that the AISC/RCSC equation closely predicts the shear strength with the threads excluded, because less than 4% of the tested bolts were below the AISC nominal value.

EXPERIMENTAL TO NOMINAL SHEAR STRENGTH WITH THE THREADS NOT EXCLUDED

Figure 8 shows the frequency distributions of the ratio of experimental to nominal strength for bolts in shear with the threads not excluded from the shear plane. The nominal shear strength with the threads not excluded from the shear plane was calculated using Equation 6.

The 228 A325 and F1852 bolts tested in shear with the threads not excluded from the shear plane, on average, showed a measured strength 12.1% (6.58%) higher than that specified by AISC/RCSC. On the other hand, the 278 A490 and F2280 bolts had an average measured shear strength with the threads not excluded from the shear plane approximately equal (99.4% ratio with 4.86% standard deviation) to the value provided by the AISC/RCSC specification (Moore, 2007). Compared to the ratios of the same lot of bolts tested in tension and shear with the threads excluded from the shear plane, these averages are somewhat lower.

Of the 203 A325 bolts tested with the threads not excluded from the shear plane, 7 bolts had a strength lower than that specified by AISC/RCSC value (the experimental to nominal ratio is lower than unity). Also there were 132 out of 228 A490 bolts tested and 23 out of 50 F2280 bolts tested that have a ratio less than unity. Consequently, about 55.8% of the A490 and F2280 bolts tested had a measured

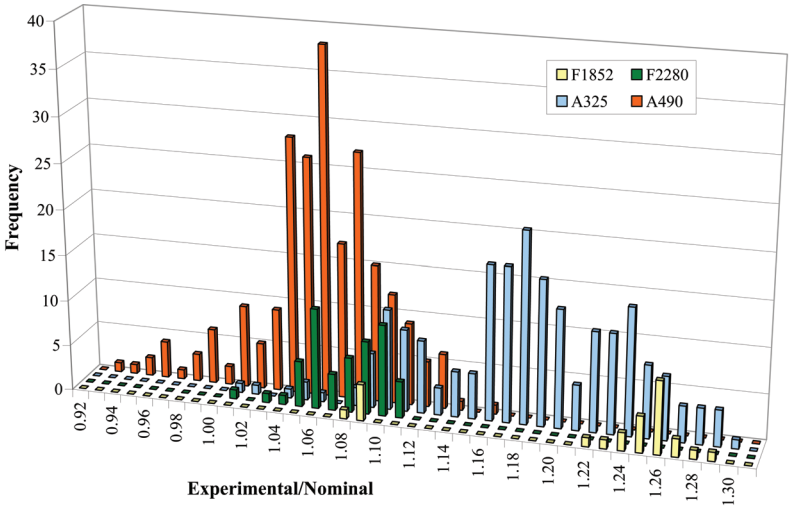

Fig. 7. Frequency distribution of experimental/nominal for strength in shear excluded.

shear strength with the threads not excluded from the shear plane below the AISC/RCSC nominal value. When looking at the 506 total bolts tested in shear with the threads not excluded, 162 (about 32%) had a measured strength below AISC/RCSC's nominal value. Thus, more than 30% of the time, AISC/RCSC's equation overpredicts the shear strength of bolts with the threads not excluded from the shear plane, based on the 506 bolts tested.

SHEAR *X* VERSUS TENSILE STRENGTH

The measured shear strength of fasteners with the threads excluded from the shear plane was compared to the measured tensile strength of bolts from the same lot. For this comparison, the shear strength with the threads excluded from the shear plane is estimated as a percentage of the bolt's tensile strength. Figure 9 shows the plot of the shear strength with the threads excluded from the shear plane versus the tensile strength for all bolts tested. It was found that the ratio of shear excluded to tensile strength is largely independent of the bolt grade (Moore, 2007), thus confirming the findings of Kulak et al. (2001). The average shear strength with the threads excluded from the shear plane is approximately 60.4% (1.49%) of the average tensile strength, based on the 100 lots tested; this compares well with the 0.62 value reported by Kulak et al. (2001).

SHEAR *N* VERSUS SHEAR *X* STRENGTH

Figure 10 shows the plot of the measured shear strength with the threads not excluded from the shear plane versus the measured shear strength with the threads excluded, based on the bolts tested. It was found that the ratio of shear not excluded to shear excluded is largely independent of the bolt grade (Moore, 2007). The average shear strength with the threads not excluded from the shear plane was found to be approximately 76.2% (2.36%) of the average shear strength with the threads excluded from the shear plane. This value is lower than the 0.83 value reported in RCSC (2004), which is approximated in the AISC provisions as 0.80. It is believed that the currently used value is based on a considerably smaller number of data points used in the statistical reduction, which results in the difference between the AISC value and the value obtained from the shear testing.

It is worth observing that the ratio of 0.76 is close to the ratio of the area of the threaded portion to the gross bolt area (which AISC takes indirectly as 0.75, as discussed earlier). This seems reasonable, because the ratio of the shear strength with the threads not excluded from the shear plane (in the threads) to the shear strength with the threads excluded (in the shank) should be proportional to the ratio of the shear areas.

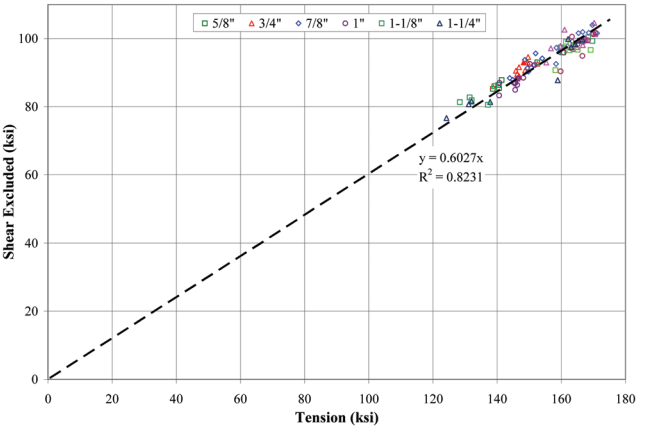

Fig. 9. Shear strength excluded versus tensile strength for all bolts tested.

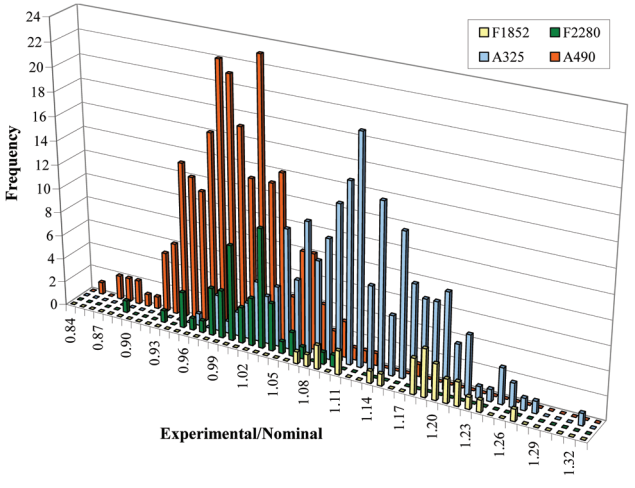

Fig. 8. Frequency distribution of experimental/nominal for strength in shear not excluded.

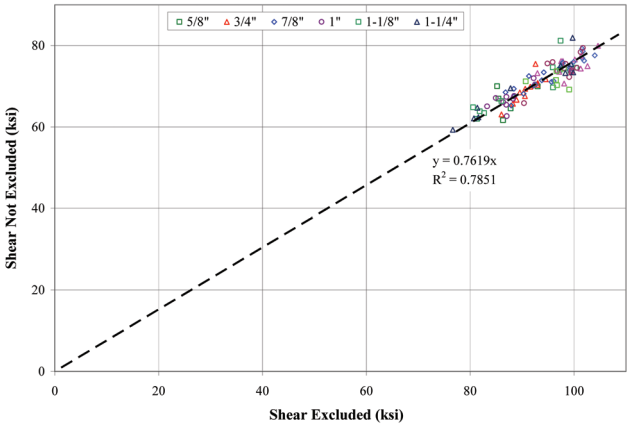

Fig. 10. Shear strength not excluded versus shear strength excluded for all bolts tested.

It is concluded that the equation currently used in the AISC provisions (AISC, 2005) to obtain the nominal value of the shear strength of a fastener with the threads not excluded from the shear plane is not always conservative. As a consequence, the calculation of the corresponding resistance factor to be used in design results in a lower value.

ELONGATION AT FAILURE

The elongation at failure of high-strength bolts was measured for the 515 bolts tested in direct tension. After the bolts were tested, the thread length was measured and compared to the initially measured thread length. This resulted in the percentage of elongation at failure of the tension bolt. Due to the reduced area in the threads, the plastic elongation occurs predominantly in this region and not in the bolt shank. The frequency distribution of the elongation at failure for all high-strength bolts tested is shown in Figure 11. The average percent elongation for A325/F1852 bolts and A490/F2280 bolts are 9.83% and 6.74%, with a standard deviation of 4.24% and 3.00%, respectively (Moore, 2007).

It is concluded that all high-strength fasteners have a considerably ductile behavior. Although higher-grade fasteners (A490 and F2280) show a reduced ductility when compared to A325 and F1852 bolts, failure will still occur after a considerable amount of energy has been absorbed by the fastener.

RELIABILITY STUDY AND RESISTANCE FACTORS

Based on the measured strength values of the 1,533 high-strength fasteners tested, a series of reliability analyses have been performed in order to evaluate resistance factors for the three cases of tension, shear with threads excluded from the shear plane, and shear with threads not excluded from the shear plane. Parameters of these analyses were the desired reliability index β (values used in the investigation were 4.0 and 4.5), the live-to–dead load ratio (values of 1.0 and 3.0 were used), the approach used to calculate the thread area (Equation 2, indicated with A, versus Equation 3, indicated with B in the tables), and the form of the resistance factor equation, chosen between Equations 8 and 9, indicated with Method I and II, respectively, in the tables:

$$\phi = \Phi_\beta \frac{R_m}{R_n} e^{-\alpha\beta V_R} \quad \text{(Fisher et al., 1978; Ravindra and Galambos, 1978)} \tag{8}$$

$$\phi = \Phi_\beta \rho_R e^{-\alpha\beta V_R} \quad \text{(Galambos, 1998)} \tag{9}$$

in which ϕ is the resistance factor; Φ_β is an adjustment factor (function of β); β is the reliability index; R_m and R_n are, respectively, the mean and nominal resistance values; α is the coefficient of separation (accounting for interdependency between loads and resistances); ρ_R is a bias coefficient for the resistance (function of geometry, material properties and equations used); and V_R is the coefficient of variation of the resistance.

A preliminary study was performed on all experimental data available in literature (which was found to be ample for tension and scarce for shear). The outcomes of this preliminary study provide values of resistance factors that compare well with those originally calculated by Fisher et al. (1978). The same approach, applied to the data acquired as part of this study, resulted in the values summarized in Tables 3 and 4. Table 3 contains the resistance factors obtained using various combinations of the parameters listed earlier, performed separately for measured strengths in tension, shear excluded, and shear not excluded (level II). Using a reliability index of 4.0 and a live-to–dead load ratio of 3.0, as recommended in the Commentary to the AISC *Specification* (AISC, 2005), it is possible to recommend a resistance factor of 0.90 for tension, 0.85 for shear excluded, and 0.80 for shear not excluded. Table 4 contains the same values, grouping together all loading cases considered, resulting in a single resistance factor (level I). Even in this case, it is possible to recommend a resistance factor of 0.80 for a live-to–dead load ratio of 3.0 and a reliability index of 4.0. The full study can be found in Moore (2007), and an in-depth summary of the approach and result can be found in Moore et al. (2008). It is concluded that it is indeed possible to increase the values of resistance factors for high-strength fasteners. Also, the resistance values for shear with the threads not excluded from the shear plane negatively affect the value of the corresponding resistance factor. In the next section, a recommendation for modifying the equation to predict the nominal values of shear resistance is presented, and the corresponding changes in resistance factors are noted.

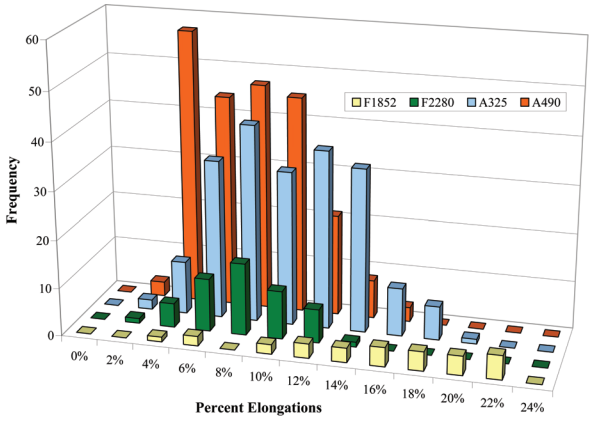

Fig. 11. Frequency distribution of percent elongation for all bolt grades.

Table 3. Resistance Factors—Level II—Summary					
		β = 4.0		β = 4.5	
		L/D = 1.0	L/D = 3.0	L/D = 1.0	L/D = 3.0
Tension	Method 1A ($0.75A_g$)	0.933	0.919	0.878	0.861
	Method 1B (A_{eff})	0.915	0.902	0.862	0.845
	Method 2A ($0.75A_g$)	0.923	0.910	0.868	0.851
	Method 2B (A_{eff})	0.912	0.899	0.859	0.842
Shear Excluded	Method 1A	0.870	0.857	0.817	0.800
	Method 2A	0.878	0.866	0.825	0.809
Shear *not* Excluded	Method 1A	0.810	0.798	0.759	0.744
	Method 2A	0.818	0.807	0.768	0.753

Table 4. Resistance Factors—Level I—Summary				
	β = 4.0		β = 4.5	
	L/D = 1.0	L/D = 3.0	L/D = 1.0	L/D = 3.0
Tension 1A Shear 1A	0.848	0.836	0.795	0.779
Tension 1B Shear 1A	0.849	0.837	0.796	0.780
Tension 2A Shear 2A	0.851	0.839	0.797	0.781
Tension 2B Shear 2A	0.853	0.841	0.800	0.784

RECOMMENDATIONS

After evaluating the resistance factors, it was found that the current values can be increased for bolts in tension, shear with the threads excluded, and shear with the threads not excluded from the shear plane without sacrificing safety, which will result in improved efficiency of bolted connections. Resistance factors of 0.90, 0.85 and 0.80 were recommended for bolts in tension, shear with the threads excluded from the shear plane, and shear with the threads not excluded from the shear plane, respectively (Moore, 2007).

It was observed that the AISC equation for the shear strength with the threads not excluded from the shear plane does not conservatively predict the strength based on the bolts tested for this research, which is why the recommended resistance factor is lower compared to tension and shear excluded. It is conceivable to modify Equations 6 and 7 using the shear-to-tension strength and shear *N*-to-*X* ratios calculated as part of this study, in the attempt to improve their prediction capabilities.

It was found from the bolts tested that the shear strength of a single high-strength bolt with the threads excluded from

Table 5. Modified Resistance Factors—Level II					
		β = 4.0		β = 4.5	
		L/D = 1.0	L/D = 3.0	L/D = 1.0	L/D = 3.0
Shear Excluded	Method 1A	0.899	0.886	0.844	0.827
	Method 2A	0.907	0.894	0.853	0.836
Shear *not* Excluded	Method 1A	0.880	0.868	0.825	0.809
	Method 2A	0.890	0.877	0.835	0.818

Table 6. Modified Resistance Factors—Level I				
	β = 4.0		β = 4.5	
	L/D = 1.0	L/D = 3.0	L/D = 1.0	L/D = 3.0
Tension 1A Shear 1A	0.903	0.890	0.848	0.831
Tension 1B Shear 1A	0.897	0.885	0.843	0.826
Tension 2A Shear 2A	0.906	0.893	0.851	0.835
Tension 2B Shear 2A	0.903	0.890	0.849	0.832

the shear plane is approximately 60% of the tensile strength regardless of the bolt grade. Therefore, based on this ratio, determined experimentally from the 100 lots tested, the nominal shear strength for a single bolt with the threads excluded from the shear plane, previously shown as Equation 7, becomes

$$R_n = 0.60F_uA_b \tag{10}$$

Regardless of the bolt grade, the shear strength with the threads not excluded from the shear plane was found to be approximately 76% of the average shear strength with the threads excluded from the shear plane for a single structural bolt, based on the bolts tested. Consequently, modifying Equation 6 to reflect the two new ratios found from the 100 lots tested, the nominal shear strength for a single high-strength bolt with the threads not excluded from the shear plane can be expressed as

$$R_n = 0.76\left(0.6F_uA_b\right) = 0.456F_uA_b \approx 0.46F_uA_b \tag{11}$$

Resistance factors have been evaluated using these modified equations for the shear strength of fasteners. To show the impact the modified shear resistance equations have on the resistance factors, Tables 5 and 6 tabulate the resistance factors based on the modified shear equations for level II and level I, respectively (Moore, 2007).

As can be seen from a comparison of Tables 3 and 4 with Tables 5 and 6, the resistance factors for shear with the threads excluded and not excluded from the shear plane increase with the modified nominal shear equations. Using these modified shear strength equations, a resistance factor of 0.85 can be recommended for bolts in shear with both the threads excluded and not excluded from the shear plane, based on a reliability index equal to 4.0 and a live-to–dead load ratio of 3.0 (Moore, 2007).

CONCLUSIONS

This paper summarizes the results of a study performed on 1,533 high-strength fasteners, measuring their geometric characteristics, strength, and ductility. Single bolts have

been tested in direct tension, in shear with the threads excluded from the shear plane, and in shear with the threads not excluded from the shear plane. The main conclusions can be summarized as follows:

- The actual thread length can be considerably different from the nominal length provided in the AISC *Manual* (AISC, 2005). While this will not have any impact for tension bolts, and for most cases of bolts in shear, this variability must be taken into account in situations in which the shear plane is close to the run-out of the threads.
- The comparison of the experimental tensile strength to the data found on the material sheets provided by manufacturers shows an excellent agreement between datasets, even when considering that the experimental data have been obtained using a wedge washer, while the data in the manufacturers' sheets have been obtained using a proof washer.
- A comparison of the experimental tensile strength to the minimum values required in the ASTM specifications and RCSC guide allows one to conclude that for A325/F1852 bolts, the strength is always larger than 120 ksi, irrespective of the diameter of the bolts. The average strength of these grades of fasteners is approximately 144 ksi. Similarly, for A490/F2280 bolts, the strength is always larger than 150 ksi. The average strength of these grades of fasteners is approximately 165 ksi. The RCSC maximum value for A490/F2280 bolts of 170 ksi is exceeded 11% of the time, while only 1% of the bolts exceed the ASTM-mandated limit of 173 ksi.
- Comparing the experimental tensile strength to the nominal values obtained using the equation in the AISC *Specification* (AISC 2005) it can be concluded that the AISC equation conservatively predicts the tensile strength of structural bolts.
- Performing the same comparison, using the effective cross-sectional area in place of the approximate area for the threaded portion of the bolt, it can be concluded that the failure load in tension is more accurately predicted.
- A calculation of the ratio of the experimental to the nominal shear strength with threads excluded from the shear plane, calculated per AISC/RCSC, allows the conclusion that, on average, A325/F1852 bolts are 18.1% stronger than predicted, while A490/F2280 bolts are 5.63% stronger than predicted. Also, 3.91% of the bolts tested (all Grade A490) show a shear strength lower than predicted. The equations in the AISC/RCSC specifications closely predict the shear strength of bolts with the threads excluded from the shear plane.
- Calculating the ratio of the experimental to the nominal shear strength with threads not excluded from the shear plane, calculated per AISC/RCSC, it can be concluded that A325/F1852 bolts are, on average, 12.1% stronger than predicted, while the strength of A490/F2280 bolts is predicted quite closely. It must be noted that 3.45% of the A325 bolts and 57.9% of the A490 bolts that were tested were weaker than predicted. Overall, more than 30% of the time the AISC/RCSC equations for the nominal shear strength with threads not excluded from the shear plane provided an unconservative value.
- The experimental ratio of shear strength with threads excluded to tensile strength is approximately equal to 60%, while the experimental ratio of shear with threads excluded to shear with threads not excluded is equal to 76%.
- The elongation at failure is 9.83% and 6.74% for A325/F1852 and A490/F2280, respectively, showing a considerable ductility in all cases.
- Resistance factors calculated using the equations in the current AISC/RCSC provisions and using the recommended modifications, taking into account the shear ratios obtained as part of this project, can be increased from the current 0.75, without sacrificing safety. Using the proposed modified equations, it is recommended to use a resistance factor of 0.90 for tension and 0.85 for shear, both with threads excluded and not excluded from the shear plane.

ACKNOWLEDGMENTS

This study was funded by the Research Council on Structural Connections, the support and guidance of which the authors gratefully acknowledge.

REFERENCES

AISC (2005), *Specification for Structural Steel Buildings,* 13th Ed., American Institute of Steel Construction, Inc., Chicago, IL.

AISC (2005), *Steel Construction Manual,* 13th Ed., American Institute of Steel Construction, Inc., Chicago, IL.

ASME B18.2.6-2006 (2006), "Fasteners for Use in Structural Applications," American Society of Mechanical Engineers, New York.

ASTM A325-04 (2004), "Standard Specification for Structural Bolts, Steel, Heat Treated, 120/105 Minimum Tensile Strength," ASTM International.

ASTM A370-05 (2002), "Standard Test Methods and Definitions for Mechanical Testing of Steel Products," ASTM International).

ASTM A490-04 (2004), "Standard Specification for Structural Bolts, Alloy Steel, Heat Treated, 150 Minimum Tensile Strength," ASTM International.

ASTM E8-04 (2004), "Standard Test Methods for Tension Testing of Metallic Materials," ASTM International.

ASTM F606-07 (2007), "Standard Test Methods for Determining the Mechanical Properties of Externally and Internally Threaded Fasteners, Washers, and Rivets," ASTM International.

ASTM F1852-05 (2005), "Standard Specification for 'Twist Off' Type Tension Control Structural Bolt/Nut/Washer Assemblies, Steel, Heat Treated, 120/105 ksi Minimum Tensile Strength," ASTM International.

ASTM F2280-06 (2006), "Standard Specification for 'Twist Off' Type Tension Control Structural Bolt/Nut/Washer Assemblies, Steel, Heat Treated, 150 ksi Minimum Tensile Strength," ASTM International.

Fisher, J.W. and Beedle, L.S. (1967). *Bibliography on Bolted and Riveted Joints,* American Society of Civil Engineers, New York, Manuals and Reports on Engineering Practice No. 48.

Fisher, J.W., Galambos, T.V., Kulak, G.L. and Ravindra, M.K. (1978) "Load and Resistance Factor Design Criteria for Connectors," *Journal of the Structural Division,* ASCE, Vol. 104, No. 9.

Galambos, T.V. (1998), *Guide to Stability Design Criteria for Metal Structures,* 5th Ed., John Wiley and Sons, Inc., New York.

Kulak, G.L., Fisher, J.W. and Struik, J.H.A. (2001), *Guide to Design Criteria for Bolted and Riveted Joints*, 2nd Ed., American Institute of Steel Construction, Inc., Chicago, IL.

Moore, A. (2007), "Evaluation of the Current Resistance Factors for High-Strength Bolts," MS Thesis, Department of Civil Engineering, University of Cincinnati, Ohio.

Moore, A.M., Rassati, G.A. and Swanson, J.A. (2008), "A Reliability Analysis of High-Strength Bolts," submitted for review to *Advances in Structural Engineering.*

Ravindra, M.K. and Galambos, T.V. (1978), "Load and Resistance Factor Design for Steel," *Journal of the Structural Division,* ASCE, Vol. 104, No. 9.

RCSC (2004), *Specification for Structural Joints Using ASTM A325 or A490 Bolts*, Research Council on Structural Connections.

A Strength Design Approach to Ponding

EDWARD SILVER

ABSTRACT

This article proposes a strength design approach to ponding resistance. It derives methods to include consideration of the impact of camber, nonuniform loading, and end fixity. The intent is to expand on the existing American Institute of Steel Construction (AISC) provisions so they may be adapted to unique framing and loading conditions.

Keywords: ponding, roof loads.

This article proposes a strength design approach to ponding resistance. The proposed procedures are constructed from the fundamentals of ponding analysis. From these fundamentals, we derive equations that help predict the behavior of beams subjected to ponding loads, then develop simplified procedure where possible.

Because the ponding demand is proportional to the ponding load—which is proportional to the total deflection—the following issues are discussed in this article:

- Beam deflection with ponding.
- Effect of camber and end fixity.
- Ponding load demand.
- Ponding moment demand.
- Beam and girder systems.

BEAM DEFLECTION WITH PONDING

The vertical load on a beam causes the beam to deflect. Water accumulates in the beam's deflected shape, inducing an additional ponding load, which induces additional deflection, which induces more water accumulation. This relationship between loading and deflection is the basis for calculating the ponded beam's deflection.

We begin by analyzing a uniformly loaded simple-span beam to determine the total deflection, including ponding effects.

Uniformly Loaded Beam

The total load along the span equals the initial, uniform load plus the ponded fluid load filling the final deflected shape of the beam:

Loading = Initial load + Ponded water

$$w(x) = w_i + \gamma S[y(x)] \tag{1}$$

where

w_i = initial uniform loading
γ = density of ponded liquid (62.4 lb/ft^3 for water)
S = beam spacing
$y(x)$ = total deflection along span, including ponding

From beam theory, the loading is proportional to the fourth derivative of the deflection:

$$w(x) = EI\frac{d^4y}{dx^4} \equiv EI\,y^{iv}(x) \tag{2}$$

Combining Equation 2 into Equation 1 gives a fourth-order linear differential equation:

$$EI\,y^{iv}(x) - \gamma S\,y(x) = w_i \tag{3}$$

The general solution to this differential equation is

$$y(x) = c_1\cos\left(\sqrt[4]{\frac{\gamma S}{EI}}\cdot x\right) + c_2\sin\left(\sqrt[4]{\frac{\gamma S}{EI}}\cdot x\right) + c_3\cosh\left(\sqrt[4]{\frac{\gamma S}{EI}}\cdot x\right) + c_4\sinh\left(\sqrt[4]{\frac{\gamma S}{EI}}\cdot x\right) - \frac{w_i}{\gamma S} \tag{4}$$

This provides the deflected shape of any prismatic, uniformly loaded beam, regardless of its end conditions.

To determine the undefined constants, c_1, c_2, c_3 and c_4, we apply the end conditions—boundary conditions—for a simply supported beam:

$$y(0) = y(L) = M(0) = M(L) = 0$$

From beam theory, $M = EIy''$. So, the boundary conditions are:

$$y(0) = y(L) = y''(0) = y''(L) = 0$$

Edward Silver, S.E., Principal, Silver and Associates, Inc., 7543 Woodley Ave., Suite 201, Van Nuys, CA, 91406. E-mail: edward.silver@esala.com

Applying these values gives:

$$y''(0) = \sqrt{\frac{\gamma S}{EI}}\left[c_1 \overset{1}{\cancel{\cos}}(0) + c_2 \overset{0}{\cancel{\sin}}(0) - c_3 \overset{1}{\cancel{\cos}}(0) - c_4 \overset{0}{\cancel{\sinh}}(0)\right]$$

$$= \sqrt{\frac{\gamma S}{EI}}\left[c_1 - c_3\right] = 0 \qquad \text{so,} \qquad c_3 = c_1$$

$$y(0) = c_1 \overset{1}{\cancel{\cos}}(0) + c_2 \overset{0}{\cancel{\sin}}(0) + c_1 \overset{1}{\cancel{\cosh}}(0) + c_4 \overset{0}{\cancel{\sinh}}(0) - \frac{w_i}{\gamma S}$$

$$= 2c_1 - \frac{w_i}{\gamma S} = 0 \qquad \text{so,} \qquad c_1 = \frac{w_i}{2\gamma S}$$

$$y(L) = \frac{w_i}{2\gamma S}\left[\cos\left(\sqrt[4]{\frac{\gamma S}{EI}} \cdot L\right) + \cosh\left(\sqrt[4]{\frac{\gamma S}{EI}} \cdot L\right) - 2\right]$$

$$+ c_2 \sin\left(\sqrt[4]{\frac{\gamma S}{EI}} \cdot L\right) + c_4 \sinh\left(\sqrt[4]{\frac{\gamma S}{EI}} \cdot L\right) = 0$$

$$y''(L) = \sqrt{\frac{\gamma S}{EI}}\left\{\begin{array}{l}\dfrac{w_i}{2\gamma S}\left[\cos\left(\sqrt[4]{\dfrac{\gamma S}{EI}} \cdot L\right) + \cosh\left(\sqrt[4]{\dfrac{\gamma S}{EI}} \cdot L\right)\right] \\ + c_2 \sin\left(\sqrt[4]{\dfrac{\gamma S}{EI}} \cdot L\right) + c_4 \sinh\left(\sqrt[4]{\dfrac{\gamma S}{EI}} \cdot L\right)\end{array}\right\} = 0$$

Solving for the remaining unknowns:

$$c_2 = \frac{w_i}{2\gamma S}\frac{1 - \cos\left(\sqrt[4]{\dfrac{\gamma S}{EI}} \cdot L\right)}{\sin\left(\sqrt[4]{\dfrac{\gamma S}{EI}} \cdot L\right)}$$

$$c_4 = \frac{w_i}{2\gamma S}\frac{1 - \cosh\left(\sqrt[4]{\dfrac{\gamma S}{EI}} \cdot L\right)}{\sinh\left(\sqrt[4]{\dfrac{\gamma S}{EI}} \cdot L\right)}$$

Applying the following identities:

$$1 - \cos(A) = 2\sin^2\left(\frac{A}{2}\right)$$

$$\sin(A) = 2\sin\left(\frac{A}{2}\right)\cos\left(\frac{A}{2}\right)$$

and

$$1 - \cosh(A) = -2\sinh^2\left(\frac{A}{2}\right)$$

$$\sinh(A) = 2\sinh\left(\frac{A}{2}\right)\cosh\left(\frac{A}{2}\right)$$

gives

$$c_2 = \frac{w_i}{2\gamma S}\frac{\sin\left(\sqrt[4]{\dfrac{\gamma S}{EI}} \cdot \dfrac{L}{2}\right)}{\cos\left(\sqrt[4]{\dfrac{\gamma S}{EI}} \cdot \dfrac{L}{2}\right)}$$

and

$$c_4 = -\frac{w_i}{2\gamma S}\frac{\sinh\left(\sqrt[4]{\dfrac{\gamma S}{EI}} \cdot \dfrac{L}{2}\right)}{\cosh\left(\sqrt[4]{\dfrac{\gamma S}{EI}} \cdot \dfrac{L}{2}\right)}$$

Substituting these last two constants and applying the following trigonometric identities:

$$\cos\left(\frac{A}{2} - x\right) = \cos\left(\frac{A}{2}\right) \cdot \cos(x) + \sin\left(\frac{A}{2}\right) \cdot \sin(x)$$

$$\cosh\left(\frac{A}{2} - x\right) = \cosh\left(\frac{A}{2}\right) \cdot \cosh(x) - \sinh\left(\frac{A}{2}\right) \cdot \sinh(x)$$

gives the deflected shape of a uniformly loaded, simple-span beam under ponding loads:

$$y(x) = \frac{w_i}{2\gamma S}\left\{\begin{array}{l}\left[\dfrac{\cos\left(\sqrt[4]{\dfrac{\gamma S}{EI}}\left(\dfrac{L}{2} - x\right)\right)}{\cos\left(\sqrt[4]{\dfrac{\gamma S}{EI}} \cdot \dfrac{L}{2}\right)} - 1\right] \\ -\left[1 - \dfrac{\cosh\left(\sqrt[4]{\dfrac{\gamma S}{EI}}\left(\dfrac{L}{2} - x\right)\right)}{\cosh\left(\sqrt[4]{\dfrac{\gamma S}{EI}} \cdot \dfrac{L}{2}\right)}\right]\end{array}\right\} \tag{5}$$

which can be written as:

$$y(x) = \frac{\Delta_i}{\dfrac{5\pi^4}{192}C}\left\{\begin{array}{l}\left[\dfrac{\cos\left(\pi\sqrt[4]{C}\left(\dfrac{1}{2} - \dfrac{x}{L}\right)\right)}{\cos\left(\dfrac{\pi}{2}\sqrt[4]{C}\right)} - 1\right] \\ -\left[1 - \dfrac{\cosh\left(\pi\sqrt[4]{C}\left(\dfrac{1}{2} - \dfrac{x}{L}\right)\right)}{\cosh\left(\dfrac{\pi}{2}\sqrt[4]{C}\right)}\right]\end{array}\right\} \tag{6}$$

where

Δ_i = initial midspan deflection $= \dfrac{5w_iL^4}{384EI}$

C = ponding factor $= \dfrac{\gamma SL^4}{\pi^4 EI}$

The ponding factor, C, is identical to the flexibility coefficient used in the 2005 AISC *Specification* Appendix 2. The AISC factor includes the density of water and adjustments for mixing units of measurements:

$$C_{\text{AISC}} = \frac{32\,SL^4}{10^7\,I} \approx \frac{62.4\ \text{pcf}\left(144\ \frac{\text{in.}^2}{\text{ft}^2}\right)SL^4}{\pi^4\left(29\cdot 10^6\ \text{ksi}\right)I}$$

The maximum deflection, Δ, occurs at midspan:

$$\Delta = \frac{\Delta_i}{\dfrac{\dfrac{5\pi^4}{192}C}{\left[\dfrac{1}{\cos\left(\dfrac{\pi}{2}\sqrt[4]{C}\right)} + \dfrac{1}{\cosh\left(\dfrac{\pi}{2}\sqrt[4]{C}\right)} - 2\right]}} \tag{7}$$

The odd formatting of this equation is intentional, so it can be more easily applied later in the article.

Nonuniform Loading

Roof loading is not always uniform. Off-center concentrated loads occur due to framing configurations and rooftop equipment. Snow drifts and rain loads on sloped roofs cause trapezoidal loading. A simple, but extreme, form of nonuniform loading is a triangular load, shown in Figure 1.

We can analyze triangular loading as we did for the uniform loads:

$$\text{Loading} = \text{Initial load} + \text{Ponded water}$$

$$w(x) = w_i\frac{x}{L} + \gamma S\,y(x) \tag{8}$$

where

w_i = the peak load at the end of the beam

Combining Equation 8 into Equation 2 gives the differential equation:

$$EI\,y^{iv}(x) - \gamma S\,y(x) = w_i\frac{x}{L} \tag{9}$$

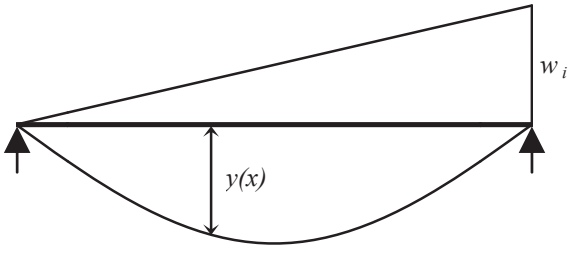

Fig. 1. Simple span with triangular load.

The general solution is:

$$y(x) = c_1\cos\left(\sqrt[4]{\frac{\gamma S}{EI}}\cdot x\right) + c_2\sin\left(\sqrt[4]{\frac{\gamma S}{EI}}\cdot x\right) + c_3\cosh\left(\sqrt[4]{\frac{\gamma S}{EI}}\cdot x\right) + c_4\sin\left(\sqrt[4]{\frac{\gamma S}{EI}}\cdot x\right) - \frac{w_i}{\gamma S}\frac{x}{L}$$

Applying the same boundary conditions as provided earlier gives:

$$y(x) = \frac{w_i}{2\gamma S}\left\{\left[\frac{\sin\left(\sqrt[4]{\dfrac{\gamma SL^4}{EI}}\dfrac{x}{L}\right)}{\sin\left(\sqrt[4]{\dfrac{\gamma SL^4}{EI}}\right)} - \frac{x}{L}\right] - \left[\frac{x}{L} - \frac{\sinh\left(\sqrt[4]{\dfrac{\gamma SL^4}{EI}}\dfrac{x}{L}\right)}{\sinh\left(\sqrt[4]{\dfrac{\gamma SL^4}{EI}}\right)}\right]\right\} \tag{10}$$

which we can write as

$$y(x) = \Delta_i\frac{76.66}{\pi^4 C}\left\{\left[\frac{\sin\left(\sqrt[4]{C}\,\dfrac{\pi x}{L}\right)}{\sin\left(\sqrt[4]{C}\cdot\pi\right)} - \frac{x}{L}\right] - \left[\frac{x}{L} - \frac{\sinh\left(\sqrt[4]{C}\,\dfrac{\pi x}{L}\right)}{\sinh\left(\sqrt[4]{C}\cdot\pi\right)}\right]\right\} \tag{11}$$

where

Δ_i = initial midspan deflection $= \dfrac{w_i L^4}{2(76.66)EI}$

C = ponding factor $= \dfrac{\gamma S\,L^4}{\pi^4 EI}$

For a triangular loaded beam, the maximum deflection occurs at $x = \sqrt{1-\sqrt{\frac{8}{15}}}\,(L) = 0.5193L$. This location shifts toward $0.50L$ with increasing ponding loads. To get the maximum moment location, we differentiate Equation 11 to get the slope and set it equal to zero, giving:

$$\frac{\cos\left(\pi\sqrt[4]{C}\cdot\dfrac{x}{L}\right)}{\sin\left(\pi\sqrt[4]{C}\right)} + \frac{\cosh\left(\pi\sqrt[4]{C}\cdot\dfrac{x}{L}\right)}{\sinh\left(\pi\sqrt[4]{C}\right)} - \frac{2}{\pi\sqrt[4]{C}} = 0 \tag{12}$$

Solving for *x/L*, numerically, over the range of possible values of *C*, gives the results shown in Figure 2.

Because the slope is zero at the maximum deflection, the deflection nearby the maximum location is fairly constant. The maximum deflection can be calculated, reasonably accurately, anywhere between 0.5*L* and 0.5193*L*. As Figure 2 shows, we can more accurately use:

$$\frac{x}{L} = 0.5193 - 0.193C(0.96 + 0.04C) \tag{13}$$

Plugging Equation 13 into Equation 11 gives the maximum deflection:

$$\Delta = \frac{\Delta_i}{\dfrac{\pi^4 C}{76.66}\left[\dfrac{\sin\left(\pi\sqrt[4]{C}\left[0.5193 - 0.193C(0.96 + 0.04C)\right]\right)}{\sin\left(\pi\sqrt[4]{C}\right)} + \dfrac{\sinh\left(\pi\sqrt[4]{C}\left[0.5193 - 0.193C\right](0.96 + 0.04C)\right)}{\sinh\left(\pi\sqrt[4]{C}\right)} - 1.02\right]} \tag{14}$$

Simplified Ponding Deflection

The deflection Equations 7 and 14 are cumbersome, so a simplified solution would be useful. The current 2005 AISC ponding analysis uses the simplifying assumption that the final deflected shape of the beam can be approximated as a sine curve:

$$y(x) = \Delta \sin\left(\frac{\pi x}{L}\right) \tag{15}$$

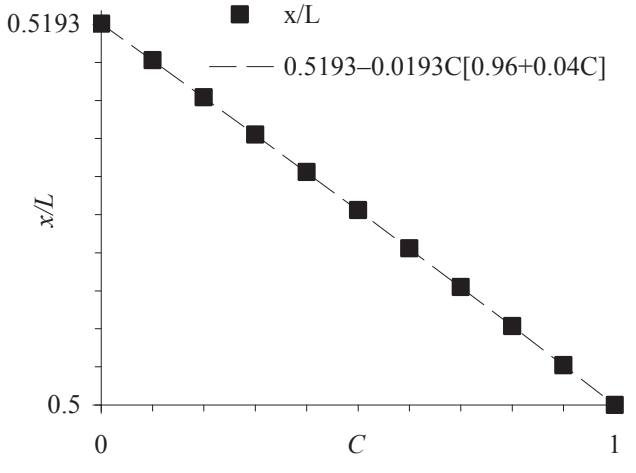

Fig. 2. Maximum deflection location.

where

Δ = total midspan deflection

Liquid ponded into this deflected shape produces a ponding load

$$w_p(x) = \gamma S \Delta \sin\left(\frac{\pi x}{L}\right) \tag{16}$$

From beam theory, the deflection is proportional to the fourth integral of the loading:

$$y_p(x) = \iiiint \frac{w_p(x)}{EI} = \frac{\gamma S}{EI} \iiiint \Delta \sin\frac{\pi x}{L} = \Delta_p \sin\frac{\pi x}{L}$$

where

$$\Delta_p = C\Delta \tag{17}$$

and

$$C = \text{ponding factor} = \frac{\gamma S L^4}{\pi^4 EI}$$

The total deflection is the sum of the initial deflection plus the ponding deflection:

$$\Delta = \Delta_i + \Delta_p \tag{18}$$

Substituting Equation 17 into Equation 18:

$$\Delta - C\Delta = \Delta_i$$

results in the basic ponding deflection equation:

$$\Delta = \frac{\Delta_i}{1 - C} \tag{19}$$

If we could use Equation 19 to estimate the deflection for beams with general loading, there will be some error, but the procedure would be greatly simplified.

Comparing the actual deflection of uniform and triangular loaded beams—Equations 7 and 14—to the approximate Equation 19 yields the data shown in Figure 3.

The graph in Figure 3 shows that Equation 19 accurately provides the total beam deflection, including ponding effects. The error between Equation 19 and the exact deflection equations is:

$$\text{Error} = \frac{\left[\dfrac{\Delta_i}{1 - C}\right]}{\Delta_{actual}} - 1$$

Plotting this error over the range of possible values of C yields the graph in Figure 4.

The error is less than half of 1 percent. So, this is nearly exact, for practical purposes.

Because the ponded fluid depth equals the total deflection, this gives the basic ponding depth as:

$$h_p = \Delta = \frac{\Delta_i}{1-C} \tag{20}$$

where

h_p = the maximum ponding depth

The maximum ponding depth term, h_p, is redundant here, but becomes useful when working with cambered beams.

End Fixity—Rotational Restraint

Though it is common to analyze simple span beams with perfectly pinned end connections, this is rarely a realistic model. For instance, conventional bolted connections on wide-flange beams provide rotational restraint, especially if the bolts are fully tensioned. In such situations, it is common for the actual beam deflection to be 20 to 30% smaller than predicted by a perfectly pinned model.

Because ponding loads are directly proportional to deflections, it is more accurate to include the effects of partial end fixity in the calculations. One way to accomplish this is to adjust the pin-ended deflection. For infinitely rigid end restraints and uniform loading:

$$\Delta_{i-FIXED} = \frac{w_i L^4}{384EI} = 0.2\frac{5w_i L^4}{384EI} = 0.2\Delta_{i-PINNED}$$

Design engineers do the same adjustment when determining camber on composite beams, where they adjust the pin-ended deflection to get the expected deflection. The adjustment is based on personal experience with some examples being shown in the table below:

Condition	$C_R = \frac{\Delta_{ACTUAL}}{\Delta_{PINNED}}$
Fixed ends	0.2
WF beam with shear connection	0.8
Open web steel joists	1.15

The values in the table are approximate numbers, and slight variations occur depending on the rotational stiffness of the supporting member. The open web joist factor is an increase due to web deformations, but it applies in the same way as the end fixity adjustment. Because the joist adjustment increases the deflection load, it should always be included in the ponding calculation.

Applying these factors to the initial deflection gives:

$$\Delta_{ACTUAL} = C_R \Delta_{PINNED}$$

With this factor, the ponding calculations are the same as for a pin-ended beam, except the deflection is reduced due to partial end fixity. Analyzing Equations 15 through 19 using this factor gives:

$$h_p = \Delta = \frac{\Delta_i}{1-C} \tag{21}$$

This is the same as Equation 20, except the ponding factor becomes $C = \frac{C_R \gamma S L^4}{\pi^4 EI}$.

The initial deflection, Δ_i, also should be adjusted for end fixity. The rest of the ponding calculations stay the same.

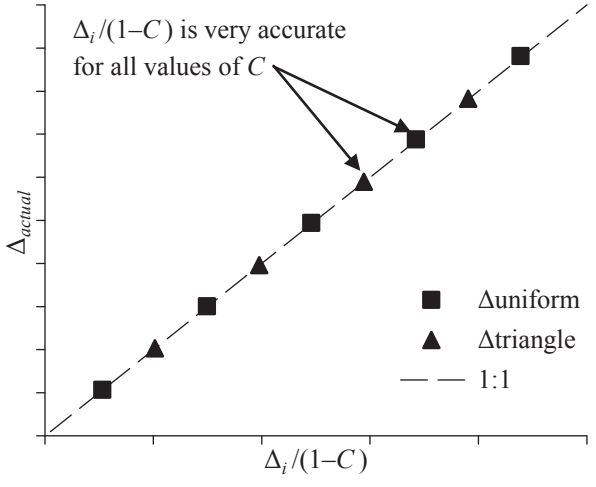

Fig. 3. Accuracy of approximate deflection equation.

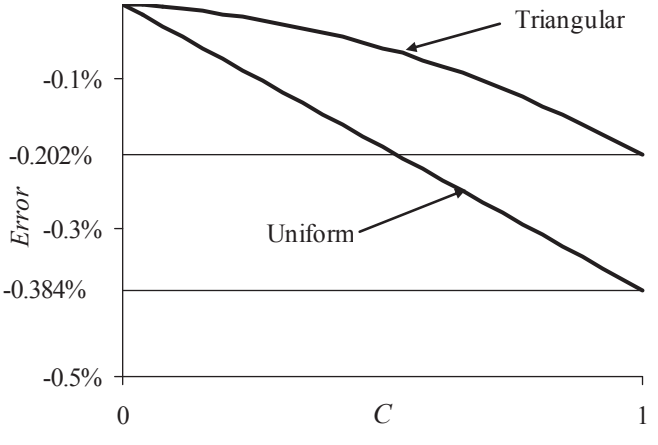

Fig. 4. Error in approximate equation $\Delta = \frac{\Delta_i}{1-C}$.

CAMBERED BEAMS

Uniform camber reduces the deflection and thus reduces the ponding load. On a cambered beam, the ponding depth is

$$h_p = \Delta - \Delta_c$$

where

Δ = the total beam deflection, including ponding
Δ_c = the upward midspan camber

If we assume the cambered shape is also a sign curve, the ponding load is:

$$w_p(x) = \gamma S h_p \sin\frac{\pi x}{L}$$

where

h_p = midspan fluid depth = $\Delta - \Delta_c$

Integrating the loading to get the ponding deflection:

$$y_p(x) = \int\int\int\int w_p(x) = \frac{\gamma S L^4}{\pi^4 EI} h_p \sin\frac{\pi x}{L}$$

giving

$$\Delta_p = \frac{\gamma S L^4}{\pi^4 EI} h_p = C h_p \tag{22}$$

Because the total deflection is the sum of the initial deflection plus the ponding deflection,

$$\Delta = \Delta_i + \Delta_p$$

and the ponding depth is the total deflection minus the camber:

$$h_p = \Delta - \Delta_c = \Delta_i + \Delta_p - \Delta_c$$

and the ponding deflection is:

$$\Delta_p = h_p - \left(\Delta_i - \Delta_c\right) = h_p - h_i$$

Substituting Equation 22:

$$C h_p = h_p - h_i$$

Solving for the midspan ponding depth:

$$h_p = \frac{h_i}{1 - C} \tag{23}$$

where

h_p = total midspan pond depth = $\Delta - \Delta_c$
h_i = initial midspan pond depth = $\Delta_i - \Delta_c$

Except for the midspan camber term, this is identical to Equations 20 and 21.

PONDING LOAD DEMAND

Summarizing the previous results provides the ponding load of a single beam:

$$w_p(x) = \gamma S h_p \sin\frac{\pi x}{L} \tag{24}$$

where

$$h_p = \frac{h_i}{1 - C} \tag{25}$$

$$C = \frac{C_R \gamma S L^4}{\pi^4 EI} \tag{26}$$

h_i = Initial midspan pond depth = $\Delta_i - \Delta_c$

PONDING MOMENT DEMAND

The water accumulated in the beam's deflected shape will add loading to the beam, thereby increasing the end shears and moments. These can be calculated from the deflected shapes.

Uniform Loading

The moment in a uniformly loaded beam with ponding can be derived from the deflection:

$$M(x) = -EI\, y''(x) \tag{27}$$

Substituting the deflection Equation 5 into Equation 27:

$$M(x) = -\frac{w_i EI}{2\gamma S}\frac{d^2}{dx^2}\left\{\left[\frac{\cos\left(\sqrt[4]{\frac{\gamma S}{EI}}\left(\frac{L}{2} - x\right)\right)}{\cos\left(\sqrt[4]{\frac{\gamma S}{EI}}\cdot\frac{L}{2}\right)} - 1\right] - \left[1 - \frac{\cosh\left(\sqrt[4]{\frac{\gamma S}{EI}}\left(\frac{L}{2} - x\right)\right)}{\cosh\left(\sqrt[4]{\frac{\gamma S}{EI}}\cdot\frac{L}{2}\right)}\right]\right\}$$

Differentiating and simplifying gives:

$$M(x) = \frac{w_i L^2}{2\pi^2\sqrt{C}}\left\{\frac{\cos\left[\pi\sqrt[4]{C}\left(\frac{1}{2} - \frac{x}{L}\right)\right]}{\cos\left(\frac{\pi}{2}\sqrt[4]{C}\right)} - \frac{\cosh\left[\pi\sqrt[4]{C}\left(\frac{1}{2} - \frac{x}{L}\right)\right]}{\cosh\left(\frac{\pi}{2}\sqrt[4]{C}\right)}\right\}$$

The maximum moment occurs at midspan:

$$M = \frac{w_i L^2}{2\pi^2\sqrt{C}}\left[\frac{1}{\cos\left(\frac{\pi}{2}\sqrt[4]{C}\right)} - \frac{1}{\cosh\left(\frac{\pi}{2}\sqrt[4]{C}\right)}\right]$$

This is the total moment, including ponding:

$$M = \frac{w_i L^2}{8} + M_p$$

Solving for the ponding moment:

$$M_p = \frac{w_i L^2}{2\pi^2\sqrt{C}}\left[\frac{1}{\cos\left(\frac{\pi}{2}\sqrt[4]{C}\right)} - \frac{1}{\cosh\left(\frac{\pi}{2}\sqrt[4]{C}\right)}\right] - \frac{w_i L^2}{8}$$

which can be written as:

$$M_p = \frac{\frac{\Delta_i \gamma S L^4}{\pi^2}}{\frac{\frac{5\pi^4}{192}C^{3/2}}{\frac{1}{\cos\left(\frac{\pi}{2}\sqrt[4]{C}\right)} - \frac{1}{\cosh\left(\frac{\pi}{2}\sqrt[4]{C}\right)} - \frac{\pi^2\sqrt{C}}{4}}} \tag{28}$$

where

Δ_i = initial midspan deflection $= \frac{5 w_i L^4}{384 EI}$

Triangular Loading

From the deflection Equations 10 and 27:

$$M(x) = -\frac{w_i EI}{2\gamma S}\frac{d^2}{dx^2}\left\{\left[\frac{\sin\left(\pi\sqrt[4]{C}\frac{x}{L}\right)}{\sin\left(\pi\sqrt[4]{C}\right)} - \frac{x}{L}\right] - \left[\frac{x}{L} - \frac{\sinh\left(\pi\sqrt[4]{C}\frac{x}{L}\right)}{\sinh\left(\pi\sqrt[4]{C}\right)}\right]\right\} \tag{29}$$

Differentiating and simplifying gives:

$$M(x) = \frac{w_i L^2}{2\pi^2\sqrt{C}}\left\{\frac{\sin\left(\pi\sqrt[4]{C}\frac{x}{L}\right)}{\sin\left(\pi\sqrt[4]{C}\right)} - \frac{\sinh\left(\pi\sqrt[4]{C}\frac{x}{L}\right)}{\sinh\left(\pi\sqrt[4]{C}\right)}\right\} \tag{30}$$

For the triangular loaded beam, the maximum moment occurs at $x = \frac{1}{\sqrt{3}}L = 0.5774L$. This location shifts toward $0.50L$ with increasing ponding loads. To get the maximum moment location, we differentiate Equation 30 to get the shear and set it equal to zero, giving:

$$\frac{\cos\left(\pi\sqrt[4]{C}\cdot\frac{x}{L}\right)}{\sin\left(\pi\sqrt[4]{C}\right)} - \frac{\cosh\left(\pi\sqrt[4]{C}\cdot\frac{x}{L}\right)}{\sinh\left(\pi\sqrt[4]{C}\right)} = 0 \tag{31}$$

Solving this numerically for *x/L*, we get the data plotted in Figure 5.

As Figure 5 shows, the maximum moment occurs very near:

$$\frac{x}{L} = 0.5774 - 0.0774\,C\,(1.07 - 0.07C) \tag{32}$$

Plugging Equation 32 into Equation 30 gives the maximum total moment:

$$M = \frac{w_i L^2}{2\pi^2\sqrt{C}} \times \left\{\frac{\sin\left(\pi\sqrt[4]{C}\,0.5774 - 0.0774\,C\,(1.07 - 0.07C)\right)}{\sin\left(\pi\sqrt[4]{C}\right)} - \frac{\sinh\left(\pi\sqrt[4]{C}\,0.5774 - 0.0774\,C\,(1.07 - 0.07C)\right)}{\sinh\left(\pi\sqrt[4]{C}\right)}\right\} \tag{33}$$

This is the total moment, which is the sum of the initial moment and the ponding moment:

$$M = M_i + M_p = \frac{w_i L^2}{9\sqrt{3}} + M_p \tag{34}$$

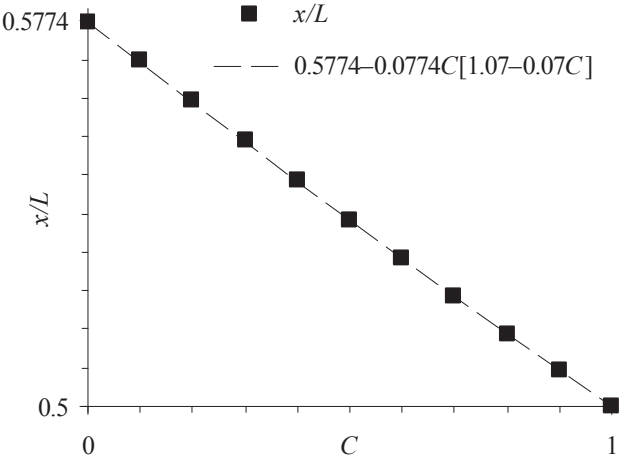

Fig. 5. Maximum deflection location.

Solving for the ponding moment:

$$M_p = \frac{w_i L^2}{2\pi^2\sqrt{C}} \times \left\{ \begin{array}{l} \dfrac{\sin\left(\pi\sqrt[4]{C}\left[0.5774 - 0.0774\,C\,(1.07 - 0.07C)\right]\right)}{\sin\left(\pi\sqrt[4]{C}\right)} \\ -\dfrac{\sinh\left(\pi\sqrt[4]{C}\left[0.5774 - 0.0774\,C\,(1.07 - 0.07C)\right]\right)}{\sinh\left(\pi\sqrt[4]{C}\right)} \end{array} \right\} - \frac{w_i L^2}{9\sqrt{3}} \quad (35)$$

which can be written as:

$$M_p = \frac{\dfrac{\Delta_i \gamma S L^4}{\pi^2}}{1.271\,C^{3/2}} \left\{ \begin{array}{l} \dfrac{\sin\left(\pi\sqrt[4]{C}\left[0.5774 - 0.0774\,C\,(1.07 - 0.07C)\right]\right)}{\sin\left(\pi\sqrt[4]{C}\right)} \\ -\dfrac{\sinh\left(\pi\sqrt[4]{C}\left[0.5774 - 0.0774\,C\,(1.07 - 0.07C)\right]\right)}{\sinh\left(\pi\sqrt[4]{C}\right)} \\ -1.266\sqrt{C} \end{array} \right\} \quad (36)$$

where

Δ_i = initial midspan deflection $= \dfrac{w_i L^4}{153.32EI}$

Simplified Ponding Moment Demand

With a sinusoidal deflected shape, the ponding load is:

$$w_p(x) = \gamma S h_p \sin\frac{\pi x}{L}$$

The ponding moment is:

$$M_p(x) = -\int\int w_p(x) = \frac{\gamma S L^2}{\pi^2} h_p \sin\frac{\pi x}{L}$$

and the ponding moment demand is:

$$M_p = \frac{\gamma S h_p L^2}{\pi^2} \quad (37)$$

where

$$h_p = \frac{h_i}{1 - C}$$

If we use Equation 37 to estimate the moment for beams with general loading, there will be some error, but the procedure is be greatly simplified.

Comparing the actual moment for a uniform and triangular loaded beam—Equations 28 and 36—to the approximate Equation 37, we get the data plotted in Figure 6.

Equation 19 accurately provides the total beam deflection, including ponding effects. The error between Equation 19 and the exact deflection equations is:

$$\text{Error} = \frac{\left[\dfrac{\Delta_i}{1 - C}\dfrac{\gamma S L^2}{\pi^2}\right]}{M_{P-actual}} - 1$$

Plotting this error over the range of possible values of C yields Figure 7.

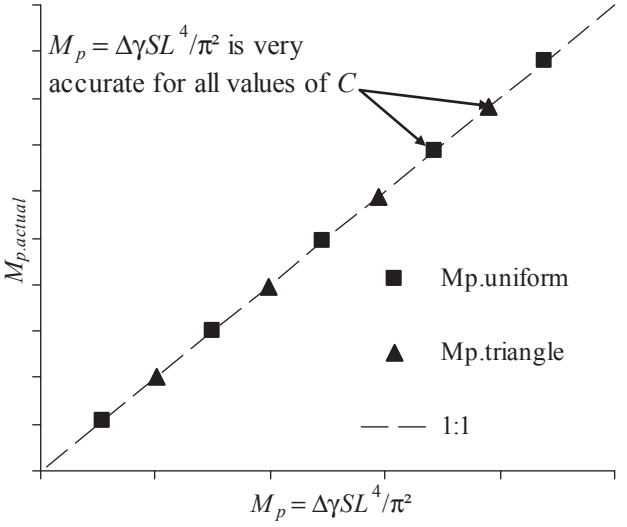

Fig. 6. Accuracy of approximate moment equation.

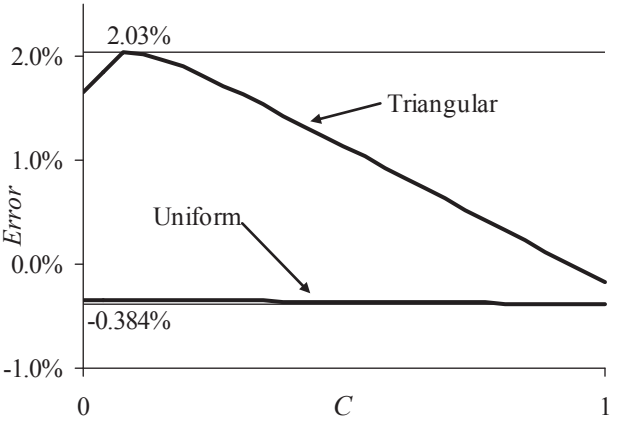

Fig. 7. Error in approximate equation $\dfrac{\Delta_i}{1 - C}\dfrac{\gamma S L^2}{\pi^2}$.

The error is very small, except for certain values of C under triangular loading, which has up to about 2% error. This is an extreme loading condition, so under common loading, the approximation is very accurate for practical purposes.

Summarizing the ponding moment demand procedure:

$$\text{Ponding moment} = M_p = \frac{h_p \gamma S L^4}{\pi^4} \tag{38}$$

where

h_p = ponding depth $= \dfrac{h_i}{1-C}$

C = ponding factor $= \dfrac{C_R \gamma S L^4}{\pi^4 EI}$

h_i = initial midspan pond depth $= \Delta_i - \Delta_c$

γ = ponding liquid density (62.4 pcf for water)

S = beam spacing

L = beam span

Example 1—Beam with Ponding

W12×14 beam; $I_x = 88.6$ in.^{4}, span = 30 ft; spacing = 6 ft; end restraint factor = $C_R = 0.8$; camber = 1 in.

Initial deflection due to $D + R$ or S:

$$\Delta_i = C_R \frac{5 w_i L^4}{384 EI} = 1.2 \text{ in.}$$

Initial depth:

$$h_i = \Delta_i - \Delta_c = 1.2 \text{ in.} - 1 \text{ in.} = 0.2 \text{ in.}$$

Ponding factor:

$$C = C_R \frac{\gamma S L^4}{\pi^4 EI} = 0.8 \frac{62.4(6)30^4(144)}{\pi^4 (29 \times 10^6) 88.6} = 0.14$$

Midspan ponding depth:

$$h_p = \frac{h_i}{1-C} = \frac{0.2 \text{ in.}}{1 - 0.14} = 0.23 \text{ in.}$$

Added ponding moment:

$$M_P = \frac{S \gamma h_p L^2}{\pi^2} = \frac{6 (62.4 \text{ pcf} \times 0.23 \text{ in.}) 30^2}{\pi^2 \times 12 \text{ in./ft}} = 0.7 \text{ k-ft}$$

Added ponding reaction:

$$R_P = \frac{S \gamma h_p L}{\pi} = \frac{6 (62.4 \text{ pcf} \times 0.23 \text{ in.}) 30}{\pi \times 12 \text{ in./ft}} = 0.1 \text{ k}$$

BEAM AND GIRDER SYSTEMS

We can expand the preceding procedures to beam and girder systems as follow:

Beam Supported by Girders

This beam has added trapezoidal ponding load due to the girder ponding depths, h_{Gp}, at each end of the beam.

Ponding load:

$$w_{Bp}(x_B) = \gamma S \left[\begin{array}{l} h_{Bp} \sin \dfrac{\pi x_B}{L_B} \\ + h_{GpR} \sin \dfrac{\pi x_{GR}}{L_{GR}} \left(\dfrac{x_B}{L_B} \right) \\ + h_{GpL} \sin \dfrac{\pi x_{GL}}{L_{GL}} \left(1 - \dfrac{x_B}{L_B} \right) \end{array} \right] \tag{39}$$

where

h_{GpL} = left girder ponding depth

h_{GpR} = right girder ponding depth

Note that the girder ponding depth varies along the length of the girder. The adjacent girders may have staggered columns, so their maximum deflections may occur at different locations. Equation 39 represents the general condition for a beam framing into any point along the girder.

The resulting beam's ponding moment demand would then be:

$$M_{Bp}(x_G) = \gamma S L_B^2 \left[\begin{array}{l} \dfrac{h_{Bp}}{\pi^2} \\ + \dfrac{h_{GpR}}{16} \sin \dfrac{\pi x_{GR}}{L_{GR}} \\ + \dfrac{h_{GpL}}{16} \sin \dfrac{\pi x_{GL}}{L_{GL}} \end{array} \right] \tag{40}$$

The deflection caused by the ponding load in Equation 39 is:

$$\Delta_{Bp}(x_G) = C_B \left[h_{Bp} + \frac{5\pi^4}{768} \left(\begin{array}{l} h_{GpR} \sin \dfrac{\pi x_{GR}}{L_{GR}} \\ + h_{GpL} \sin \dfrac{\pi x_{GL}}{L_{GL}} \end{array} \right) \right]$$

where

$$C_B = \frac{C_R \gamma S L_B^4}{\pi^4 E I_B}$$

Substituting:

$$h_{Bp} = \Delta_{Bp} + h_{Bi}$$

and solving for the beam ponding depth,

$$h_{Bp}(x_G) = \frac{h_{Bi}}{1-C_B} + \frac{5\pi^4}{768}\frac{C_B}{1-C_B}\begin{pmatrix} h_{GpR}\sin\dfrac{\pi x_{GR}}{L_{GR}} \\ + h_{GpL}\sin\dfrac{\pi x_{GL}}{L_{GL}} \end{pmatrix} \quad (41)$$

If the beam frames into both girder midspans, then the maximum beam ponding depth is:

$$h_{Bp} = \frac{h_{Bi}}{1-C_B} + \frac{5\pi^4}{384}\frac{C_B}{1-C_B}\left(\frac{h_{GpR}+h_{GpL}}{2}\right) \quad (42)$$

and the corresponding maximum beam ponding moment demand is:

$$M_{Bp} = \gamma S L_B^{\,2}\left[\frac{h_{Bp}}{\pi^2} + \frac{h_{GpL}+h_{GpR}}{16}\right] \quad (43)$$

Solving Equation 39 for the end reaction:

$$R_{BpL}(x_G) = \gamma S L_B\begin{bmatrix} \dfrac{h_{Bp}}{\pi} \\ + \dfrac{h_{GpL}}{3}\sin\dfrac{\pi x_{GL}}{L_{GL}} \\ + \dfrac{h_{GpR}}{6}\sin\dfrac{\pi x_{GR}}{L_{GR}} \end{bmatrix} \quad (44)$$

Substituting Equation 41:

$$R_{BpL}(x_G) = \frac{\gamma S L_B}{\pi}\begin{bmatrix} \dfrac{h_{Bp}}{1-C_B} \\ + \left(\dfrac{\pi}{3} + \dfrac{C_B}{1-C_B}\dfrac{5\pi^4}{768}\right) h_{GpL}\sin\dfrac{\pi x_{GL}}{L_{GL}} \\ + \left(\dfrac{\pi}{6} + \dfrac{C_B}{1-C_B}\dfrac{5\pi^4}{768}\right) h_{GpR}\sin\dfrac{\pi x_{GR}}{L_{GR}} \end{bmatrix} \quad (45)$$

Girder Ponding

The girder supports the end reactions from the beams on each side of the girder.

$$w_G(x_G) = \frac{R_{BpL} + R_{BpR}}{S}$$

Substituting from Equation 45, we get the ponding load on the girder:

$$w_{Gp}(x_G) = \frac{\gamma}{\pi}\left\{\begin{array}{l} \dfrac{h_{Bp1}L_{B1}}{1-C_{B1}} + \dfrac{h_{Bp2}L_{B2}}{1-C_{B2}} \\ + \left[\begin{array}{l} \left(\dfrac{\pi}{3} + \dfrac{C_{B1}}{1-C_{B1}}\dfrac{5\pi^4}{768}\right) L_{B1} \\ + \left(\dfrac{\pi}{3} \quad \dfrac{C_{B2}}{1-C_{B2}}\dfrac{5\pi^4}{768}\right) L_{B2} \end{array}\right] h_{Gp}\sin\dfrac{\pi x_G}{L_G} \\ + \left(\dfrac{\pi}{6} + \dfrac{C_{B1}}{1-C_{B1}}\dfrac{5\pi^4}{768}\right) L_{B1} h_{Gp1}\sin\dfrac{\pi x_{G1}}{L_{G1}} \\ + \left(\dfrac{\pi}{6} + \dfrac{C_{B2}}{1-C_{B2}}\dfrac{5\pi^4}{768}\right) L_{B2} h_{Gp2}\sin\dfrac{\pi x_{G2}}{L_{G2}} \end{array}\right\} \quad (46)$$

The adjacent girders may have staggered columns, so their maximum deflections may occur at different locations. Equation 46 represents the general loading condition. It can be used to solve complex framing patterns by modeling all the girders and beams, then iterating to find the ponding depths of all the framing members.

We will next look at some conditions that allow for closed-form solutions.

Identical Beams and Girders

If the nearby beams and girders are all identical, with the same loading, then the solution can be simplified. The beam ponding depth becomes:

$$h_{Bp}(x_G) = \frac{h_{Bi}}{1-C_B} + \frac{5\pi^4}{384}\frac{C_B}{1-C_B}h_{Gp}\sin\frac{\pi x_G}{L_G} \quad (47)$$

The girder loading is

$$w_{Gp}(x_G) = \gamma L_B\begin{bmatrix} \dfrac{2}{\pi}\dfrac{h_{Bi}}{1-C_B} \\ + \left(1 + \dfrac{5\pi^3}{192}\dfrac{C_B}{1-C_B}\right) h_{Gp}\sin\dfrac{\pi x_G}{L_G} \end{bmatrix} \quad (48)$$

The girder deflection due to ponding is

$$\Delta_{Gp} = C_G\left[\frac{5\pi^3}{192}\frac{h_{Bi}}{1-C_B} + \left(1 + \frac{5\pi^3}{192}\frac{C_B}{1-C_B}\right)h_{Gp}\right]$$

where

$$C_G = \frac{C_R\gamma L_B L_G^{\,4}}{\pi^4 E I_G}$$

Substituting $h_{Gp} = h_{Gi} + \Delta_{Gp}$:

$$h_{Gp} = \frac{\dfrac{h_{Gi}}{C_G} + \dfrac{5\pi^3}{192}\dfrac{h_{Bi}}{1-C_B}}{\dfrac{1-C_G}{C_G} - \dfrac{5\pi^3}{192}\dfrac{C_B}{1-C_B}} \tag{49}$$

The beam framing into the girder midspan has a ponding depth of:

$$h_{Bp} = \frac{h_{Bi}}{1-C_B} + \frac{5\pi^4}{384}\frac{C_B}{1-C_B}h_{Gp} \tag{50}$$

Using the ponding depths from Equations 49 and 50, the ponding moment demands can be computed as follows.

Beam at girder midspan from Equation 40:

$$M_{Bp} = \gamma S L_B^{\,2}\left(\frac{h_{Bp}}{\pi^2} + \frac{h_{Gp}}{8}\right) \tag{51}$$

Using Equation 40 to calculate the moment demand for beams framing into different locations on the girder yields the following.

Beam at girder third-points:

$$M_{Bp} = \gamma S L_B^{\,2}\left(\frac{h_{Bp}}{\pi^2} + \frac{\sqrt{3}}{16}h_{Gp}\right) \tag{52}$$

Beam and girder quarter-points:

$$M_{Bp} = \gamma S L_B^{\,2}\left(\frac{h_{Bp}}{\pi^2} + \frac{h_{Gp}}{8\sqrt{2}}\right) \tag{53}$$

Girder moment:

$$\begin{aligned} M_{Gp} &= \gamma L_B L_G^{\,2}\left\{\frac{h_{Bp}}{4\pi} + \left[1 - \left(\frac{\pi^2}{8} - 1\right)\frac{5\pi^3}{192}\cdot\frac{C_B}{1-C_B}\right]\frac{h_{Gp}}{\pi^2}\right\} \\ &= \frac{\gamma L_B L_G^{\,2}}{4\pi}\left[h_{Bp} + \left(5.3 - \frac{C_B}{1-C_B}\right)\frac{h_{Gp}}{4.2}\right] \end{aligned} \tag{54}$$

The total moment demand, including rain and/or snow, can then be compared against the beam's flexural capacity.

Example 2—Uniform Beam and Girder System

End restraint factor = $C_R = 0.8$

W12×14 beam; $I_x = 88.6$ in.^{4}; span = 30 ft; spacing = 6 ft; camber = 1 in.; deflection due to $D + R$ or S: $\Delta_i = 1.2$ in.
$h_{Bi} = 1.2 - 1 = 0.2$ in.

W18×35 girder; $I_x = 510$ in.^{4}; span = 31 ft; camber = 1 in.; deflection due to $D + R$ or S: $\Delta_i = 1.3$ in.
$h_{Gi} = 1.3 - 1 = 0.3$ in.
$C_G = 0.14$

The girder ponding depth is:

$$\begin{aligned} h_{Gp} &= \frac{\dfrac{h_{Gi}}{C_G} + \dfrac{5\pi^3}{192}\dfrac{h_{Bi}}{1-C_B}}{\dfrac{1-C_G}{C_G} - \dfrac{5\pi^3}{192}\dfrac{C_B}{1-C_B}} \\ &= \frac{\dfrac{0.3}{0.14} + \dfrac{5\pi^3}{192}\dfrac{0.2}{1-0.14}}{\dfrac{1-0.14}{0.14} - \dfrac{5\pi^3}{192}\dfrac{0.14}{1-0.14}} = 0.39 \text{ in.} \end{aligned} \tag{55}$$

The beam framing into the girder midspan has a ponding depth of:

$$\begin{aligned} h_{Bp} &= \frac{h_{Bi}}{1-C_B} + \frac{5\pi^4}{384}\frac{C_B}{1-C_B}h_{Gp} \\ &= \frac{0.2}{1-0.14} + \frac{5\pi^4}{384}\frac{0.14}{1-0.14}0.39 = 0.31 \text{ in.} \end{aligned} \tag{56}$$

The moment in the beam at the girder midspan is:

$$\begin{aligned} M_{Bp} &= \gamma S L_B^{\,2}\left(\frac{h_{Bp}}{\pi^2} + \frac{h_{Gp}}{8}\right) \\ &= \frac{62.4(6)30^2}{12{,}000}\left(\frac{0.39}{\pi^2} + \frac{0.31}{8}\right) \\ &= 2.2 \text{ k-ft} \end{aligned} \tag{57}$$

The girder moment is:

$$\begin{aligned} M_{Gp} &= \frac{\gamma L_B L_G^{\,2}}{4\pi}\left[h_{Bp} + \left(5.3 - \frac{C_B}{1-C_B}\right)\frac{h_{Gp}}{4.2}\right] \\ &= \frac{62.4(30)31^2}{4\pi(12{,}000)}\left[0.31 + \left(5.3 - \frac{C_B}{1-C_B}\right)\frac{0.39}{4.2}\right] \\ &= 9.4 \text{ k-ft} \end{aligned} \tag{58}$$

Beam Framing into a Wall—Identical Adjacent Framing

The beam ponding depth is

$$h_{Bp}(x_G) = \frac{h_{Bi}}{1-C_B} + \frac{5\pi^4}{768}\frac{C_B}{1-C_B}h_{Gp}\sin\frac{\pi x_G}{L_G} \tag{59}$$

If the adjacent beams and girders are identical and similarly loaded, then the girder loading is:

$$w_{Gp}(x_G) = \gamma L_B\left[\begin{aligned}&\frac{2}{\pi}\frac{h_{Bi}}{1-C_B} \\ &+\left(\frac{5}{6} + \frac{5\pi^3}{256}\frac{C_B}{1-C_B}\right)h_{Gp}\sin\frac{\pi x_G}{L_G}\end{aligned}\right] \tag{60}$$

The girder deflection due to ponding is:

$$\Delta_{Gp} = C_G \left[\frac{5\pi^3}{192} \frac{h_{Bi}}{1-C_B} + \left(\frac{5}{6} + \frac{5\pi^3}{256} \frac{C_B}{1-C_B} \right) h_{Gp} \right]$$

The girder ponding depth is:

$$h_{Gp} = \frac{\frac{h_{Gi}}{C_G} + \frac{5\pi^3}{192} \frac{h_{Bi}}{1-C_B}}{\frac{1-\frac{5}{6}C_G}{C_G} - \frac{5\pi^3}{256} \frac{C_B}{1-C_B}} \tag{61}$$

The beam framing into the wall and the girder midspan has a ponding depth of:

$$h_{Bp} = \frac{h_{Bi}}{1-C_B} + \frac{5\pi^4}{768} \frac{C_B}{1-C_B} h_{Gp} \tag{62}$$

The ponding moment demands are as follows.

Beam at girder midspan from Equation 40:

$$M_{Bp} = \gamma S L_B^{\,2} \left(\frac{h_{Bp}}{\pi^2} + \frac{h_{Gp}}{16} \right) \tag{63}$$

Beam at girder third-points:

$$M_{Bp} = \gamma S L_B^{\,2} \left(\frac{h_{Bp}}{\pi^2} + \frac{\sqrt{3}}{32} h_{Gp} \right) \tag{64}$$

Beam and girder quarter-points:

$$M_{Bp} = \gamma S L_B^{\,2} \left(\frac{h_{Bp}}{\pi^2} + \frac{h_{Gp}}{16\sqrt{2}} \right) \tag{65}$$

Girder moment:

$$\begin{aligned} M_{Gp} &= \gamma L_B L_G^{\,2} \left\{ \frac{h_{Bp}}{4\pi} + \left[\frac{5}{6} + \left(1 - \frac{\pi^2}{12} \right) \frac{5\pi^3}{256} \cdot \frac{C_B}{1-C_B} \right] \frac{h_{Gp}}{\pi^2} \right\} \\ &= \frac{\gamma L_B L_G^{\,2}}{4\pi} \left[h_{Bp} + \left(7.75 - \frac{C_B}{1-C_B} \right) \frac{h_{Gp}}{7.3} \right] \end{aligned} \tag{66}$$

STRENGTH CAPACITY PONDING CHECK

To design for ponding, a designer can include the ponding moment demands—from this article—in the appropriate ASCE 7-05 load combination and then compare it to the capacity from Chapter F of the 2005 AISC *Specification*:

$$\begin{aligned} M_u &\le \phi M_n \\ 1.2M_D + 1.6\left(M_{R\,or\,S} + M_P\right) &\le 0.9M_n \end{aligned} \tag{67}$$

or

$$\begin{aligned} M_u &\le \frac{M_n}{\Omega_b} \\ M_D + M_{R\,or\,S} + M_P &\le \frac{M_n}{1.67} \end{aligned} \tag{68}$$

This is consistent with the general provisions of ASCE 7-05 and AISC; however, it conflicts with the provisions of Appendix 2 of the 2005 AISC *Specification*.

Present Code Provisions

In Appendix 2 of the 2005 AISC *Specification*, the ponding check is a service load stress check:

$$f_b = f_o + f_w = \frac{M_o + M_w}{S_x} \le 0.8F_y$$

At the time this ponding stress check was adopted, the AISC flexural capacity was also a service load stress check, but with a different safety factor:

$$M_o \le 0.66F_y$$

Thus, the present AISC ponding design provision allows a stress increase for the ponding moment of 0.8/0.66 = 1.21. Conversely, the ponding demand was reduced by 0.66/0.8 = 0.825.

The reason behind this stress increase appears to be an assumption that the current snow and rain load demands already account for some amount of ponding load. Thus, combining ponding with the other loading is slightly redundant. Incorporating this into the demand capacity check gives:

$$0.83\left[1.2\,M_D + 1.6\left(M_{R\,or\,S} + M_P\right)\right] \le 0.9\,M_n \tag{69}$$

and

$$0.83\left(M_D + M_{R\,or\,S} + M_P\right) \le \frac{M_n}{1.67} \tag{70}$$

Another inherent assumption in the current AISC ponding provision is that the beam's compression flanges can be assumed fully braced regardless of the actual conditions. By allowing $0.8F_y$ flexural stress, without checking for flange bracing, the current code implies that lateral-torsional buckling can be ignored.

Rain Loading on Roof Areas away from Drains

For rain loading, ASCE 7-05 specifies the depth of water due to clogged primary roof drains. If the roof is sloped, then this loading only applies near the roof drains. No loading is specified for the roof area away from the water pooled around the drain.

It would be reasonable to include a rain load for ponding checks away from this area. This can be calculated using the

rainfall rate, the tributary area of roof uphill from the beam, and an open channel flow depth calculation. For most roofs, this would be a very shallow flow depth and loading. This author recommends a minimum rain load of 5 psf.

CONCLUSION

The current ponding provisions of the 2005 AISC *Specification* can be expanded to include more unique conditions. There also may be a benefit to formatting the analysis to more closely mesh with the other code provisions. This would allow the ponding analysis to be interpreted, adapted to unique conditions, improved, and calibrated to other provisions of the code.

The current AISC procedure frames a specific condition simply and directly, but obscures its inner workings, making it difficult to adapt to other conditions.

There are some actions not included in this model. Inelastic action would induce larger deflections for moments above the beam's yield limit, though this is usually not the case. Residual stresses in rolled beams can affect the deflection in ways similar to inelastic action. Camber variability is very common and would also induce errors in this calculation.

There have been few, if any, documented failures due to ponding—though it is possible that ponding played a role in past snow load– or clogged-roof-drain–induced failures. It is likely that the current procedure is too conservative. This is a paradox, because the current procedure uses a lower factor of safety than the ASCE and AISC codes. With a more accurate design calculation, and refinement in the procedures, it is possible that less structural steel could be used on future roofs.

REFERENCES

AISC (2005), *Specification for Structural Steel Buildings*, American Institute of Steel Construction, Chicago, IL.

ASCE (2005), *Minimum Design Loads for Buildings and Other Structures, ASCE 7-05*, American Society of Civil Engineers, Reston, VA.

Avent, R.R. and Stewart, G.S. (1975), "Rainwater Ponding on Beam-Girder Roof Systems," *Journal of the Structural Divisions*, ASCE, Vol. 101, No. ST9, September, pp. 1913–1927.

Carter, C.J. and Zuo, J. (1999), "Ponding Calculations in LRFD and ASD," *Engineering Journal*, AISC, Vol. 36, No. 3, 3rd quarter.

Chinn, J. (1965), "Failure of Simply-Supported Flat Roofs by Ponding of Rain," *Engineering Journal*, AISC, April.

Marino, F.J. (1966), "Ponding of Two-Way Roof Systems," *Engineering Journal*, AISC, Vol. 3, No. 3.

Milbradt, K.P. (2000), "Discussion–Ponding Calculations in LRFD and ASD Paper by Charles J. Carter and Jiahong Zuo," *Engineering Journal*, AISC, Vol. 37, No. 4, 4th quarter.

Ruddy, J.L., (1986), "Ponding of Concrete Deck Floors," *Engineering Journal*, AISC, 3rd quarter.

Sawyer, D.A. (1967), "Ponding of Rainwater on Flexible Roof Systems," *Journal of Structural Division*, ASCE, Vol. 94, No. ST1, Proc. Paper 5094, pp. 127–147.

Single-Plate Shear Connection Design to Meet Structural Integrity Requirements

LOUIS F. GESCHWINDNER and KURT D. GUSTAFSON

ABSTRACT

Specific prescriptive structural integrity provisions have been added to both model and local building codes since the collapse of the buildings at the World Trade Center site in 2001. The first building code to incorporate specific requirements was the 2008 New York City Building Code, which was followed quickly by the 2009 International Building Code. This paper demonstrates how properly designed single-plate shear connections comply with the structural integrity provisions of IBC 2009 and also make appropriate comparisons with NYC 2008.

Keywords: building code, structural integrity, single-plate shear connection.

Structural integrity has always been one of the goals for the structural engineer carrying out an engineering design and for the committees writing design standards. However, it has only been since the collapse of the buildings at the World Trade Center site that requirements with the stated purpose of addressing structural integrity have appeared in U.S. building codes. The first building code to incorporate specific requirements was the New York City Building Code (NYC, 2008) which was followed quickly by the International Building Code (ICC, 2009). Although the requirements of these two building codes are similar, there are some specifics that make their application different. Appendix A presents the provisions of the New York City code that are pertinent to this discussion, and Appendix B presents the appropriate International Building Code provisions. Appendix C summarizes the AISC *Specification* equations referenced in this paper.

This paper will demonstrate how properly designed single-plate shear connections comply with the structural integrity provisions of IBC 2009 and will also make appropriate comparisons with NYC 2008.

INTERNATIONAL BUILDING CODE REQUIREMENTS

Section 1614 of IBC 2009 provides structural integrity requirements that apply to high-rise buildings in occupancy categories III and IV. Simply stated, this means buildings with an occupied floor more than 75 ft above fire department vehicle access that represent a substantial hazard to human life in the event of failure or that are essential facilities. Thus, the number of buildings that these requirements apply to is limited.

Two types of member connections are addressed for steel frame structures, Section 1614.3.2.1 addresses column splices and 1614.3.2.2 addresses beam connections. This paper looks at one particular beam connection, the single-plate shear connection as shown in Figure 1. The provisions state that "all beams and girders shall have a minimum nominal axial tensile strength equal to the required vertical shear strength for allowable stress design (ASD) or two-thirds of the required shear strength for load and resistance factor design (LRFD) but not less than 10 kips." It also states that "For the purpose of this section, the shear force and axial tensile force need not be considered to act simultaneously." Using the terminology of AISC 360-05 *Specification for Structural Steel Buildings* (AISC, 2005a), these requirements can be stated as

$$T_n \geq V_a \qquad \text{(ASD)} \tag{1}$$

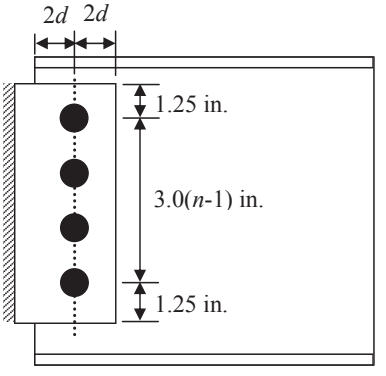

Fig. 1. Conventional configuration single-plate shear connection.

Louis F. Geschwindner, P.E., Ph.D., Vice President, American Institute of Steel Construction, Chicago, IL (corresponding author). E-mail: geschwindner@aisc.org

Kurt D. Gustafson, S.E., P.E., Director of Technical Assistance, American Institute of Steel Construction, Chicago, IL. E-mail: solutions@aisc.org

$$T_n \geq \frac{2}{3} V_a \qquad \text{(LRFD)} \tag{2}$$

and

$$T_n \geq 10.0 \text{ kips} \tag{3}$$

where

T_n = nominal tensile strength
V_a = required shear strength for ASD
V_u = required shear strength for LRFD

Section 1614.3.2.2 provides an exception that will be addressed later.

Design of the connection for shear under normal loading requires that available strength be greater than or equal to required strength. This can be stated as

$$V_a \leq \frac{V_n}{\Omega} \qquad \text{(ASD)} \tag{4}$$

or

$$V_u \leq \phi V_n \qquad \text{(LRFD)} \tag{5}$$

where

V_n = nominal shear strength
Ω = safety factor for ASD
ϕ = resistance factor for LRFD

The right hand side of Equations 4 and 5 is the available shear strength for ASD and LRFD, respectively. Although the required shear strength must always be less than or equal to the available shear strength, it will be useful in this presentation to look at the limit where required shear strength is equal to the available shear strength. Thus, solving Equations 4 and 5 at the limit for V_n yields

$$\Omega V_a = V_n \qquad \text{(ASD)} \tag{6}$$

$$\frac{V_u}{\phi} = V_n \qquad \text{(LRFD)} \tag{7}$$

Setting Equations 6 and 7 equal and solving for V_a yields

$$V_a = \frac{V_u}{\phi \Omega} \tag{8}$$

Calibration of the ASD and LRFD provisions in AISC 360-05 is based on the fixed relationship $\phi\Omega = 1.5$. Thus, Equation 8 becomes

$$V_a = \frac{V_u}{1.5} = \frac{2}{3} V_u \tag{9}$$

If Equation 9 is substituted into Equation 1, the structural integrity requirements for ASD are seen to be exactly the same as those for LRFD, thus

$$T_n \geq \frac{2}{3} V_u \tag{10}$$

Equation 10 has the nominal tension strength on one side and the required shear strength on the other. If it is again recognized that the required strength cannot exceed the minimum design strength, $V_u = \phi V_n$ may be substituted into Equation 10 and the building code requirement restated as

$$1.5 T_n \geq \phi V_n \tag{11}$$

Using Equation 11, all limit states may be checked without regard to any actual loading condition. If it can be shown that $1.5T_n$ is greater than the design shear strength for any particular limit state, Equation 11 is satisfied and the building code requirements have been satisfied.

In addition, it is not necessary to know the exact minimum available shear strength for every possible limit state if an upper-bound shear strength and a lower-bound tension strength are used. If it can be shown that $1.5T_n$ is greater than the available shear strength for any one shear limit state, it will be greater than the controlling minimum available shear strength. For many of the limit states to be checked in this paper, similar limit states will be considered for shear and tension because this will likely make the comparisons easiest. However, for some limit states, it will be easier to compare the results from different limit states.

SINGLE-PLATE SHEAR CONNECTION—CONVENTIONAL CONFIGURATION

Conventional configuration single-plate shear connections are defined in Part 10, page 10-101 of the 13th Edition *Steel Construction Manual* (AISC, 2005b). Design strength values are provided in Tables 10-9a and 10-9b.

The following eight limit states must be checked for a tension force applied to the single-plate shear connection shown in Figure 1:

- Bolt shear
- Weld
- Plate yield
- Plate rupture
- Bolt bearing and tearout on plate
- Bolt bearing and tearout on beam web
- Block shear on plate
- Block shear on beam web

1. Bolt Shear

Bolt shear strength is controlled by AISC *Specification* Eq. J3-1 and is independent of the direction of application of the load. Thus, the nominal shear strength of a bolt can be taken as r_n. With $\phi = 0.75$ and n being the number of bolts,

$$\phi V_n = 0.75 n r_n \tag{12}$$

and

$$1.5 T_n = 1.5 n r_n \tag{13}$$

Thus, it can be seen that Equation 11 is always satisfied for bolt shear since

$$1.5nr_n > 0.75nr_n \tag{14}$$

2. Weld

The conventional configuration single-plate shear connection is required to have two fillet welds ⅝ the thickness of the plate, t_p. This ensures that the weld will not be a critical element when using 36-ksi or 50-ksi plate material. The design strength of the weld, based on AISC *Specification* Eq. J2-4 and $\phi = 0.75$, is

$$\phi R_n = 1.392Dl \tag{15}$$

where D is the weld size in sixteenths of an inch and l is the length in inches. For two ⅝-in. welds, $D = 20$ and the design shear strength is

$$\phi V_n = 1.392\left(20t_p\right)l = 27.8t_p l \tag{16}$$

For tension, two modifications will be made. First, the tension force is applied at 90° to the longitudinal axis of the weld so an increase of 1.5 in the strength is applicable according to AISC *Specification* Eq. J2-5. Second, the design strength of the weld as given in Equation 15 includes the resistance factor, $\phi = 0.75$, so this factor must be removed. Thus,

$$1.5T_n = 1.5\left(1.5\left[1.392\left(20t_p\right)l\right] / 0.75\right) = 83.5t_p l \tag{17}$$

From Equations 16 and 17, it can be seen that Equation 11 is always satisfied for weld strength because

$$83.5t_p l > 27.8t_p l \tag{18}$$

3. Plate Yield

The limit state for yielding of the plate in shear is controlled by AISC *Specification* Eq. J4-3. Therefore, with $\phi = 1.00$,

$$\phi V_n = 1.00\left(0.6F_y\right)t_p l = 0.6F_y t_p l \tag{19}$$

For the limit state of yielding of the plate in tension, AISC *Specification* Eq. J4-1 controls. Thus,

$$1.5T_n = 1.5F_y t_p l \tag{20}$$

From Equations 19 and 20, it can be seen that Equation 11 is always satisfied for plate yielding because

$$1.5F_y t_p l > 0.6F_y t_p l \tag{21}$$

Table 1. Design Shear Strength as a Function of Bolt Diameter

Bolt diameter, d (in.)	Design shear strength, ϕV_n
¾	$1.35nt_pF_u$
⅝	$1.58nt_pF_u$
1	$1.80nt_pF_u$
1⅛	$2.03nt_pF_u$

4. Plate Rupture

The limit state for plate rupture in shear is given by AISC *Specification* Eq. J4-4. Therefore, with $\phi = 0.75$,

$$\phi V_n = 0.75\left(0.6F_u t_p l_n\right) = 0.45F_u t_p l_n \tag{22}$$

where l_n is the net shear area. Tensile rupture is given by AISC *Specification* Eq. J4-2. By definition, the net area of the plate for shear and tension are the same. Thus,

$$1.5T_n = 1.5F_u t_p l_n \tag{23}$$

From Equations 22 and 23, it can be seen that Equation 11 is always satisfied for plate rupture because

$$1.5F_u t_p l_n > 0.45F_u t_p l_n \tag{24}$$

5. Bolt Bearing and Tearout on Plate

Bearing and tearout are controlled by the provisions of AISC *Specification* Section J3.10. For shear, deformation at service load is a normal design consideration. The requirements stated in AISC *Specification* Eq. J3-6a apply when using standard or short slotted holes, both of which are permitted for conventional configuration single-plate shear connections. For the design shear strength, all bolts are assumed to be at their full bearing strength as given by the right side of AISC *Specification* Eq. J3-6a. This is an upper limit on the design shear strength, so its use will be conservative, regardless of the tearout strength dictated by the distance L_{ev}. Thus, with $\phi = 0.75$,

$$\phi V_n = n\left[0.75\left(2.4d\right)t_p F_u\right] = 1.8ndt_p F_u \tag{25}$$

where d is the bolt diameter.

With strength seen as a function of bolt diameter, Table 1 shows the solution of Equation 25 for four different bolt diameters used in the conventional configuration single-plate shear connection.

Table 2. Bolt Tearout Length and Tensile Strength for SSL Holes		
Bolt diameter, d (in.)	Tearout length, L_c (in.)	Tensile strength, $1.5T_n$
¾	1.000	$2.25nt_pF_u$
⅝	1.188	$2.67nt_pF_u$
1	1.344	$3.02nt_pF_u$
1⅛	1.500	$3.38nt_pF_u$

For consideration of structural integrity, deformation does not need to be a design consideration, as provided in Section B3.2 of the final draft of the 2010 AISC *Specification*. Thus, the nominal tensile strength is controlled by 2005 AISC *Specification* Eq. J3-6b. The conventional configuration, *Manual* page 10-102, requires that the horizontal distance from the bolt hole center to the loaded edge, L_{eh}, be at least $2d$. Thus, tearout would control over bearing and

$$1.5T_n = 1.5\left[n\left(1.5L_c t_p F_u\right)\right] = 2.25nL_c t_p F_u \qquad (26)$$

With $L_{eh} = 2d$ as stated earlier, the clear distance for tearout with standard holes is $L_c = 2d - 0.5(d + 1/16) = 1.5d - 0.0313$. For short slotted holes, hole dimensions are given in AISC *Specification* Table J3.3. Table 2 shows the clear distance for tearout, L_c, as a function of bolt diameter for short slotted holes and the corresponding tensile strength, $1.5T_n$. Because the tearout strength will be greater for standard holes than for short slotted holes, short slotted holes will provide a conservative comparison.

A comparison between Tables 1 and 2 shows that for each bolt size and either standard holes or short slotted holes, Equation 11 is satisfied for bolt bearing and tearout of the plate. If deformation were to be a design consideration for tension, the tensile strength in Table 2 would be reduced by 0.8 and the tensile strength would still be greater than the shear strength.

6. Bolt Bearing and Tearout on Beam Web

The assessment of bolt bearing and tearout on the beam web follows the same procedure as for the plate. For shear, all bolts are assumed to be at their full bearing strength. This will be used even if the beam is coped because it gives an upper bound on the shear strength. The tearout distance for the beam web is taken as $2d$, as it was for the plate. Thus, the values in Tables 1 and 2 may be used for the beam web by simply replacing t_p with t_b. Thus, Equation 11 is satisfied for bolt bearing and tearout of the beam web for standard and short slotted holes.

Table 3. Bolt Tearout Length and Tensile Strength for Standard Holes with $L_{eh} = 1.5d$		
Bolt diameter, d (in.)	Tearout length, L_c (in.)	Tensile strength, $1.5T_n$
¾	0.719	$1.62nt_pF_u$
⅝	0.844	$1.90nt_pF_u$
1	0.969	$2.18nt_pF_u$
1⅛	1.094	$2.46nt_pF_u$

Table 4. Net Length for Determination of Ultimate Shear Strength	
Bolt diameter, d (in.)	Net length, l_{n2} (in.)
¾	1.06
⅝	1.25
1	1.44
1⅛	1.63

If only standard holes are used in the beam web, the tearout distance can be reduced to $1.5d$ and Equation 11 is still satisfied as seen by comparing the results in Table 3 with those in Table 1.

7. Block Shear on Plate

Block shear strength is controlled by the provisions of AISC *Specification* Section J4.3 and specifically Eq. J4-5. For the design shear strength, it will be assumed that shear rupture in combination with tension rupture will control. This will give an upper-bound strength if shear yielding happened to control. In addition, for one line of bolts $U_{bs} = 1.0$. Figure 2(a) shows the single-plate with the block shear failure planes for a shear loading noted. AISC *Specification* Eq. J4-5, considering only rupture and $\phi = 0.75$, can be written as

$$\phi V_n = 0.75\left(F_u l_{n2} t_p + 0.6F_u l_{n1} t_p + 0.6F_u l_{n3} t_p\right) \qquad (27)$$

For the geometry of the conventional configuration single-plate shear connection, with a bolt spacing of 3.0 in., $l_1 = 3.0(n - 1)$ in., $l_2 = 2d$ in., $l_3 = 1.25$ in. For standard holes and short slotted holes, the net length for line 2 will always be greater than the net length for line 3. Thus, it will be conservative to let $l_{n3} = l_{n2}$. Therefore

$$\phi V_n = \left(0.45l_{n1} + 1.2l_{n2}\right)F_u t_p \qquad (28)$$

Table 4 shows the net length, l_{n2}, for standard holes to be used in Equation 28.

Table 5. Determination of Controlling Limit State for Tension				
Bolt diameter, d (in.)	Gross length, $l_{g2} = 2d$ (in.)	Net length, l_{n2} (in.)	$\frac{F_y}{F_u} l_{g2}$ (in.)	
			A36	A572 Gr. 50
¾	1.50	0.969	0.932	1.15
⅝	1.75	1.16	1.09	1.35
1	2.00	1.31	1.24	1.54
1⅛	2.25	1.47	1.40	1.73

The block shear planes for the tension force are shown in Figure 2(b). With the shear rupture terms controlling, AISC *Specification* Eq. J4-5 becomes

$$1.5T_n = 1.5\left[F_u l_{n1} t_p + 2\left(0.6F_u l_{n2} t_p\right)\right] = \left[1.5l_{n1} + 1.2\left(1.5l_{n2}\right)\right] F_u t_p \quad (29)$$

and with shear yielding terms controlling, Eq. J4-5 becomes

$$1.5T_n = 1.5\left(F_u l_{n1} t_p + 1.2F_y l_{g2} t_p\right) = \left[1.5l_{n1} + 1.2\left(1.5\frac{F_y}{F_u} l_{g2}\right)\right] F_u t_p \quad (30)$$

A comparison of Equations 29 and 30 shows that the smaller of l_{n2} or $(F_y/F_u)l_{g2}$ will give the lower bound tensile strength. Table 5 shows the lengths needed to determine which limit state controls for the four considered bolt diameters using short slotted holes with $l_{n2} = 2d - 0.5(SSL + 1/16)$.

For these four bolt diameters and A36 steel, $(F_y/F_u)l_{g2}$ is smaller than l_{n2}, so yielding will control and the comparisons required to satisfy Equation 11 will be between Equations 28 and 30. For A572 Gr. 50 steel, l_{n2} is smaller than $(F_y/F_u)l_{g2}$, so rupture controls and the comparisons required to satisfy Equation 11 will be between Equations 28 and 29.

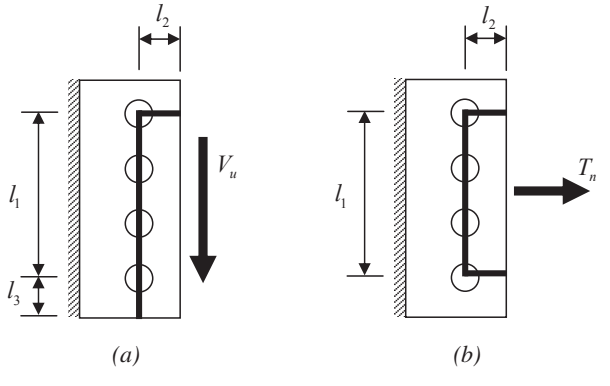

Figure 2. Geometry for block shear on plate.

Table 6. Second Term in Equations 29 and 30				
Bolt diameter, d (in.)	A36		A570 Gr. 50	
	$\frac{F_y}{F_u} l_{g2}$ (in.)	$1.5\left(\frac{F_y}{F_u} l_{g2}\right)$ (in.)	Net length, l_{n2} (in.)	$1.5l_{n2}$ (in.)
¾	0.932	1.40	0.969	1.45
⅝	1.09	1.64	1.16	1.74
1	1.24	1.86	1.31	1.97
1⅛	1.40	2.10	1.47	2.21

Table 7. Bearing and Tearout on Beam Web	
Bolt diameter, d (in.)	Design shear strength, ϕV_n
¾	$1.35nt_bF_u$
⅝	$1.58nt_bF_u$
1	$1.80nt_bF_u$
1⅛	$2.03nt_bF_u$

The comparison between shear and tension will be made in two parts. First, because the definition of l_{n1} is the same for shear and tension, the contribution for length l_{n1} will always be greater in resisting tension. That leaves the comparison to be based on the second term of each equation. The definition of l_{n2} is different for shear and tension because standard holes are used to get the maximum for shear and short slotted holes are used to get the minimum for tension. Table 6 gives the appropriate second term for tension strength to be compared to the second term for shear strength.

A comparison between Tables 4 and 6 shows that Equation 11 is satisfied for block shear in the plate for the four bolt diameters considered, for standard or short slotted holes, and for both A36 and A572 Gr. 50 steels.

8. Block Shear on Beam Web

For the first seven limit states considered in this paper for the single-plate shear connection, the same limit state was assessed for design shear strength and nominal tension strength. Although it is not imperative that it be done this way, it generally makes the comparisons easier because the same parameters are being used for each strength. For the case of block shear on the beam web, it will be easier to consider block shear for the tension force while considering bearing and tearout for the shear force. Table 7, taken from

Table 8a. Block Shear Strength for Tension Force—Tension Component		
Bolt diameter, d (in.)	$l_{n1} = (n - 1)(3.0 - d - 1/8)$ (in.)	T_n (tension)
3/4	$2.125(n - 1)$	$2.125(n - 1)t_bF_u$
5/8	$2.00(n - 1)$	$2.00(n - 1)t_bF_u$
1	$1.875(n - 1)$	$1.875(n - 1)t_bF_u$
1 1/8	$1.75(n - 1)$	$1.75(n - 1)t_bF_u$

Table 8b. Block Shear Strength for Tension Force—Shear Component		
Bolt diameter, d (in.)	$l_{n2} = 2d - 0.5(SSL + 1/16)$. (in.)	T_n (shear)
3/4	0.969	$1.16t_bF_u$
5/8	1.16	$1.39t_bF_u$
1	1.31	$1.57t_bF_u$
1 1/8	1.47	$1.76t_bF_u$

Table 1 with the beam web thickness replacing the plate thickness (limit state 6), gives the shear strength that will be used to assess the beam web for block shear in tension.

Figure 3 shows the beam web with the block shear planes defined for resisting the tension force. Because the beam will be A992 steel, the controlling limit state for the shear planes will be rupture and Equation 29, modified to represent the beam web rather than the plate, is

$$1.5T_n = \left[1.5l_{n1} + 1.2\left(1.5l_{n2}\right)\right]F_u t_b \tag{31}$$

The net length for the tension rupture term, l_{n1}, is a function of the number of bolts and bolt spacing. Using a standard spacing of 3.0 in. yields

$$l_{n1} = (n-1)\left(3.0 - d - 1/8\right) \tag{32}$$

The net length for the shear rupture term, l_{n2}, with $L_{eh} = 2d$ and short slotted holes can be determined from

$$l_{n2} = 2d - 0.5\left(SSL + 1/16\right) \tag{33}$$

where SSL is the slot length as defined in AISC *Specification* Table J3.3.

Tables 8a, 8b and 8c give the net lengths and the nominal tensile strength as a function of the number of bolts, n.

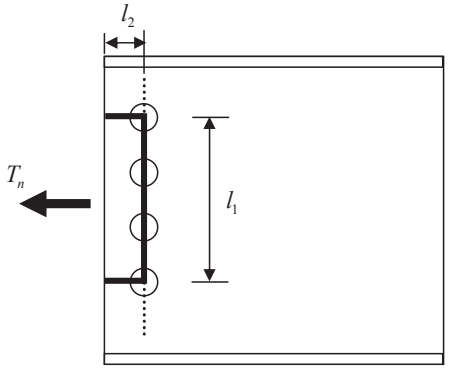

Figure 3. Geometry for block shear on beam web.

Table 8c. Block Shear Strength for Tension Force Total	
Bolt diameter, d (in.)	$1.5T_n$
3/4	$(3.19(n - 1) + 1.74)t_bF_u$
5/8	$(3.00(n - 1) + 2.09)t_bF_u$
1	$(2.81(n - 1) + 2.36)t_bF_u$
1 1/8	$(2.63(n - 1) + 2.64)t_bF_u$

In order to make the necessary comparisons called for by Equation 11, an assessment must be made for number of bolts from 2 through 12, as provided in the conventional configuration definition. As an example, five 1.00-in.-diameter bolts will be checked. From Table 7,

$$\phi V_n = 1.80nt_bF_u = 9.00t_bF_u \tag{34}$$

and from Table 8c,

$$1.5T_n = \left[2.81(n-1) + 2.36\right]t_bF_u = 13.6t_bF_u \tag{35}$$

Similarly, in all cases, Equation 11 is satisfied for the block shear pattern shown in Figure 3.

If the beam is coped, a comparison can be made using only one shear plane for the tension strength. That is accomplished by considering only one half of the value given in Table 8b. Equation 11 is satisfied for all combinations of bolts considered in this way for the coped beam except for two bolts with 1.125-in. diameter. However, for this one condition, a very small contribution from the tension plane above the top hole will add sufficient strength to satisfy Equation 11. Thus, block shear on the beam web is satisfied for all conditions considered.

Summary for IBC

It has been shown that for every applicable limit state required to resist the structural integrity tensile force, the single-plate shear connection has sufficient strength. These connections have been shown to satisfy the basic

Table 9. Minimum Edge Distance for NYC 2008					
	Standard Holes			Short Slotted Holes	
Bolt diameter, d (in.)	L_{eh} (in.)	L_{eh}/d	SSL	L_{eh} (in.)	L_{eh}/d
¾	1.606	2.14	1.0000	1.700	2.27
⅝	1.869	2.14	1.1250	1.963	2.24
1	2.131	2.13	1.3125	2.256	2.26
1⅛	2.394	2.13	1.5000	2.550	2.27

requirement without relying on the exception provided in IBC 2009 Section 1614.3.2.2. Thus, no further calculations will be required in the design phase for conventional configuration single-plate shear connections to show compliance with the IBC structural integrity provisions.

NYC BUILDING CODE REQUIREMENTS

The requirements of the New York City Building Code (NYC, 2008) are given in Appendix A. A review of these requirements shows that all bolted connections must have two bolts and that in connections that are part of the lateral load resisting system, bearing type connections are acceptable but that the bolts must be pretensioned. For beam end connections that are not part of the lateral load resisting system, "all beams and girders shall have a design axial tension strength equal to the larger of the provided vertical shear strength of the connection at either end but not less than 10 kips." This edition of the NYC Building Code permits design by ASD according to the 1989 ASD *Specification* or LRFD according to the 1999 LRFD *Specification*. Unfortunately, the terminology used in the building code is not consistent with the specifications referenced. Using AISC 360-05, these requirements, in the form of Equations 1 and 2, can be stated as

$$\frac{T_n}{\Omega} \geq \frac{V_n}{\Omega} \qquad \text{(ASD)} \qquad (36)$$

$$\phi T_n \geq \phi V_n \qquad \text{(LRFD)} \qquad (37)$$

It should be noted that the safety factors, Ω, and the resistance factors, ϕ, shown are not necessarily equal on each side of Equations 36 and 37 because they will vary depending on the limit state being considered. For single-plate shear connections, the only limit state to be evaluated for resisting the structural integrity tension force, as given in Section 2213.2.3.1, is bolt bearing and tearout without deformation being a design consideration. Bolt shear is not mentioned in the NYC Building Code because the available strength of the bolts in shear is the same when they are resisting beam shear or beam tension.

Thus, the nominal axial tension strength is to be determined according to AISC *Specification* Eq. J3-6b, where deformation is not a design consideration. The right side of Equation 37 is the same as the right side of Equation 11. Thus, an approach similar to that used to show compliance with the requirements of IBC 2009 can be used here. The bearing and tearout limit states were addressed in cases 5 and 6 for IBC 2009. From Equation 26, without the 1.5 increase,

$$T_n = \left[n\left(1.5L_c t_p F_u\right)\right] = 1.5nL_c t_p F_u \qquad (38)$$

In order to satisfy Equation 37, using Equation 25 for the provided shear strength, Equation 38 for the nominal tensile strength, and $\phi = 0.75$,

$$0.75\left(1.5nL_c t_p F_u\right) \geq 1.8nt_p dF_u \qquad (39)$$

This results in the requirement that

$$L_c \geq 1.6d \qquad (40)$$

For standard holes,

$$L_c = L_{eh} - \frac{1}{2}\left(d + \frac{1}{16}\right) \qquad (41)$$

Using Equations 40 and 41, the minimum edge distance for standard holes is

$$L_{eh} = 2.1d + 0.0313 \qquad (42)$$

For short slotted holes,

$$L_c = L_{eh} - \frac{1}{2}(SSL) \qquad (43)$$

Using Equations 42 and 43, the minimum edge distance for short slotted holes is

$$L_{eh} = 1.6d + \frac{SSL}{2} \qquad (44)$$

Table 9 shows the minimum edge distances to permit the conclusion that Equation 39 would always be satisfied.

With a slight increase in the conventional configuration edge distance from 2*d* to 2.3*d* in both the plate and the beam web, single-plate shear connections will always be adequate to resist the structural integrity tension force. However, that is not the best way to show compliance with the NYC Building Code requirements. Because there is only one limit state to be considered in resisting the structural integrity tension force, it will be a relatively simple task to determine the design strength, ϕT_n, of each conventional configuration single-plate shear connection given in the 13th Edition *Manual*. This strength is given in Appendix D of this paper—Table D-1 for standard holes and Table D-2 for short slotted holes, based on Equation 38 and $\phi = 0.75$. A comparison of the data in Appendix D with that in *Manual* Table 10-9 shows that in all cases the conventional configuration single-plate shear connection has sufficient design strength in tension to satisfy the NYC Building Code structural integrity provisions.

For any case where the beam web controls the shear strength of the connection, the tension strength can be determined using the results shown in Appendix D, modified proportionally for the appropriate beam web thickness. This would then be compared to the shear strength of the connection to confirm that Equation 37 is satisfied.

There is one additional issue that must be addressed with regard to the NYC Building Code provisions. That is the requirement that the structural integrity tension force for beams that are not symmetrically loaded be determined using the largest provided shear strength on either end of the member. There are an infinite number of combinations possible for the required shear strength at a beam end. The simplest way to satisfy this requirement, if the beam is not symmetrical, is to the make the connections symmetrical. That way, the connection at each end will be guaranteed to meet the structural integrity requirements.

CONCLUSIONS

Conventional configuration single-plate shear connections, as provided in Tables 10-9a and 10-9b of the 13th Edition *Steel Construction Manual*, were evaluated for compliance with the structural integrity provisions of the 2009 International Building Code (ICC, 2009) and the 2008 New York City Building Code (NYC, 2008). It was shown that these connections, when designed to resist shear according to the provisions of ANSI/AISC 360-05, will satisfy the structural integrity provisions of both building codes without any modification to their design. Clearly for conventional configuration single-plate shear connections, structural integrity, as defined by these two building codes, has already been assured by the provisions of the AISC *Specification* (AISC, 2005a) and the *Steel Construction Manual* (AISC, 2005b), without the need for the special requirements of building codes.

REFERENCES

AISC (2005a), *Specification for Structural Steel Buildings*, AISC/ANSI 360, American Institute of Steel Construction, Chicago, IL.

AISC (2005b), *Steel Construction Manual*, 13th Edition, American Institute of Steel Construction, Chicago, IL.

ICC (2009), *International Building Code*, International Code Council, Country Club Hills, IL.

NYC (2008), 2008 New York City *Building Code*, NYCBC, New York, NY.

APPENDIX A

2008 New York City Building Code Structural Integrity Provisions

SECTION BC 2213
STRUCTURAL INTEGRITY REQUIREMENTS

2213.2 Continuity and ties. The following requirements shall be met:

1. All bolted connections shall have at least two bolts.
2. Bolted connections of all columns, beams, braces and other structural elements that are part of the lateral load resisting system shall be designed as bearing-type connections with pretensioned bolts or as slip critical connections.
3. End connections of all beams and girders shall have a design axial tension strength equal to the larger of the provided vertical shear strength of the connections at either end, but not less than 10 kips (45 kN). For the design of the connections, the shear force and axial tensile force need not be considered to act simultaneously. For the purpose of this provision, a connection shall be considered compliant if it meets the following requirements:

   3.1 For single plate shear connections, the nominal axial tension strength shall be determined for the limit state of bolt bearing, where deformation is not a consideration, on the plate and beam web.

   3.2 For single angle and double angle shear connections, the nominal tension strength shall be determined for the limit state of bolt bearing, where deformation is not a consideration, on the angles and beam web and for tension yielding on the gross area of the angles.

   3.3 All other connections shall be designed for the required tension force in accordance with either AISC-LRFD, AISC 335, or AISC-HSS.

For the purpose of meeting this integrity provision only, bolts in connections with short-slotted holes parallel to the direction of the tension force are permitted. For the purpose of checking bearing, these bolts shall be assumed to be located at the end of the slots.

APPENDIX B

2009 International Building Code Structural Integrity Provisions

SECTION 1614
STRUCTURAL INTEGRITY

1614.1 General. Buildings classified as high-rise buildings in accordance with Section 403 and assigned to *Occupancy Category* III or IV shall comply with the requirements of this section. Frame structures shall comply with the requirements of Section 1614.3. Bearing wall structures shall comply with the requirements of Section 1614.4.

1614.3.2 Structural steel, open web steel joist or joist girder, or composite steel and concrete frame structures. Frame structures constructed with a structural steel frame or a frame composed of open web steel joists, joist girders with or without other structural steel elements or a frame composed of steel or composite steel joists and reinforced concrete elements shall conform to the requirements of this section.

1614.3.2.1 Columns. Each column splice shall have the minimum design strength in tension to transfer the design dead and live load tributary to the column between the splice and the splice or base immediately below.

1614.3.2.2 Beams. End connections of all beams and girders shall have a minimum nominal axial tensile strength equal to the required vertical shear strength for *allowable stress design* (ASD) or two-thirds of the required shear strength for *load and resistance factor design* (LRFD) but not less than 10 kips (45 kN). For the purpose of this section, the shear force and the axial tensile force need not be considered to act simultaneously.

Exception: Where beams, girders, open web joist and joist girders support a concrete slab or concrete slab on metal deck that is attached to the beam or girder with not less than 3/8-inch-diameter (9.5 mm) headed shear studs, at spacing of not more that 12 inches (305 mm) on center, averaged over the length of the member, or other attachment having equivalent shear strength, and the slab contains continuous distributed reinforcement in each of two orthogonal directions with an area not less than 0.0015 times the concrete area, the nominal axial tension strength of the end connection shall be permitted to be taken as half the required vertical shear strength for ASD or one-third of the required shear strength for LRFD, but not less than 10 kips (45 kN).

APPENDIX C

REFERENCED AISC 360-05 EQUATIONS

The following equations from the 2005 AISC *Specification for Structural Steel Buildings* have been referenced in this paper.

J2. Welds

$$R_n = F_w A_w \tag{J2-4}$$

$$F_w = 0.60F_{EXX}\left(1.0 + 0.50\sin^{1.5}\theta\right) \tag{J2-5}$$
$$\phi = 0.75$$

J3. Bolts and Threaded Parts

$$R_n = F_n A_b \tag{J3-1}$$

$$R_n = 1.2L_c tF_u \le 2.4dtF_u \tag{J3-6a}$$

$$R_n = 1.5L_c tF_u \le 3.0dtF_u \tag{J3-6b}$$
$$\phi = 0.75$$

J4. Affected Elements of Members and Connecting Elements

$$R_n = F_y A_g \tag{J4-1}$$
$$\phi = 0.90$$

$$R_n = F_u A_e \tag{J4-2}$$
$$\phi = 0.75$$

$$R_n = 0.60F_y A_g \tag{J4-3}$$
$$\phi = 1.0$$

$$R_n = 0.60F_u A_{nv} \tag{J4-4}$$
$$\phi = 0.75$$

$$R_n = 0.6F_u A_{nv} + U_{bs}F_u A_{nt} \le 0.6F_y A_{gv} + U_{bs}F_u A_{nt} \tag{J4-5}$$
$$\phi = 0.75$$

APPENDIX D

TENSION STRENGTH FOR USE WITH THE 2008 NEW YORK CITY BUILDING CODE

Table D-1. Design Tensile Strength for Plates with Standard Holes

F_y = 36 ksi
Bolt Diameter, ¾ in.
Standard Holes, clear distance, L_c = 1.0938 in.

n	Plate Thickness, in.					
	¼	5/16	⅜	7/16	½	9/16
12	214	268	321	375	428	482
11	196	245	294	344	393	442
10	178	223	268	312	357	401
9	161	201	241	281	321	361
8	143	178	214	250	286	321
7	125	156	187	219	250	281
6	107	134	161	187	214	241
5	89.2	112	134	156	178	201
4	71.4	89.2	107	125	143	161
3	53.5	66.9	80.3	93.7	107	120
2	35.7	44.6	53.5	62.4	71.4	80.3

F_y = 36 ksi
Bolt Diameter, ⅞-in.
Standard Holes, clear distance, L_c = 1.2813 in.

n	Plate Thickness, in.					
	¼	5/16	⅜	7/16	½	9/16
12	251	314	376	439	502	564
11	230	287	345	402	460	517
10	209	261	314	366	418	470
9	188	235	282	329	376	423
8	167	209	251	293	334	376
7	146	183	220	256	293	329
6	125	157	188	220	251	282
5	105	131	157	183	209	235
4	83.6	105	125	146	167	188
3	62.7	78.4	94.1	110	125	141
2	41.8	52.3	62.7	73.2	83.6	94.1

Table D-1. Design Tensile Strength for Plates with Standard Holes (cont.)

F_y = 36 ksi
Bolt Diameter, 1 in.
Standard Holes, clear distance, L_c = 1.4688 in.

n	Plate Thickness, in.					
	¼	5/16	3/8	7/16	½	9/16
12	288	359	431	503	575	647
11	264	329	395	461	527	593
10	240	300	359	419	479	539
9	216	270	323	377	431	485
8	192	240	288	335	383	431
7	168	210	252	294	335	377
6	144	180	216	252	288	323
5	120	150	180	210	240	270
4	95.8	120	144	168	192	216
3	71.9	89.8	108	126	144	162
2	47.9	59.9	71.9	83.9	95.8	108

F_y = 36 ksi
Bolt Diameter, 1⅛ in.
Standard Holes, clear distance, L_c = 1.6563 in.

n	Plate Thickness, in.					
	¼	5/16	3/8	7/16	½	9/16
12	324	405	486	567	648	730
11	297	372	446	520	594	669
10	270	338	405	473	540	608
9	243	304	365	426	486	547
8	216	270	324	378	432	486
7	189	236	284	331	378	426
6	162	203	243	284	324	365
5	135	169	203	236	270	304
4	108	135	162	189	216	243
3	81.1	101	122	142	162	182
2	54.0	67.5	81.1	94.6	108	122

Table D-1. Design Tensile Strength for Plates with Standard Holes (cont.)

F_y = 50 ksi
Bolt Diameter, ¾ in.
Standard Holes, clear distance, L_c = 1.0938 in.

n	Plate Thickness, in.					
	¼	5/16	3/8	7/16	½	9/16
12	240	300	360	420	480	540
11	220	275	330	385	440	495
10	200	250	300	350	400	450
9	180	225	270	315	360	405
8	160	200	240	280	320	360
7	140	175	210	245	280	315
6	120	150	180	210	240	270
5	100	125	150	175	200	225
4	80.0	100	120	140	160	180
3	60.0	75.0	90.0	105	120	135
2	40.0	50.0	60.0	70.0	80.0	90.0

F_y = 50 ksi
Bolt Diameter, ⅞ in.
Standard Holes, clear distance, L_c = 1.2813 in.

n	Plate Thickness, in.					
	¼	5/16	3/8	7/16	½	9/16
12	281	351	422	492	562	632
11	258	322	387	451	515	580
10	234	293	351	410	469	527
9	211	264	316	369	422	474
8	187	234	281	328	375	422
7	164	205	246	287	328	369
6	141	176	211	246	281	316
5	117	146	176	205	234	264
4	93.7	117	141	164	187	211
3	70.3	87.8	105	123	141	158
2	46.8	58.6	70.3	82.0	93.7	105

Table D-1. Design Tensile Strength for Plates with Standard Holes (cont.)

F_y = 50 ksi
Bolt Diameter, 1 in.
Standard Holes, clear distance, L_c = 1.4688 in.

n	Plate Thickness, in.					
	¼	5/16	⅜	7/16	½	9/16
12	322	403	483	564	644	725
11	295	369	443	517	591	665
10	269	336	403	470	537	604
9	242	302	363	423	483	544
8	215	269	322	376	430	483
7	188	235	282	329	376	423
6	161	201	242	282	322	363
5	134	168	201	235	269	302
4	107	134	161	188	215	242
3	80.6	101	121	141	161	181
2	53.7	67.1	80.6	94.0	107	121

F_y = 50 ksi
Bolt Diameter, 1⅛ in.
Standard Holes, clear distance, L_c = 1.6563 in.

n	Plate Thickness, in.					
	¼	5/16	⅜	7/16	½	9/16
12	363	454	545	636	727	818
11	333	416	500	583	666	749
10	303	379	454	530	606	681
9	273	341	409	477	545	613
8	242	303	363	424	485	545
7	212	265	318	371	424	477
6	182	227	273	318	363	409
5	151	189	227	265	303	341
4	121	151	182	212	242	273
3	90.8	114	136	159	182	204
2	60.6	75.7	90.8	106	121	136

Table D-2. Design Tensile Strength for Plates with Short Slotted Holes

F_y = 36 ksi
Bolt Diameter, ¾ in.
Short Slotted Holes, clear distance, L_c = 1.00 in.

n	Plate Thickness, in.					
	¼	5/16	⅜	7/16	½	9/16
12	196	245	294	343	392	440
11	179	224	269	314	359	404
10	163	204	245	286	326	367
9	147	184	220	257	294	330
8	131	163	196	228	261	294
7	114	143	171	200	228	257
6	97.9	122	147	171	196	220
5	81.6	102	122	143	163	184
4	65.3	81.6	97.9	114	131	147
3	48.9	61.2	73.4	85.6	97.9	110
2	32.6	40.8	48.9	57.1	65.3	73.4

F_y = 36 ksi
Bolt Diameter, ⅞ in.
Short Slotted Holes, clear distance, L_c = 1.188 in.

n	Plate Thickness, in.					
	¼	5/16	⅜	7/16	½	9/16
12	233	291	349	407	465	523
11	213	267	320	373	426	480
10	194	242	291	339	388	436
9	174	218	262	305	349	392
8	155	194	233	271	310	349
7	136	170	204	237	271	305
6	116	145	174	204	233	262
5	96.9	121	145	170	194	218
4	77.5	96.9	116	136	155	174
3	58.1	72.7	87.2	102	116	131
2	38.8	48.4	58.1	67.8	77.5	87.2

Table D-2. Design Tensile Strength for Plates with Short Slotted Holes (cont.)

F_y = 36 ksi
Bolt Diameter, 1 in.
Short Slotted Holes, clear distance, L_c = 1.344 in.

n	Plate Thickness, in.					
	¼	5/16	3/8	7/16	½	9/16
12	263	329	395	460	526	592
11	241	302	362	422	482	543
10	219	274	329	384	439	493
9	197	247	296	345	395	444
8	175	219	263	307	351	395
7	154	192	230	269	307	345
6	132	164	197	230	263	296
5	110	137	164	192	219	247
4	87.7	110	132	154	175	197
3	65.8	82.2	98.7	115	132	148
2	43.8	54.8	65.8	76.7	87.7	98.7

F_y = 36 ksi
Bolt Diameter, 1⅛ in.
Short Slotted Holes, clear distance, L_c = 1.50 in.

n	Plate Thickness, in.					
	¼	5/16	3/8	7/16	½	9/16
12	294	367	440	514	587	661
11	269	336	404	471	538	606
10	245	306	367	428	489	551
9	220	275	330	385	440	496
8	196	245	294	343	392	440
7	171	214	257	300	343	385
6	147	184	220	257	294	330
5	122	153	184	214	245	275
4	97.9	122	147	171	196	220
3	73.4	91.8	110	129	147	165
2	48.9	61.2	73.4	85.6	97.9	110

Table D-2. Design Tensile Strength for Plates with Short Slotted Holes (cont.)

Fy = 50 ksi
Bolt Diameter, ¾ in.
Short Slotted Holes, clear distance, L_c = 1.00 in.

n	Plate Thickness, in.					
	¼	5/16	3/8	7/16	½	9/16
12	219	274	329	384	439	494
11	201	251	302	352	402	453
10	183	229	274	320	366	411
9	165	206	247	288	329	370
8	146	183	219	256	293	329
7	128	160	192	224	256	288
6	110	137	165	192	219	247
5	91.4	114	137	160	183	206
4	73.1	91.4	110	128	146	165
3	54.8	68.6	82.3	96.0	110	123
2	36.6	45.7	54.8	64.0	73.1	82.3

F_y = 50 ksi
Bolt Diameter, ⅞ in.
Short Slotted Holes, clear distance, L_c = 1.188 in.

n	Plate Thickness, in.					
	¼	5/16	3/8	7/16	½	9/16
12	261	326	391	456	521	586
11	239	299	358	418	478	538
10	217	272	326	380	434	489
9	196	244	293	342	391	440
8	174	217	261	304	348	391
7	152	190	228	266	304	342
6	130	163	196	228	261	293
5	109	136	163	190	217	244
4	86.9	109	130	152	174	196
3	65.2	81.4	97.7	114	130	147
2	43.4	54.3	65.2	76.0	86.9	97.7

Table D-2. Design Tensile Strength for Plates with Short Slotted Holes (cont.)

F_y = 50 ksi
Bolt Diameter, 1 in.
Short Slotted Holes, clear distance, L_c = 1.344 in.

n	Plate Thickness, in.					
	¼	5/16	3/8	7/16	½	9/16
12	295	369	442	516	590	663
11	270	338	405	473	541	608
10	246	307	369	430	491	553
9	221	276	332	387	442	498
8	197	246	295	344	393	442
7	172	215	258	301	344	387
6	147	184	221	258	295	332
5	123	154	184	215	246	276
4	98.3	123	147	172	197	221
3	73.7	92.1	111	129	147	166
2	49.1	61.4	73.7	86.0	98.3	111

F_y = 50 ksi
Bolt Diameter, 1⅛ in.
Short Slotted Holes, clear distance, L_c = 1.50 in.

n	Plate Thickness, in.					
	¼	5/16	3/8	7/16	½	9/16
12	329	411	494	576	658	740
11	302	377	453	528	603	679
10	274	343	411	480	548	617
9	247	309	370	432	494	555
8	219	274	329	384	439	494
7	192	240	288	336	384	432
6	165	206	247	288	329	370
5	137	171	206	240	274	309
4	110	137	165	192	219	247
3	82.3	103	123	144	165	185
2	54.8	68.6	82.3	96.0	110	123

Current Steel Structures Research

REIDAR BJORHOVDE

The new feature that was introduced for the steel structures research papers in the second quarter issue for 2010 of the *Engineering Journal* continues with ongoing work at three major European universities. While we will not be able to discuss all of the current projects at the schools, a selection of studies will provide a representative picture of the research efforts and demonstrate the schools' importance to the efforts of industry and the profession worldwide.

The universities are very well known in the world of steel construction: Imperial College in London, England; Delft University of Technology in Delft, the Netherlands; and the University of Liège in Liège, Belgium. Researchers at the three schools have been very active for many years, as evidenced by their participation and leading roles in the standards development committees of Europe and for the past number of years in the committees of the European Union (EU) and the European Convention for Constructional Steelwork (ECCS). Faculty and staff have authored large numbers of outstanding technical papers, reports and conference presentations.

Some of the findings have also been adopted by the design specifications of North America. For example, the equation for the equivalent moment factor C_b that is used in the 2005 AISC *Specification* was developed by Professor Nethercot, and many parts of the classical plastic analysis techniques were based on work by Professors Massonnet and Maquoi at the University of Liège.

References are provided throughout the paper, whenever such are available in the public domain. However, much of the work is still in progress, and in some cases reports or publications have not yet been prepared for public dissemination.

IMPERIAL COLLEGE—SELECTED PROJECTS

Progressive Collapse of Steel and Composite Building Structures: Professor David A. Nethercot has been the director of the project, with Professors B. A. Izzuddin and A. Y. Elghazouli also as members of the research team. The project was initiated six years ago and is now reaching the practical application stage with a design approach that addresses all of the key features of progressive collapse (Izzuddin et al., 2008; Nethercot et al., 2009).

The method is based on the alternative load path approach as well as the threat-independent column removal concept. The procedure is based on a simplified process that transforms the static response of the gravity loads into a dynamic response. Using a multilevel approach, the response at any level of structural modeling can be assembled from the known responses at lower levels. The modeling considers levels such as floor system, substructures and the complete structure.

In an interesting twist, a hand calculation procedure has been introduced that improves and clarifies the analysis approach (Nethercot et al, 2009). For example, the response of a connection to bending moment and axial load during column removal is represented by an explicit, simplified model (Stylianidis and Nethercot, 2010). This was then utilized to develop the hand calculation method that predicts the nonlinear response under gravity load. Figure 1 illustrates these stages as they evolve, following the removal of the column.

Apart from the practical uses of the procedure, this method also facilitates parametric evaluations that are critical to understanding the mechanics of the phenomenon. Indeed, recent studies have shown that the response characteristics of the beam-to-column connections are the most important feature of a progressive collapse scenario. Further, both the form of the response and the inherent resistance against progressive collapse depend on the interaction between the various elements of the structure. Primary among these are of course the moment-rotation response of the connections and their individual elements, including the ability to resist axial loads and deformations. This applies equally to steel and composite structures, for which strength (axial tension and compression), stiffness and ductility are paramount. The span-to-depth ratio of the beam appears to be significant, and this also depends on the position of the removed column within the frame and the axial restraint that is afforded by the connections (Nethercot et al., 2009).

Current project work aims at developing the relationships between causes and effects, by evaluating the interaction between the structural parameters and taking into account the dynamic nature of the response. This also includes the characteristics of the behavior of the floor system, for which a grillage model may prove useful.

Reidar Bjorhovde, Ph.D., Research Editor for *Engineering Journal,* Tucson, AZ. E-mail: rbj@bjorhovde.com

Behavior of Semi-Rigid (PR) Wide-Flange Beam-to-Tubular Column Connections: Professor A. Y. Elghazouli has been the director of the project. Sometimes referred to as "open beam-to-tubular column connections," questions have been raised about their strength, stiffness and ductility, in particular the ability of the wall of the tube to provide adequate deformation capacity. This applies especially when cyclic loading has to be considered.

Despite the relatively high cost of some connections involving HSS columns, they do offer certain architectural and structural advantages. The perceived complexity of connecting wide-flange shapes to HSS columns sometimes means that such connections do not get selected for a project. The project was therefore undertaken to develop suitable, practical and economical PR connections with appropriate performance characteristics. The chosen connections were (1) top and seat angle connections, (2) top, seat and web angle connections, and (3) combined channel-and-angle connections, where a channel is shop-welded with the legs against the wall of the HSS, using a typical bolted connection from the beam to the channel (this could be a top and seat angle connection, or a top and seat angle with a web angle connection). For the Type 1 connections blind bolts were used to connect to the HSS, with so-called Lindapter Hollo-bolts (Elghazouli et al., 2009).

The analytical and experimental results have shown that these connections provide more than adequate rotation capacities for "typical design scenarios" (which are not defined, but presumably compare to typical U.S. practice). The connections exhibited stable hysteresis loops in the cyclical tests that were conducted, with reasonable ductility and energy absorption. Further, it has been found that it is very important to ensure that there is a reliable mechanism for the transfer of compression forces to the column. Finally, the tests also showed that significant improvements in stiffness and strength were achieved when Grade 10.9 (same as ASTM A490) Hollo-bolts were used, as compared to the connections that used Grade 8.8 bolts (same as ASTM A325). Figure 2(a) shows a Type 1 connection after the test; Figure 2(b) shows a combined channel-angle connection.

For the analytical and design procedure developments, simplified mechanical models have been created for providing initial connection stiffness and moment capacity. More refined models are currently being examined, including procedures that can be used to design for various extreme loading conditions.

Finally, related projects at Imperial College include studies of connections between tubular columns and reinforced concrete flat slabs, as well as the seismic performance of concentrically braced frames and composite moment-resisting frames.

Structural Use of Stainless Steel: The project director has been Dr. Leroy Gardner. Recognizing that stainless steel offers certain behavior and performance advantages for structures, the availability of stainless steel rolled shapes is still very limited, and cost figures are not available.

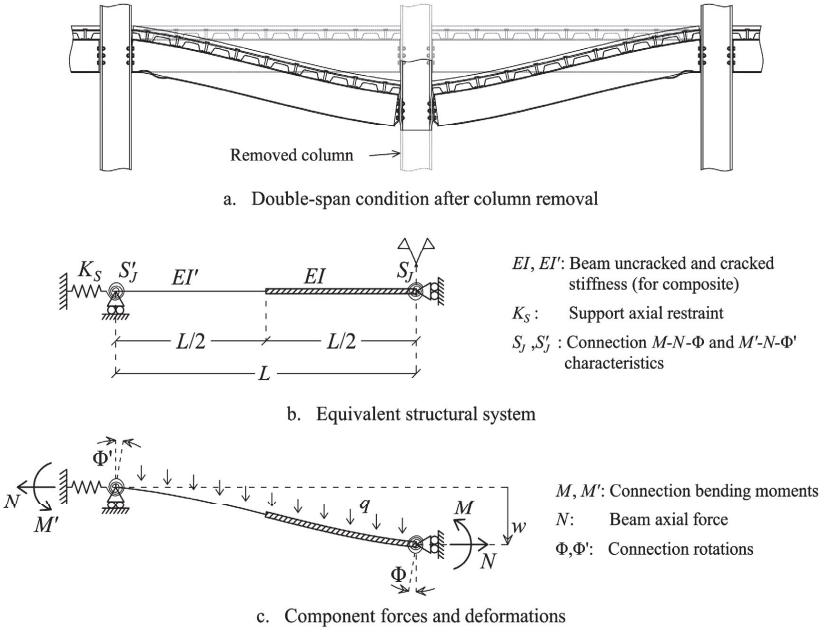

Fig. 1. Static load-deflection beam response following column removal (Figure courtesy of Professor D. A. Nethercot).

The primary stainless steel research efforts at Imperial College have focused on the following general subjects:

1. Improving the accuracy and efficiency of the design criteria, by taking into account the strength increases that are provided through the cold-forming process (Cruise and Gardner, 2008) and by considering the actual (rounded) stress-strain characteristic and strain hardening under load, using an innovative deformation-based design approach (Ashraf et al., 2008).
2. Examining the performance of stainless steel under fire and under seismic loading. For example, austenitic stainless steel performs better than carbon steel (no steel grade given) under elevated temperatures, but the larger thermal expansion of the stainless steel is problematic due to the increased axial restraint (Gardner and Baddoo, 2006). For seismic conditions, austenitic stainless steel offers improved energy dissipation than comparable carbon steel (no steel grade given), due to the delayed local buckling (Nip et al., 2010).
3. Studying the suitability of new grades of stainless steel for construction, especially the so-called "lean duplex" grades. On the European market, this steel is twice the strength of the more common austenitic stainless steel, and it costs less. Preliminary studies have verified the structural performance of the material, but further studies are needed (Theofanous and Gardner, 2010).

Structural Steel Elliptical Hollow Sections: Dr. Leroy Gardner has been the director for this project. These sections have found favor with a number of architectural firms, but they are still somewhat of a rarity. The studies at Imperial College have focused on physical tests and numerical analyses, with the aim of providing design criteria for international specifications. Column, beam bending and shear tests have been conducted (Chan and Gardner, 2008, 2009), and Figure 3 shows two examples of the tests.

The design criteria have aimed at developing an equivalent circular cross section (CHS) and that way to be able to take advantage of existing code provisions.

The Continuous Strength Method for Structural Steel Design: This is an ongoing research and development effort, headed by Dr. Leroy Gardner. Essentially, the work focuses on an improvement of the approach that is used in most current design specifications to account for nonlinear response characteristics. Traditional approaches represent the material behavior by simplified elastic-plastic or rigid-plastic models, and strain hardening is generally ignored, although the spread of plasticity throughout the cross sections and redistribution of moments in the frame are taken into account.

The study by Dr. Gardner focuses on what is now known as the continuous strength method (CSM). CSM uses a systematic procedure to account for strain hardening, and it is based on the deformation capacity of the cross section (Gardner, 2008). By incorporating the effects of strain hardening, the method allows for compressive strengths greater than the yield load and bending capacities higher than the plastic moment. The approach provides for a more accurate representation of the structural behavior. For compact (stocky) sections, for example, member strength increases of 15% can be achieved, when compared to current methods. Additional criteria are currently being developed.

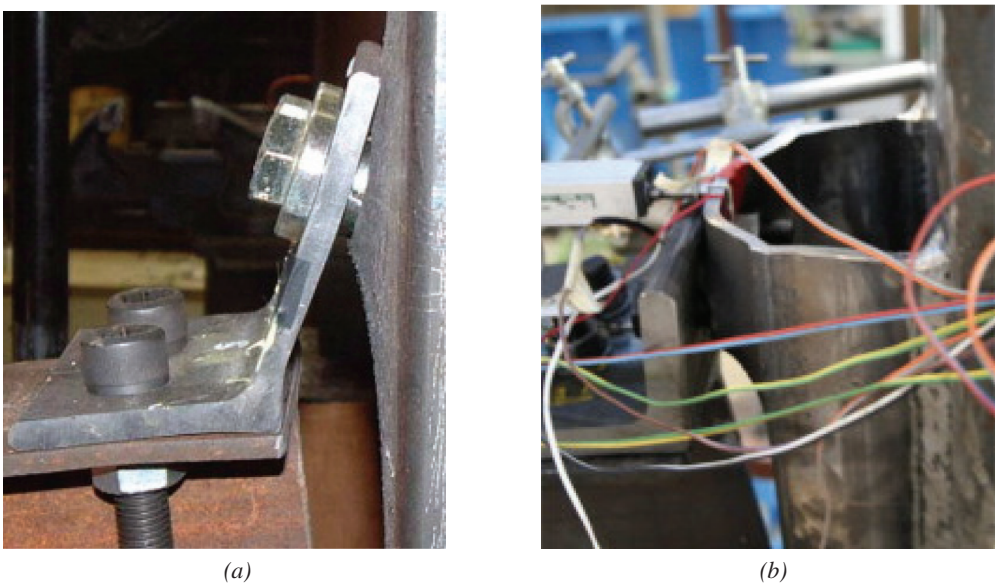

(a) *(b)*

Fig. 2. Semi-rigid connection tests: (a) top and seat angles with blind bolts; (b) combined channel and angle connection (Photos courtesy of Professor A. Y. Elghazouli).

DELFT UNIVERSITY OF TECHNOLOGY—SELECTED PROJECTS

Application of Cast Nodes and Very High Strength Steel in the Offshore Industry: This project has been sponsored by Materials Innovation Institute (M2i) of the Netherlands and Bouwen met Staal, the Dutch steel construction society. Professor Frans Bijlaard is the project director.

The very high strength steels (VHSS) that are part of the project have been available in the European market for a number of years. Nominal yield stress values are up to 160 ksi (1,100 MPa), but such steels have not seen much use within the civil engineering and offshore construction industries. The primary reason is simply that design and fabrication methods and data are very scarce, and at this time design standards do not recognize these steel grades. Among potential advantages would be smaller size members and reduced fabrication costs. On the other hand, the fatigue performance of VHSS structures is likely to be problematic, because stress levels and stress ranges will be much higher than what is the case for structures in lower strength steels. Furthermore, VHSS welded connections require much higher fabrication quality, to avoid large stress concentrations in the connections and to use optimal configurations of the welded joints.

Fatigue Strength of Hybrid Truss Girders: This project is a part of the study of cast nodes and very high strength steel. Professor Frans Bijlaard is the project director.

Hybrid truss girders appear to be an effective application for very high strength steel. These girders are very stiff

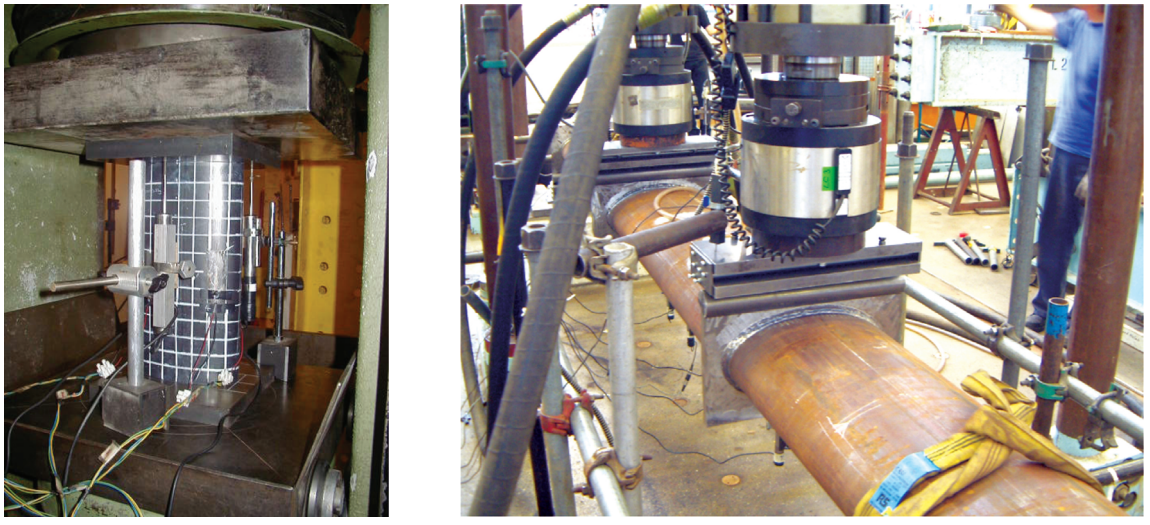

(a) (b)

Fig. 3. Stub column test (a) and bending test (b) of eliptical hollow cross sections (Photos courtesy of Dr. Leroy Gardner).

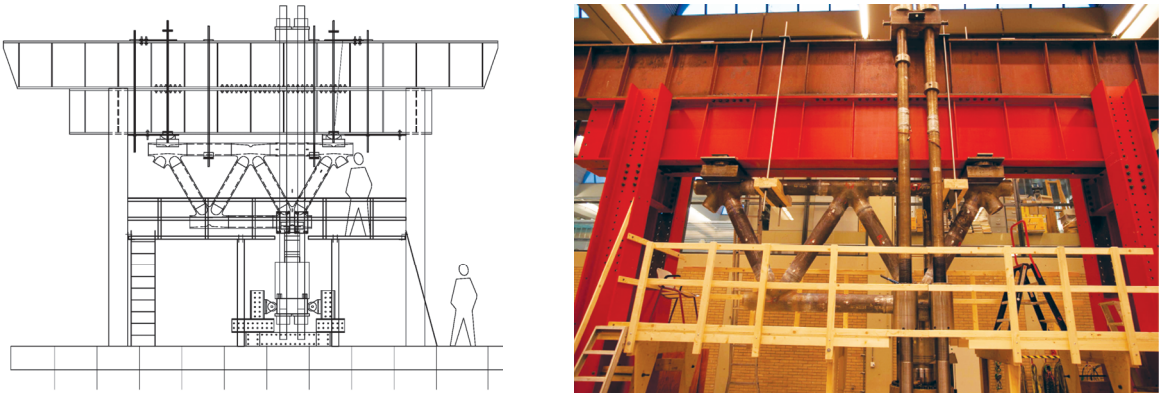

Fig. 4. Hybrid truss girder test specimen (Drawing and photo courtesy of Professor Frans Bijlaard).

and are typically produced with circular hollow sections (CHS). The use of cast steel nodes in combination with CHS elements would provide structures with highly fatigue-resistant connections. At this time, such solutions for bridges and offshore structures use steels with yield stress magnitudes up to 65 ksi (460 MPa). With this background, a program featuring fatigue tests of a truss girder was formulated, using welded CHS elements with K-joints in cast steel with yield stresses of 100 and 130 ksi (690 and 890 MPa). Figure 4 shows a schematic of the test assembly, along with a photograph of the installation in the Stevin Laboratory in Delft.

The large-scale tests were started in January 2010, and the initial results are now becoming available. It is anticipated that the test will be continued for some time. No evaluations of performance and the like are available at this time.

UNIVERSITY OF LIÈGE—SELECTED PROJECTS

Development of an Improved Design Method for Cold-Formed Stainless Steel Members: This is a very long-term research program, having been initiated in 2005. It is anticipated that the effort will be concluded in 2012. Professor Jean-Pierre Jaspart has been the project director.

The University of Liège has excellent testing laboratories, but the school also houses a major software development operation. This is particularly helpful to the researchers studying nonlinear materials, elements and connections.

As already observed in the discussion of some of the research projects being conducted at Imperial College, the actual use of stainless steel for structures has been fairly limited for many years. Part of the problem has been that the material properties of the steel have not been properly reflected in the code criteria, using formulations that were developed for carbon steel. Further, cold-formed elements, connections and structures require detailed attention to very small material thicknesses, local and distortional buckling, cross sections that are only partially effective (due to local buckling effects), and very complex connection details and fasteners.

The studies of stainless steel at Liège have involved extensive analyses and physical tests. In particular, the modeling of the elements has taken into account the nonlinear behavior of the material, biaxial loading, strain hardening, Bauschinger effects, and work-hardening stagnation under reversed deformations at large strain levels (Rossi, 2009).

In line with current advanced application of approaches such as the direct strength method (Schafer, 2006), the overall aim of the project was to arrive at advanced—but above all practical—design formulations. Conducting full-scale tests to confirm the theoretical evaluations, additional finite element models were developed and used to generate further results. The correlation between tests and theory were very good.

Figure 5 illustrates the finite element model that was developed in conjunction with the test program.

REFERENCES

Ashraf, M., Gardner, L. and Nethercot, D.A. (2008), "Structural Stainless Steel Design: Resistance Based on Deformation Capacity," *Journal of Structural Engineering*, ASCE, Vol. 134, No. 3 (pp. 402–411).

Chan, T.M. and Gardner, L. (2008), "Bending Strength of Hot-Rolled Elliptical Hollow Sections," *Journal of Constructional Steel Research*, Vol. 64, No. 9 (pp. 971–986).

Chan, T.M. and Gardner, L. (2009), "Flexural Buckling of Elliptical Hollow Section Columns," *Journal of Structural Engineering*, ASCE, Vol. 135, No. 5 (pp. 546–557).

Cruise, R.B. and Gardner, L. (2008), "Strength Enhancements Induced During Cold Forming of Stainless Steel Sections," *Journal of Constructional Steel Research*, Vol. 64, No. 11 (pp. 1310–1316).

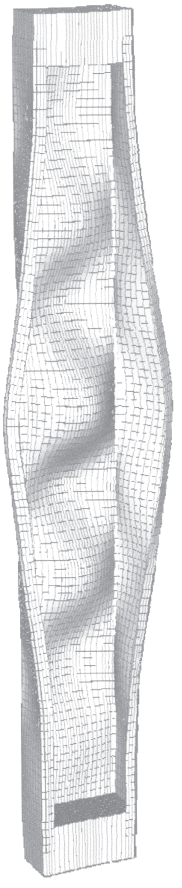

Fig. 5. Finite element model of locally buckled stainless steel cold-formed column (Figure courtesy of Dr. Barbara Rossi).

Elghazouli, A.Y., Málaga-Chuquitaype, C., Castro, J.M. and Orton, A.H. (2009), "Experimental Monotonic and Cyclic Behaviour of Blind-Bolted Angle Connections," *Engineering Structures*, Vol. 31, No. 11 (pp. 2540–2553).

Gardner, L. (2008), "The Continuous Strength Method," *Proceedings of the Institution of Civil Engineers—Structures and Buildings*, Vol. 161, No. 3 (pp. 127–133).

Gardner, L. and Baddoo, N.R. (2006), "Fire Testing and Design of Stainless Steel Structures," *Journal of Constructional Steel Research*, Vol. 62, No. 6 (pp. 532–543).

Izzuddin, B.A., Vlassis, A.G., Elghazouli, A.Y. and Nethercot, D.A. (2008), "Progressive Collapse of Multi-Storey Buildings Due to Sudden Column Loss—Part I: Simplified Assessment Framework," *Engineering Structures*, Vol. 30, No. 5 (pp. 1308–1318).

Nethercot, D.A., Stylianidis, P., Izzuddin, B.A. and Elghazouli, A.Y. (2009), "Enhancing the Robustness of Steel and Composite Buildings," in *Advances in Steel Structures (ICASS '09)*, S.L. Chan (ed.), Hong Kong Institute of Steel Construction, Hong Kong (pp. 105–122).

Nip, K.H., Gardner, L. and Elghazouli, A.Y. (2010), "Cyclic Testing and Numerical Modeling of Carbon Steel and Stainless Steel Tubular Bracing Members," *Engineering Structures*, Vol. 32, No. 2 (pp. 424–441).

Rossi, B. (2009), "Strength, Behavior and the Direct Strength Method for Stainless Steel Cold-Formed Columns," Ph.D. Dissertation, University of Liège, Liège, Belgium.

Schafer, B.W. (2006), *Direct Strength Method (DSM) Design Guide*, American Iron and Steel Institute, Washington, D.C.

Stylianidis, P. and Nethercot, D.A. (2010), "Representation of Connection Behaviour for Progressive Collapse Response," *International Journal of Structural Engineering* (accepted for publication).

Theofanous, M. and Gardner, L. (2010), "Experimental and Numerical Studies of Lean Duplex Stainless Steel Beams," *Journal of Constructional Steel Research*, Vol. 66, No. 6 (pp. 816–825).

ACKNOWLEDGMENTS

Assistance has been provided by ISSRA members Frans Bijlaard, Delft University of Technology; Jean-Pierre Jaspart, University of Liège; and Dr. David Moore, British Constructional Steel Association.

Significant special assistance has been extended by Professors David A. Nethercot, A. Y. Elghazouli, B. A. Izzuddin and Dr. Leroy Gardner of Imperial College; Dr. A. M. Gresnigt of Delft University of Technology; and Dr. Barbara Rossi of the University of Liège.